Master's thesis
2020
Kristian Stråbø

NTNU
Norwegian University of
Science and Technology
Faculty of Information Technology and Electrical
Engineering
Department of Engineering Cybernetics

Kristian Stråbø

Metamodeling and inverse metamodeling electrical conditions in ferromanganese furnaces

June 2020

NTNU
Norwegian University of
Science and Technology

NTNU
Norwegian University of
Science and Technology

NTNU
Norwegian University of
Science and Technology

Metamodeling and inverse metamodeling electrical conditions in ferromanganese furnaces

Kristian Stråbø

Industrial Cybernetics
Submission date: June 2020
Supervisor: Damiano Varagnolo
Co-supervisor: Manuel Sparta

Norwegian University of Science and Technology
Department of Engineering Cybernetics

Sammendrag

Denne masteroppgaven fokuserte på å beskrive og analysere en metallurgisk smelteovn for produksjon av ferromangan (FeMn) legeringer. Den spesifikke utfordringen som blir tatt opp i oppgaven er at det er vanskelig å vite den eksakte tilstanden til ovnen på grunn av et begrenset antall målinger er tilgjengelig.

For å overkomme mangelen på direkte målinger ble en "finite element method" (FEM) modell bygd for å innhente informasjon om forhold mellom indre parametere og elektriske variabler i ovnen. I praksis simulerer FEM modellen de elektriske forholdene med en spesifikk konfigurasjon av parameterne (geometriske parametere, materielle egenskaper) i ovnen. FEM modellen er tung å kjøre, trenger en spesifikk programvare og bruker relativt lang tid for å gi resultatene fra simulering.

En av ideene som ble utforsket i arbeidet var å lage data-drevne modeller av FEM modellen. I denne sammenhengen ble en metamodell laget som en estimering av FEM modellen for å få en raskere modell. I tillegg, så ble en invers metamodell bygd for å finne den inverse sammenhengen mellom input og output, noe som FEM modellen ikke er i stand til å gjøre. Ved å bruke den inverse metamodellen så kan ukjente tilstander i ovnen bli funnet. Modellene kan bli brukt som et hjelpemiddel for å ta avgjørelser da modellen innehar informasjon om ovnen. På denne måten kan modellene bli brukt til å sjekke om modellene stemmer overens med operatørenes kunnskap.

Ikke alle inputene til metamodellene er målt i ovnen. Ved å bygge en estimator som kun bruker variabler som blir målt som input, kan estimatoren bli brukt i sanntid for estimering av den indre tilstanden til ovnen. For at estimatoren skal kunne brukes som et hjelpemiddel for operatørene eller som en del av et kontrollsystem er det veldig viktig at estimatoren er nøyaktig. Derfor ble estimatoren evaluert på ekte data. Evalueringen forteller hvor bra estimatoren er, og til hvilken grad den kan brukes på en ekte ovn. Estimatoren ble prøvd ut på ulike måter med at nye variabler ble lagt til som input for å se hvordan det påvirket ytelsen på estimatoren.

Abstract

This thesis focused on the description and analysis of the metallurgical furnace for the production of the ferromanganese (FeMn) alloy. The specific challenge the thesis addresses is the difficulty of knowing the exact conditions of the industrial furnace during operations due to limited measurements available.

To overcome the scarcity of direct measurements, a finite element method (FEM) model has been built to gain information regarding the relationship between the internal conditions of the furnace and the electrical conditions. In practice, the FEM model simulates the electrical conditions for a specific configuration (geometrical parameters, material properties) in the furnace. The FEM model is computational heavy, it requires dedicated software and it uses a relatively long time to give the simulation results.

One of the ideas explored in this work is to obtain data-driven models of the FEM model. In this context, a metamodel was built as an estimation of the FEM model that runs much faster. An inverse metamodel was also built to give the inverse relationship between input and output, which the FEM model is unable to provide. Thus, unknown internal conditions can be predicted. The models can be used as an assistive tool for the operators for making decisions as the models gain information of the furnace. In this way, the models can be used to check if the models correspond to the operator's knowledge.

Not all the inputs of the metamodels are measured in the plant. By building an estimator that uses only variables that are measured as input, the estimator can be used in real-time for estimation of unknown internal conditions. For using the estimator as an assistive tool or as a part of the control system, the estimator must be accurate. Therefore, the estimator was assessed on real data. The assessment provides how good the estimator is and state to what extent the estimator can be used on the real furnace. Different cases were tested where new variables were included in the input. As the new variables do not have measurement, the variables were estimated to see how the estimator will perform with additional information.

Preface

This master's thesis was written as a part of a 2-year master's degree in Industrial Cybernetics at the Faculty of Information Technology and Electrical Engineering at Norwegian University of Science and Technology (NTNU). The thesis is a part of the "*Electrical Conditions and their Process Interactions in High Temperature Metallurgical Reactors (ElMet)*" project lead by NORCE, Project No.: 247791; with financial support from The Research Council of Norway and the companies Elkem and Eramet Norway. The work was supervised by Damiano Varagnolo (professor at NTNU), and co-supervised by Manuel Sparta (researcher at NORCE).

First of all I want to thank my supervisors for guiding me through the thesis, giving constructive feedback and providing ideas to be explored in the thesis. I also want to thank the people at the plant in Sauda for helping me understand the process of producing ferromanganese (FeMn), and for giving me necessary data.

Personally, I have learned a lot from the writing the thesis. From a technical perspective I have learnt a lot about the production of FeMn, how metamodels of FeMn furnaces can be built using digital twins, and how these two can be combined to gain knowledge about the FeMn furnace. From a personal perspective I have learned a lot from being a part of a bigger project and collaborating with industrial contacts. I hope that this thesis can be a step in the direction of understanding what is going on inside a FeMn furnace, and that the stakeholders of the project can get use of the thesis' output.

Table of Contents

List of Tables

List of Figures

Abbreviations

PLSR	=	Partial Least Squares Regression
FeMn	=	Ferromanganese
FEM	=	Finite Element Method
CI	=	Confidence Interval
PI	=	Prediction Interval
SiMn	=	Silicomanganese
HC	=	High Carbon

Chapter 1

Introduction

This thesis is the continuation of the work done in the project report *"Metamodelling of large ferromanganese furnaces"*. It contributes to the competence project *"Electrical Conditions and their Process Interactions in High Temperature Metallurgical Reactors (ElMet)"*, a research project coordinated by NORCE [1, chap. 1]. In this context, NORCE has developed an ad-hoc finite element method (FEM) model that describes the electrical conditions in a large submerged arc furnace for the production of ferromanganese. The main industrial challenge that drives the project is *understanding what is going on inside the furnace by combining data- and physics-driven models.* In collaboration with NORCE, this thesis focuses on contributing to the understanding of the process by analyzing simulated data from the FEM-model, which can then give a greater knowledge of the process and possibly optimize the control of the furnace [1, chap. 1].

Figure 1.1 visualizes and describes the project's structure. The FEM model possesses well-defined internal conditions of the furnace that gives the outcome of a simulation (1). By utilizing statistical analysis tools, we construct a metamodel that links the inputs and outputs and, in this way, unveils the relative importance of the parameters in the FEM model (2). Importantly, the metamodel can run in milliseconds (i.e., compute outputs starting from some given inputs in a computationally fast way), and in the process, give not only predictions but also predictions intervals. These are favorable properties that the FEM model does not possess. Then we perform an inverse analysis, and in this way, provide an inverse metamodel that links the outputs to the inputs (3). By making an inverse metamodel that uses the same observables as the real furnace, this inverse metamodel can predict the furnace's internal conditions using real data (3'). With the knowledge gained, new control strategies can be implemented to monitor, control, and optimize the furnace (4) [1, chap 1].

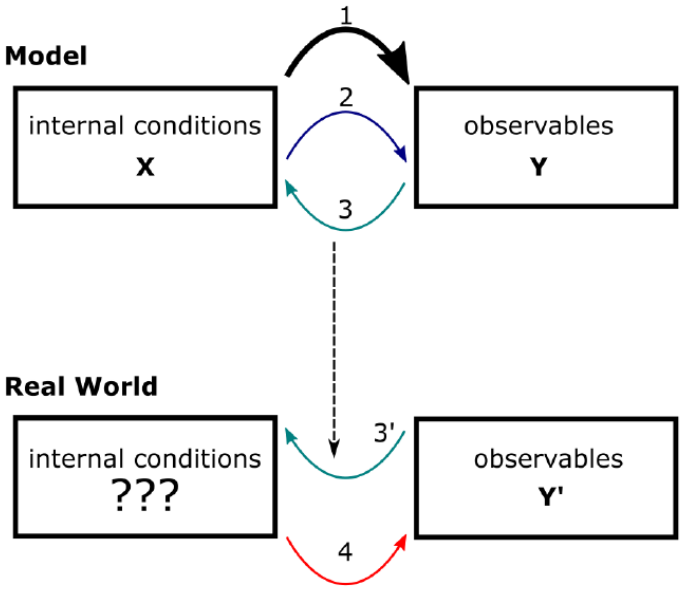

Figure 1.1: The project structure [1, p. 2]. As a first step, a FEM model is used to simulate observable outputs by defining opportune internal working conditions of the furnace (1). The second step is using the simulated output data to build a metamodel of the FEM model (2). Third, this simulated data is used to obtain an inverse metamodel, i.e., a function that takes some given observable outputs, and associates to them the most likely internal working conditions that led to that outputs (3). This means that the inverse metamodel can map real data into estimates of the internal conditions of a real furnace (3'). This information may then be used to monitor, control, and optimize the furnace itself (4).

1.1 Confidentiality

In respect to the stakeholders of the project, some of the values in this report have been obfuscated due to confidentiality. This has been solved by choosing a not given reference value for all variables that contain confidential information. In the report, the values will be given as a percentage of the reference. For example, if one variable has a reference value of 100, and the actual value of the variable is 50, the value given in the report is 50 %. The not given reference values are set for the variables: current, resistance, reactance, voltage, active power, and holder position.

Chapter 2

Project structure

Chapter 1 presented the overall plan. This chapter describes the project structure in more detail. The project started in the summer of 2019 with a visit to a plant in Sauda. This visit focused on talking with professionals within the control and metallurgy of the furnace, with the purpose of gaining an overview of the furnace's overall control strategy, and a list of the measurements that are available at the plant. The information from the plant were supplied with internal documents on the furnace. In the autumn of 2019, the work started by modeling the FEM model's direct and inverse metamodels. This work is continued in this thesis. With respect to the project work, the most important novel contributions brought by this thesis are:

1. Make a direct and inverse metamodel of the FEM model using a partial least square regression (PLSR) approach. More precisely:
   (a) Create a PLSR metamodel that links the inputs and the outputs of the FEM model, creating a function that is a representation of the FEM model but that is at the same time computationally fast to be executed.
   (b) Create an inverse metamodel that links the outputs to the inputs of the FEM model. As the input of the FEM model includes properties that are unknown in operation of the real furnace, the inverse metamodel can extract valuable information that can gain knowledge about the furnace.
2. Make an estimator of the FEM model that only uses electrical conditions that are known in a real furnace to predict interesting conditions given by the FEM model. In this way, the estimator can use real-time measurements of the real furnace to predict the furnace's internal conditions. More precisely:
   (a) The estimator does not link the input to the output as the metamodels. The input of the model are variables in the FEM model that are measured in the real furnace, and the output will be interesting parameters in the FEM model. The parameters are interesting in the sense that they are unknown for a real furnace. With an accurate prediction of the unknown internal conditions, one

can gain knowledge, and possibly implement the estimator as a part of the control system for improved control of the furnace.

This means that the thesis's goal is to make a direct metamodel, an inverse metamodel, and an estimator. These models will be based on the FEM model and will thus represent the FEM model. Representative simulations are done using an experimental design approach to make data-driven models of the FEM model. The design is made in such a way that the simulations will cover most of the furnace operational area.

The models are assessed using classical statistical performance indexes and other ad-hoc features. Thus, it is possible to give indicators of how good, for example, the metamodels represent the original FEM model. Besides this, as the direct and inverse metamodels' main purpose is to both represent the FEM model (one in the input $\rightarrow$ output way, and the other vice versa), they have also been implemented in a specially designed user-interface that is meant to help plant owners to gain insights in the ways the furnace works. The interface moreover displays prediction intervals for the predictions with a given confidence interval, to provide certainty in the prediction.

In the same way as the metamodels, the estimator will be assessed using performance indexes and other ad-hoc features. The estimator is built on a data foundation based on simulations of the FEM model. This means that it is a representation of the FEM model, and the assessment gives an indication of how well the estimator is recreating the FEM model. As the estimator should not only be used for representing the FEM model, but be used on the real furnace, the estimator should be further assessed. The FEM model is also a model of the real furnace, and contains simplification and other factors that can make the FEM model an inaccurate representation of the furnace. Therefore, to make a more thorough assessment, the estimator is tested on real data to explore the performance of the estimator on a real furnace. As there are almost no measurements of the estimated variables, it is hard to compare the estimations with reality. Therefore, knowledge about the processes occurring in the furnace is used to see if the behavior of the estimator corresponds with the understanding of the furnace.

Chapter 3

Theory

This chapter explains the essential theoretical concepts used in the thesis. The theory mainly focuses on modeling and then specifically on partial least square regression (PLSR). Formulas for finding confidence intervals for parameters and estimations will be given and validated.

3.1 Direct and inverse modeling

Consider a system of the form:

$$y(k) = \int_0^k g(k,\tau)u(\tau) + v(k), \tag{3.1}$$

where $y(k)$ is the outcome of a measurement system, $u(\tau)$ is the input of the system, $g(k,\tau)$ is a known function describing the operator transforming the input to the noiseless output and $v(k)$ is the measurement noise. In direct modeling, the aim is to estimate $g(k,\tau)$ such that the output, $y(k)$, can be estimated using the input $u(\tau)$. In the inverse modelling, the aim is to estimate the inverse relation of $g(k,\tau)$ such that the output of the system, $y(k)$, can be used to estimate the input $u(\tau)$.

3.1.1 Metamodeling

A metamodel is a data-driven model based on a complex mathematical model (i.e., a model of a model). Metamodeling aims to obtain an approximated model that is more computationally effective than the original model. This makes the model more practical to use and to implement in, for example, control. Typically, a mathematical model gives a system on the form given in Equation 3.1. This means that the metamodel uses the input, u, to predict the output, y. An inverse metamodel gives the inverse relation, a model that predicts the input, u, given the output y [2].

3.2 Partial least squares

The partial least square regression (PLSR) is a way to predict variables using a linear approach. The PLSR model has a training set consisting of $\boldsymbol{x}_k$ variables ($k = 1, \ldots, K$) and $\boldsymbol{y}_m$ variables ($m = 1, \ldots, M$) with a finite number of samples, N. The training set, therefore, consists of a matrix $\boldsymbol{X}$ with a size of ($N \times K$) and a matrix $\boldsymbol{Y}$ with a size of ($N \times M$). The PLSR finds new latent variables for $\boldsymbol{X}$ that are used in predicting $\boldsymbol{Y}$, as shown in Figure 3.1. The underlying model for PLSR is given by [3]:

$$\boldsymbol{X} = \boldsymbol{T}\boldsymbol{P}^T + \boldsymbol{E} = \sum_{a=1}^{A} \boldsymbol{t}_a \boldsymbol{p}_a^T + \mathbf{E} \tag{3.2a}$$

$$\boldsymbol{Y} = \boldsymbol{U}\boldsymbol{Q}^T + \boldsymbol{F} = \sum_{a=1}^{A} \boldsymbol{u}_a \boldsymbol{q}_a^T + \mathbf{F} \tag{3.2b}$$

where $\boldsymbol{t}_a$ is the $\boldsymbol{X}$-scores and $\boldsymbol{p}_a$ is the corresponding loadings of $\boldsymbol{X}$. In the same way, $\boldsymbol{u}_a$ is the $\boldsymbol{Y}$-scores and $\boldsymbol{q}_a$ is the corresponding loadings of $\boldsymbol{Y}$. By choosing the number of components in the model less than the number of $\boldsymbol{X}$ variables, $A < K$, gives a compressed regression. The scores can be described as a summary of the data and can be used for finding clusters, outliers, and interesting patterns. The loadings gives the structure of the $\boldsymbol{X}$ and $\boldsymbol{Y}$, and can be used to see correlations between variables. Highly correlated variables will cluster together for all dimensions. The purpose of the PLSR is to maximize the covariance of $\boldsymbol{T}$ and $\boldsymbol{U}$, such that $\boldsymbol{T}$ can be used as a predictor of $\boldsymbol{Y}$. In this way, a relation between the $\boldsymbol{X}$ and $\boldsymbol{Y}$ variables can be obtained given by the linear PLSR model [3] [4, Chap. 13.3]:

$$\boldsymbol{Y} = \boldsymbol{X}\boldsymbol{B} + \boldsymbol{b}_0 + \boldsymbol{E} \tag{3.3}$$

where $\boldsymbol{B}$ is a matrix containing the regression coefficients of the model, $\boldsymbol{b}_0$ is the interception vector and $\boldsymbol{E}$ is the error matrix. The regression coefficients can be used to see the relative importance for the variables in predicting $\boldsymbol{Y}$. In this thesis the SIMPLS [5] algorithm is used for estimating the parameters in the PLSR.

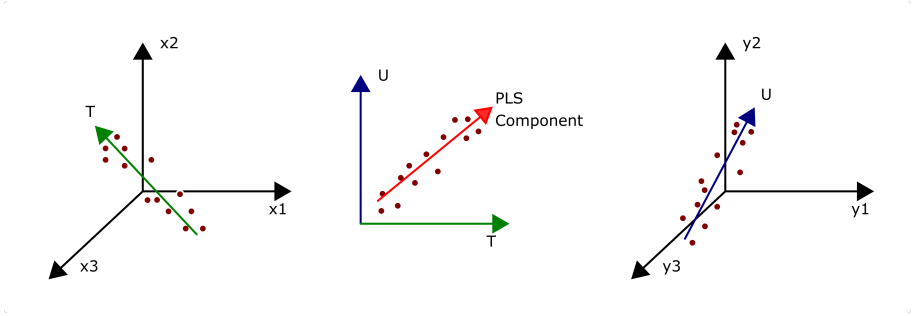

Figure 3.1: Visualization of how the vectors $\boldsymbol{U}$ and $\boldsymbol{T}$ are chosen to get maximum covariance between the vectors (based on Lambert [6]).

3.2.1 Backnormalizing the model coefficients

Since the dataset often has variables with different units of measurements, it is often beneficial to normalize the data before performing PLSR. In the PLSR, the $\boldsymbol{X}$ and $\boldsymbol{Y}$ variables are normalized, such that each column of the respective set has a mean value of 0 and a standard deviation of 1. This means that the matrix $\boldsymbol{B}$ and the interception term $\boldsymbol{b}_0$ given in Equation 3.3, are also corresponding to the normalized set. We are therefore to make an expression with $\boldsymbol{\beta}_{raw}$ and $\boldsymbol{\beta}_{0,raw}$ that can predict $\boldsymbol{y}$ using $\boldsymbol{x}$ without normalizing the vectors. From the PLSR model we really obtain the equation where the $\boldsymbol{B}$ and $\boldsymbol{b}_0$ are normalized:

$$\hat{\boldsymbol{y}}_{norm} = \boldsymbol{x}_{norm}\hat{\boldsymbol{\beta}}_{norm} + \hat{\boldsymbol{\beta}}_{0,norm}, \tag{3.4}$$

where $\boldsymbol{y}_{norm}$ and $\boldsymbol{x}_{norm}$ are given as following:

$$\hat{\boldsymbol{y}}_{norm} = (\hat{\boldsymbol{y}} - \bar{\boldsymbol{y}})diag\left(\frac{1}{\sigma_{y,i}}\right) \quad \text{and} \quad \boldsymbol{x}_{norm} = (\boldsymbol{x} - \bar{\boldsymbol{x}})diag\left(\frac{1}{\sigma_{x,j}}\right),$$

where i denotes the variable number in the $\boldsymbol{y}$ vector and j denotes the variable number in the $\boldsymbol{x}$ vector. By substitution, we can extract the backnormalized $\hat{\boldsymbol{\beta}}_{raw}$ and $\hat{\boldsymbol{\beta}}_{0,raw}$:

$$(\hat{\boldsymbol{y}} - \bar{\boldsymbol{y}})diag\left(\frac{1}{\sigma_{y,i}}\right) = (\boldsymbol{x} - \bar{\boldsymbol{x}})diag\left(\frac{1}{\sigma_{x,j}}\right)\hat{\boldsymbol{\beta}}_{norm} + \hat{\boldsymbol{\beta}}_{0,norm} \tag{3.5a}$$

$$\begin{aligned}\hat{\boldsymbol{y}} = \underbrace{\boldsymbol{x}\, diag\left(\frac{\sigma_{y,i}}{\sigma_{x,j}}\right)\hat{\boldsymbol{\beta}}_{norm}}_{\hat{\boldsymbol{\beta}}_{raw}} \\ \underbrace{-\bar{\boldsymbol{x}}diag\left(\frac{\sigma_{y,i}}{\sigma_{x,j}}\right)\hat{\boldsymbol{\beta}}_{norm} + diag\left(\sigma_{y,i}\right)\hat{\boldsymbol{\beta}}_{0,norm} + \bar{\boldsymbol{y}}}_{\hat{\boldsymbol{\beta}}_{0,raw}}\end{aligned} \tag{3.5b}$$

The expression can then be rewritten as:

$$\hat{\boldsymbol{y}} = \boldsymbol{x}\hat{\boldsymbol{\beta}}_{raw} + \hat{\boldsymbol{\beta}}_{0,raw} \tag{3.6}$$

This gives us a faster regression model where there is no need for normalizing the $\boldsymbol{x}$ and $\boldsymbol{y}$ for each prediction.

3.2.2 Estimating the confidence intervals for the model coefficients

The confidence intervals of the $\hat{\boldsymbol{\beta}}$ coefficients are a way of expressing the uncertainty in our estimates. More precisely, and from intuitive perspectives, a confidence interval gives a range of values for an unknown parameter with an associated confidence level that the true parameter is in the given range. Formally speaking, see Dekking et al. [7, Chap. 23].

For the specific case of confidence intervals in PLSR settings, Nomikos and MacGregor [8] have developed an approximate confidence interval for $\hat{\boldsymbol{\beta}}$, which can be derived in a computationally efficient manner. More precisely, the estimated variance of $\hat{\boldsymbol{\beta}}$ is given as:

$$\text{Var}(\hat{\boldsymbol{\beta}}) = \underbrace{\boldsymbol{W}(\boldsymbol{P}^T\boldsymbol{W})^{-1}(\boldsymbol{T}^T\boldsymbol{T})^{-1}(\boldsymbol{W}^T\boldsymbol{P})^{-1}\boldsymbol{W}^T}_{\boldsymbol{Z}}\sigma^2, \tag{3.7}$$

where $\boldsymbol{W}$ is the weight matrix of the $\boldsymbol{X}$ set in the PLSR, $\boldsymbol{P}$ is the loading matrix for the $\boldsymbol{X}$ set in the PLSR and $\boldsymbol{T}$ is the score matrix for the $\boldsymbol{X}$ set in the PLSR. The variance σ^2 can be estimated by [8]:

$$\hat{\sigma}^2 = \frac{1}{N - A - 1} \sum_{l=1}^{N} (y_l - \hat{y}_l)^2, \tag{3.8}$$

where N is the number of training cases, and A is the number of components in the PLSR. We now assume that the deviations of $\boldsymbol{Y}$ around its expectation is Gaussian which gives us the following expression for the confidence intervals for the $\hat{\boldsymbol{\beta}}$:

$$\hat{\boldsymbol{\beta}}_i \pm t_{N-A-1}^{(\alpha/2)} \hat{\sigma} \sqrt{\boldsymbol{Z}_{ii}}. \tag{3.9}$$

Validating the confidence intervals

In this section, we use Equation 3.9 to validate the estimated confidence intervals using a test. As the confidence interval (CI) given in equation 3.9 is an approximation, an algorithm is designed to test the accuracy of the CI. In the first step, the algorithm creates a linear model containing the $\boldsymbol{\beta}$ parameters. An estimated model is then found by performing a PLSR step on the simulated data for $\boldsymbol{X}$ and $\boldsymbol{Y}$. The CI's can then be computed for the $\hat{\boldsymbol{\beta}}$ and, in this way, one can detect whether the true $\boldsymbol{\beta}$ is outside the CI. The CI can be estimated by doing this in a for loop for a representative number of times. By generating the model inside of the for loop, 1000 different models are built, meaning that the validation takes into consideration different models.

1. For i = 1, . . . , 1000

   (a) Generate a random $\boldsymbol{\beta}$ for a linear model $\boldsymbol{y} = \boldsymbol{X}\boldsymbol{\beta} + \boldsymbol{error}$.

   (b) Generate randomly a $\boldsymbol{X}$ and $\boldsymbol{error}$ set used to calculate a $\boldsymbol{y}$ set.

   (c) Make a regression model based on the $\boldsymbol{X}$ set and $\boldsymbol{y}$ set which gives an estimate $\hat{\boldsymbol{\beta}}$.

   (d) Compute the CI of 95 % for each $\hat{\boldsymbol{\beta}}$ component.

   (e) Count how many times $\boldsymbol{\beta}$ is outside of the CI for each component.

2. Return how many times $\boldsymbol{\beta}$ is outside the CI as a percentage for each component.

The results of the test given in Figure 3.2 was satisfying with the simulations gathered around 5 % outside the CI's.

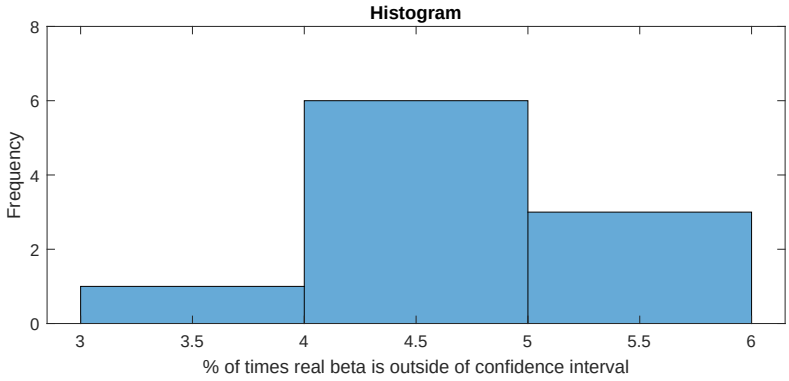

Figure 3.2: Histogram of how often the real beta is outside of the calculated beta confidence intervals for 1000 simulations with 10 beta parameters.

3.2.3 Estimating the prediction intervals

The uncertainties of $\hat{\boldsymbol{\beta}}$ give a good measure of the uncertainty in the model. But, when using a new set of predictors, $\boldsymbol{x}_0$, it is useful to know the prediction intervals for the prediction, $\hat{f}_0(\boldsymbol{x}_0) = \boldsymbol{x}_0^T\hat{\boldsymbol{\beta}}$. The expression for the prediction interval for a single prediction is given by [8]:

$$\hat{f}_{PI} = \hat{f}_0 \pm t_{N-A-1}^{(\alpha/2)}\hat{\sigma}\sqrt{1 + \hat{\boldsymbol{t}}(\boldsymbol{T}^T\boldsymbol{T})^{-1}\hat{\boldsymbol{t}}^T} \tag{3.10}$$

where $\boldsymbol{x}_0$ is decomposed as $\hat{\boldsymbol{x}}_0 = \hat{\boldsymbol{t}}\boldsymbol{P}^T$. $\boldsymbol{T}$ is the score matrix for the $\boldsymbol{X}$ set and $\boldsymbol{P}$ is the loading matrix for the $\boldsymbol{X}$ set. The $t_{N-A-1}^{(\alpha/2)}$ is the critical value of the Studentized variable with $N - A - 1$ degrees of freedom at significance level $\alpha/2$, and $\hat{\sigma}$ is given by Equation 3.8. In the SIMPLS algorithm one tries to find $\boldsymbol{R}$ such that $\boldsymbol{t} = \boldsymbol{x}_0\boldsymbol{R}$, where $\boldsymbol{R}$ can be calculated by $\boldsymbol{R} = \boldsymbol{W}(\boldsymbol{P}^T\boldsymbol{W})^{-1}$. By substitution this gives $\boldsymbol{t} = \boldsymbol{x}_0\boldsymbol{W}(\boldsymbol{P}^T\boldsymbol{W})^{-1}$. This can then be inserted into the Equation 3.10 which gives:

$$\hat{f}_{PI} = \hat{f}_0 \pm t_{N-p-1}^{(\alpha/2)}\hat{\sigma}\sqrt{1 + \boldsymbol{x}_0\boldsymbol{W}(\boldsymbol{P}^T\boldsymbol{W})^{-1}(\boldsymbol{T}^T\boldsymbol{T})^{-1}(\boldsymbol{W}^T\boldsymbol{P})^{-1}\boldsymbol{W}^T\boldsymbol{x}_0^T} \tag{3.11a}$$

$$\hat{f}_{PI} = \hat{f}_0 \pm t_{N-p-1}^{(\alpha/2)}\hat{\sigma}\sqrt{1 + \boldsymbol{x}_0\boldsymbol{Z}\boldsymbol{x}_0^T} \tag{3.11b}$$

As $\boldsymbol{Z}$ can be calculated once, this gives a fast calculation of the prediction interval.

Validating the prediction intervals

In this section, we use the prediction interval (PI) formula presented in Equation 3.10. Since the formula contains simplifications, we will test whether these simplifications introduce non-tolerable distortions for random PLSR models. The algorithm is similar to the algorithm for validating the confidence intervals for $\boldsymbol{\beta}$ parameters. In the same fashion, it finds a true model containing $\boldsymbol{\beta}$ parameters. An estimated model is found using PLSR based on simulated data of the true model. The PLSR model is then predicting $\hat{y}_0$ with a 95 % confidence level based on new simulated $\boldsymbol{x_0}$ data. By extracting the number of

times the true y_0 is outside the PI one can find the predicted confidence level for the given model. The algorithm was performed 100 times to get a representative test for different models.

1. Generate a random $\boldsymbol{\beta}$ for a linear model $\boldsymbol{y} = \boldsymbol{X\beta} + \boldsymbol{error}$.
2. Generate randomly a $\boldsymbol{X}$ and $\boldsymbol{error}$ set used to calculate a $\boldsymbol{y}$ set.
3. Make a regression model based on the $\boldsymbol{X}$ set and $\boldsymbol{y}$ set which gives an estimate $\hat{\boldsymbol{\beta}}$.
4. For i = 1...1000:
   (a) Generate a new input, $\boldsymbol{x_0}$.
   (b) Regress $\boldsymbol{x_0}$ to find an estimate $\hat{y}_0$.
   (c) Compute the PI of 95 % for each $\hat{y}_0$.
   (d) Count how many times y_0 is outside the PI.
5. Return how many times y is outside the PI as a percentage.

The results of the test are given in Figure 3.3, and were deemed as satisfying. We can indeed see that out of the hundred simulations, there exists a clustering around 5 %. It should also be commented that for some models, the confidence level is calculated to be around 10 %.

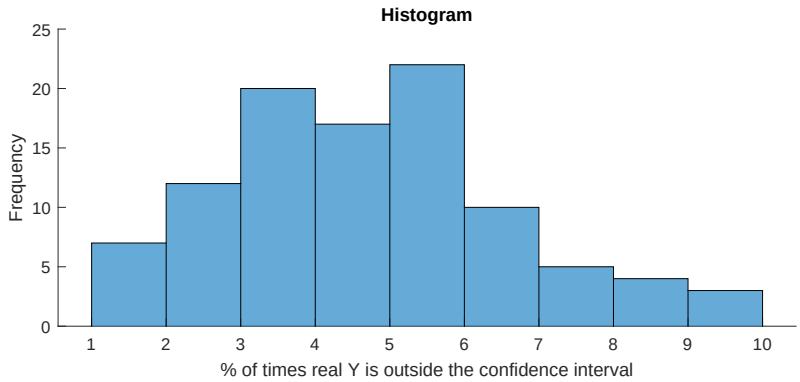

Figure 3.3: Histogram of how many % of the times a real y value is outside a prediction interval for 100 models with 1000 simulations each.

3.3 Model selection and validation

Friedman et al. [9, p. 219] states: "The *generalization* performance of a learning method relates to its prediction capability on independent test data". Practically speaking, a data-driven model must be tested on "unseen" data to assess the performance. Unseen data can be defined as data that the model has not used in training the model. This section explains different methods for assessing the performance of a data-driven model and why the assessment is important.

3.3.1 bias-variance tradeoff in model order selection

All models presented in this thesis are built using a PLSR approach. A PLSR model has one complexity parameter: the number of components used for the model. The number of components should be chosen such that the model not only performs well on the training data, but also performs well for unseen data. Intuitively, using the maximum number of components in the model can give a perfect fit for the training data, but the performance on unseen data can be poor. This is the bias-variance tradeoff [9, chap. 2.9]. A good choice of the number of components is when an increase in the number of components are not giving a significantly increase in the performance of the model.

Mathematically, the bias-variance tradeoff can be presented as given in Friedman et al. [9, chap 2.9]:

Firstly, we can define a training set consisting of a set of points $x_i, ..., x_n$ and real values y_i associated with each point x_i. We can assume that there exists a function given by $y = f(x) + \varepsilon$, where ε is noise with zero mean and variance σ^2. The best estimator, $\hat{f}(x)$, can be found measuring the mean square error between y and $\hat{f}(x)$. To obtain an estimator that is generalizable for unseen data, we want that $(y - \hat{f}(x))^2$ is minimal both for the training samples, $x_i, ..., x_n$, and for points outside our sample. The expected error on an unseen sample x for the estimator $\hat{f}$ can be decomposed as follows:

$$\boldsymbol{E}[(y - \hat{f}(x))^2] = (Bias[\hat{f}(x)])^2 + Var[\hat{f}(x)] + \sigma^2 \tag{3.12}$$

where $Bias[\hat{f}(x)] = \boldsymbol{E}[\hat{f}(x)] - \boldsymbol{E}[f(x)]$ and $Var[\hat{f}(x)] = \boldsymbol{E}[\hat{f}(x)^2] - \boldsymbol{E}[f(x)]^2$.

Figure 3.4 visualizes the bias-variance tradeoff. By increasing the model complexity (i.e., for a PLSR model: increasing the number of components), the prediction error decreases for the training set, while the prediction error increases for the test set. Having a low bias and high variance is often referred to as "overfitting". Practically speaking, this is when the model fits the training set very well, but the performance on an unseen test set is worse. The opposite effect is called "underfitting". This means that the model complexity is too low for giving a good representation of both test and training data. See Burnham and Anderson [10, pp. 29–35] for more details regarding under- and overfitting.

3.3.2 Validation of a model

The validation of a model is important in assessing the model's performance on unseen data. There are several ways to validate the model. If the amount of data is large, it is possible to split the data into a training, a validation, and a test set. In this case, we fit the models to the data in the training set, and validate the model on the validation set. The model with the best fit on the validation set is selected. The final assessment of the chosen model is done on the test set [9, Chap. 7.2].

Using a validation set for assessing the performance of the model is the ideal case. However, if the amount of data is scarce, it is possible to use cross-validation. K-fold cross-validation uses a part of the available data in the training set to fit the model, and a different part to test the model in K iterations. This means that the data is split up into $k = 1, 2, ..., K$ folds. For the kth part, the model is fitted using the other $K-1$ parts of the data, and calculates the model's performance on the kth part of data. When the performance

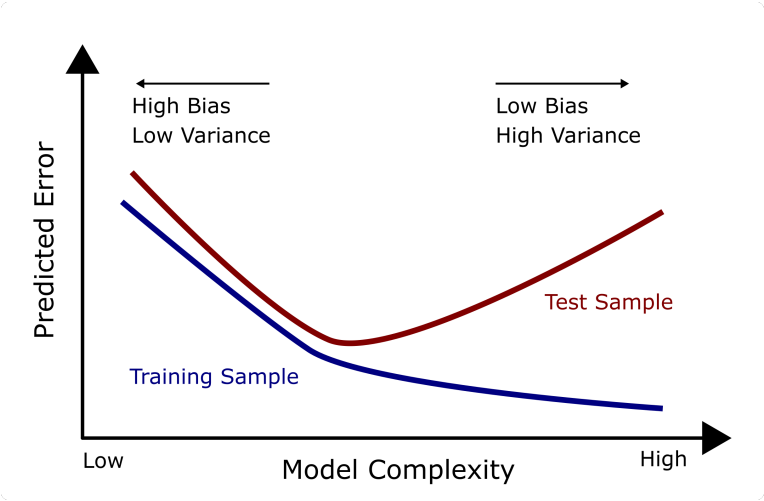

Figure 3.4: The prediction error for the test and training set as a function of model complexity (based on Friedman et al. [9, p. 38].)

is found for each k, the mean of the performance is calculated [9, Chap. 7.10.1]. A 3-fold cross-validation is visualized in Figure 3.5. The case when K equals the number of samples, N, is known as leave-one-out cross-validation [9, Chap. 7.10.1].

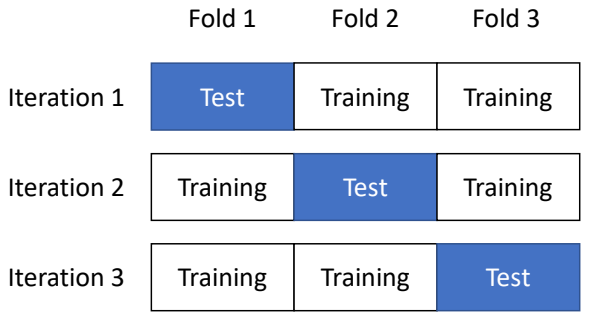

Figure 3.5: The concept of K-fold cross-validation using three folds.

Chapter 4

Details about the modeled FeMn furnace

This chapter presents general information regarding the FeMn furnace, and highlights the challenges of controlling the furnace. Generally, the reactions that take place in the furnace are well known. What makes the control of the furnace difficult is that the furnace's actual condition at a given time is hard to measure. The material composition is not uniform, and the reactions happens at different rates. This means that the operators do not have information that can be valuable in controlling the furnace. The main focus will be on the control aspect of the furnace, and less from the metallurgical side. This chapter is based on meetings with professionals with long experience of FeMn furnaces from a visit to the plant in Sauda, and the internal document by Asphaug [11]. A summary of the visit can be found in the internal document [12].

4.1 A brief overview of the considered FeMn furnace

Firstly, it is essential to know what manganese is. Manganese is a metallic element with the chemical symbol Mn. The appearance of the manganese metal is gray-white and is resembling iron, but it is harder and very brittle. Manganese and iron also appear very close in the periodic system of elements, with atomic numbers 25 and 26, respectively [11, Chap. 1.1]. The most common use of manganese is as a desulfurizing and deoxidizing agent in steelmaking for increasing hardenability [13]. The manganese used in steelmaking is mostly in the form of ferroalloys, as ferromanganese (FeMn) or silicomanganese (SiMn) [11, Chap. 1.1].

Large modern electrical furnaces for the production of FeMn are rated at more than 40 MW and have a size of 10 - 15 meters in diameter [1]. The furnaces are three-phase with three "Søderberg" electrodes of a size of 1.5 - 2 meters in diameter going into the furnace. The temperatures in the furnace can go up to 1700 °C [11, Chap. 1.3].

Manganese ore is the main raw material fed to the furnace [11, Chap. 4.1.1]. As

manganese cannot be found in its pure form in nature, the ore contains other metals and minerals depending on the type of ore. If it is not used self-fluxing ore, it is needed flux material in the charge to obtain desired properties as melting point, viscosity, chemical activities and electrical resistivity [11, Chap. 2.3.1]. The most commonly used flux materials are limestone ($CaCaO_3$), dolomite ($CaMg(CO_3)_2$), olivine ($(Mg,Fe)_2SiO_4$) and quartzite (SiO_2). The last main group of raw materials used in the furnace is the reductants. In High Carbon (HC) FeMn production, coke is the most used reductant [11, Chap. 4.1.1].

The different raw material components that are to be smelted in the furnace are proportioned out according to a recipe given by the metallurgists. The materials are weighed out, mixed and transported to hoppers above the furnace, where they are fed through the cover [11, Chap. 1.3].

The raw materials at the top of the charge inside the furnace are heated by the hot gases rising from the reaction zone deeper in the furnace. Here, higher oxides partly react with CO to CO_2 and partly dissociate. The reduction of the higher oxides with CO is exothermic and adds heat to the process [11, Chap. 1.3].

The final reduction from MnO to Mn takes place with solid carbon in the "coke bed". The coke bed is the area of molten slag and coke mixture. As the coke bed is soaked with slag, it acts as a resistance element between the electrode and the metal bath. Therefore, this is the region of the furnace where most of the electric energy dissipates. In this way, the size and properties of the coke bed is vital in giving the electrical conditions in the furnace. The gangue (undesirable oxides in the manganese ore) and flux materials such as CaO, MgO, and Al_2O_3 all require higher temperatures than MnO for reduction to metal, and ends up in the slag without being reduced. For iron, the reduction of FeO to Fe takes place at a lower temperature than the reduction of MnO to Mn, which means that practically all the iron ends up in the metal. Unfortunately, the undesired oxides of phosphorus and arsenic easily reduce and end up in the metal. For the production of HC FeMn, the alloy typically consists of 79% Mn, 13 % Fe, 7 % C, and minor amounts of Si, P, and S [11, Chap. 1.3].

The melted metal and slag are tapped from the bottom of the furnace. Since the slag is lighter than the metal, it floats atop of the metal and can easily be separated from the metal [11, Chap. 1.3]. The metal is cast into "sandbeds", and once the metal has cooled sufficiently, it goes through a crushing and screening process to meet the sizing requirements for the various steel customers. The slag is often processed and reused in the production of SiMn alloy [1, Chap. 3.1] [12, Chap. 2]. Figure 4.1 gives an illustration of the furnace.

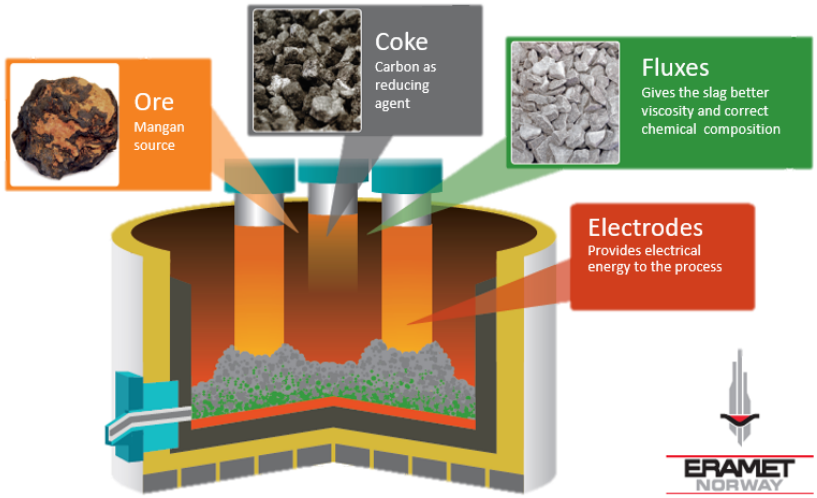

Figure 4.1: The concept of a ferromanganese furnace with three electrodes. The manganese ore, coke and fluxes are smelted in the furnace and tapped at the bottom as metal and slag. Figure courtesy of Eramet Norway.

4.2 Notes about the furnace's control system

A general description of the FeMn furnace has now been provided. We will now go deeper into the furnace's control aspect and go into each part of the block diagram of the furnace given in Figure 4.2.

4.2.1 The reference signals

A reference is set on the total power, and resistance and holder position for each electrode. The reference on the resistance and total power gives the wanted conditions in the furnace. The holder position's reference is often in the middle of the span of what the holder can move up or down. That is to give the maximum allowance to the movement of the electrode both up and down.

4.2.2 The purpose of the control system

The controller minimizes the error between reference and measurement of total power and the resistances. Few details of the controller are known because the controller is regarded as an "industrial secret". What is known is that the controller gives the voltage on each electrode to reach the desired reference of the total power. As the voltage is given in distinct steps (voltage transformer), the power reference cannot be met exactly. The power setpoint is, therefore, less important than the reference of the resistances. The voltage

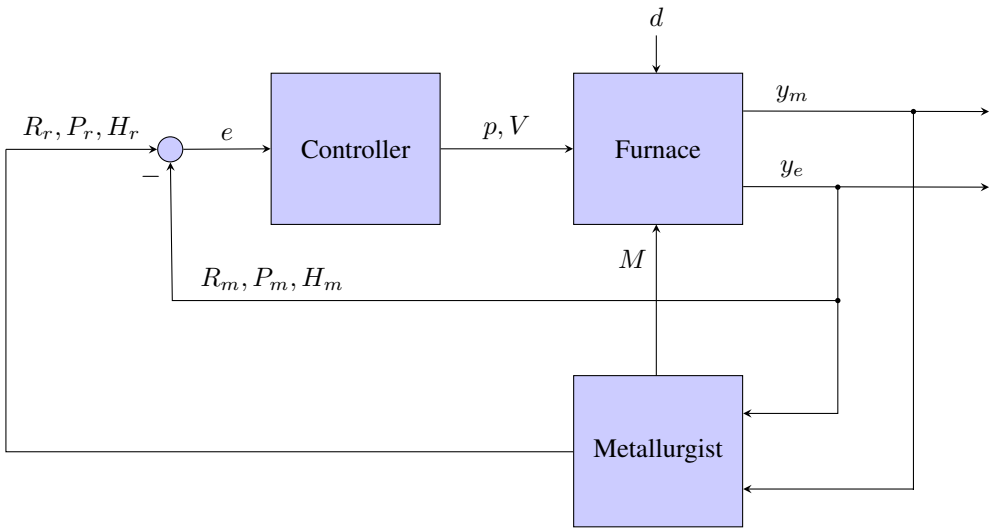

Figure 4.2: The block diagram of the furnace. The block diagram shows that the metallurgist is a part of the feedback loop. The metallurgist has the role of ensuring a stable furnace, and have two control actions: (1) give the material composition (M) applied to the furnace and (2) change the setpoints on the resistance (R_r), power (P_r), and holder position (H_r) for each electrode. The controller is designed to keep the error (e) minimized between the setpoints and measurements of resistance, power and holder position given some constraints. The controller gives the electrode position (p_r) and the step on the voltage transformers for each electrode, which gives the furnace's electrical conditions. The disturbance (d) of the furnace is regarded as everything chemical reactions that make the furnace hard to control. The output is divided into electrical conditions (y_e) and the metallurgical conditions (y_m). The metallurgist uses both outputs in making decisions. The controller uses only the measured resistance (R_m), power (P_m) and holder position (H_m) for each electrode of the electrical variables.

transformers can be asymmetrical, such that the voltage transformers are on different steps, but they have a limitation on the maximum difference in the steps.

The resistance is regulated by moving the electrode up or down. There is an upper and lower boundary on the resistance. If the measured resistance goes below the lower boundary (i.e., the resistance is lower than wanted), the electrode is raised, and the resistance increases. Otherwise, if the measured resistance is above the upper boundary (i.e., the resistance is higher than wanted), the electrode is lowered, and the resistance decreases.

In addition to change in holder position, the electrode position is given by the "slipping". The slipping is primarily to compensate for the electrode consumption during operation, and over a long period of time, the slipping must be equal to the total consumption. In the short period, however, one can modify the slipping rate to help to keep the holder in the optimal central position. The frequency of the slip cycles is increased or decreased based on the actual holder position versus a setpoint for the holder position. For example, if the holder position is near the top position, the slipping frequency is slowed down, and if the electrode is below the setpoint, the slipping frequency increases. This is to keep the holder position at the reference without affecting the resistance in the furnace.

What is described above is implemented in an automatic control system. But the metallurgists control a big part of the furnace. They specify the amount of charge material and its composition loaded into the furnace. The material gives the conductivity in the furnace and influences the electrical conditions in the furnace. In this way, the control system is partially "manual". The electrical control differs a lot to the chemical control in a time perspective. The electrical conditions are much faster (electrodes lift in minutes) compared to the chemical control by changing the composition of the charge. It takes hours/days before the mix with new composition reaches the reactive zones in the core and starts affecting the process. In this section, the metallurgists part in the control system is not described in detail.

4.2.3 The actuation system

As explained in Section 4.2.2, we have three control actions that are possible [11, Chap. 5.1]:

1. Changing electrode position to give the wanted resistance.
2. Changing the step on the voltage transformers to give the wanted power.
3. Changing the amount of charge material and its composition to give the conductivity in the furnace.

The electrode position can be changed by regulating the holder position and slipping cycle. A big issue is that there is no measurement of the electrode position, which makes the control of the furnace challenging. We note that the slipping rate and holder position is known, but the electrode consumes in the furnace due to chemical reactions. This means that the positions of the electrodes' tips are unknown. To compensate for the fact that the electrodes' losses are unknown, the electrode's consumption is estimated, and the electrode slipped according to the estimation. Note that to the best of our knowledge, estimating the positions of these tips accurately is yet an open problem, since the current solutions do not meet the accuracy requirements that are wished by the plants' managers and operators.

4.2.4 The furnace

The system controlled is the furnace. See Section 4.1 for more information regarding the furnace.

4.2.5 Some notes about the disturbances

The disturbances of the furnaces makes the control of the furnace difficult. All reactions in the furnace are regarded as a disturbance that influences the material distributions and the electrode positions. Since the material distributions and electrode positions impact the electrical conditions, the disturbances also impact the electrical conditions.

The tapping of the furnace occurs at regular intervals. During tapping, the amount of metal and slag decreases, which affects the conductivity in the furnace. Tapping intervals are known, but how exactly the tapping influences the conditions in the furnace are uncertain. Therefore are the tapping cycles regarded as a disturbance of the system.

4.2.6 The available measurements

The furnace's output is all electrical variables measured in and around the furnace (voltages, currents, resistances, reactances, powers), temperature sensors in the lining and bottom of the furnaces, gas measurements, and pressure measurements. Not all the electrical variables are measured directly, and some of them are measured inaccurate. The electrical measurements are presented below:

Voltage

It is inaccurate to measure the furnace's voltage because the strong alternating magnetic field around the furnace induces currents in any measuring circuits. The most used method is to measure the voltage through the Bøckman principle, and is given by Asphaug in the following way:

> *Three measuring leads in approximately 120° symmetry are used to reproduce the furnace bottom potential above the furnace, where it is connected to the star point above between the electrode voltages. The idea is that the voltages induced in the three measuring leads will compensate each other. Deviation from ideal 120° symmetry which may be necessary for practical reasons is compensated by adjusting a resistor network connecting the three leads* [11, p. 51].

Power

The active power (P) in the furnace is found using voltage (U), current and phase angle (θ) in a power measuring converter. The equation is given as [11, Chap. 5.2.1]:

$$P = UI\cos(\theta) \tag{4.1}$$

This means that the power is found based on the voltage, which is an inaccurate measurement.

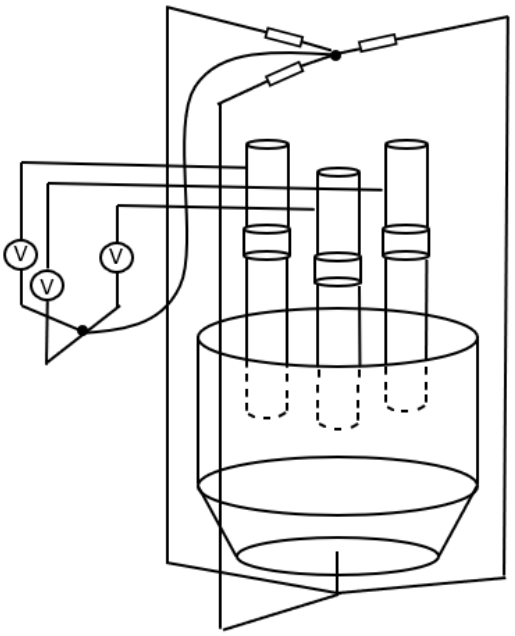

Figure 4.3: Visualization of the Bøckman principle. The bottom voltage is moved to an area with weak magnetic fields above the furnace using a three-lead compensating network [11, Chap. 5.2.1].

Current

Accurate measurement of currents is not possible with current transformers because of high currents. This is, however, not a problem as the currents can be derived from the primary side without loss of accuracy [11, Chap. 5.2.1].

Resistance

The resistance measurement is complex. The resistance between each electrode and the furnace bottom should be known to control the electrical conditions in the furnace. To determine the resistance, we need the active power obtained in by the power (P) measuring unit, which is given in Equation 4.1 and the current (I). The equation can then determine the resistance [11, Chap. 5.2.1]:

$$R = \frac{P}{I^2} \tag{4.2}$$

This means that the resistance is found based on the power, which again is based on the inaccurate measurement of voltage.

Reactance

The reactance (X) can be calculated using electrode current (I), electrode voltage (V) and electrode power (P) by the formula [11, Chap. 5.2.1]:

$$X = \sqrt{\left(\frac{V}{I}\right)^2 - \left(\frac{P}{I}\right)^2} \tag{4.3}$$

This means that the reactance is found based on the voltage, which is an inaccurate measurement.

4.3 A qualitative analysis of the dynamics of the FeMn furnace

A qualitative analysis of the FeMn furnace's dynamics is performed to gain a deeper understanding of the various dynamics of the furnace. This analysis will show the different span of time constants that occurs in the furnace.

4.3.1 Dynamics of the thermal phenomena

In January 2019, a short stop (approx. 400 min) due to technical necessities was exploited to collect the data needed to determine if and where heat generated by Eddy currents in the steel shell can be detected. The underlying assumption is that to have any chance to carry information about the induced currents; the temperature profiles must react fast to shutdowns and change in currents [14].

The results from the experiment showed that some temperature probes responded both to the shutdown and restart. In Figure 4.4, two representative cases of the probes are

shown. The plot shows that Sensor 1 reacts on the shutdown while Sensor 2 does not seem to be influenced by the shutdown. Since all electrical conditions in the furnace are reduced during shutdown, it indicates that Sensor 1 correlates with the electrical conditions. This means that Sensor 1, and the equivalent sensors, are sensitive to the Eddy currents.

The problem with the temperatures is that they have a very long time constant. If we assume that the temperature has reached its peak at the end of the time-series, the time constant of Sensor 1 is 320 minutes. In total, the sensor 1 uses 16 hours and 50 minutes to reach the steady-state after shutdown.

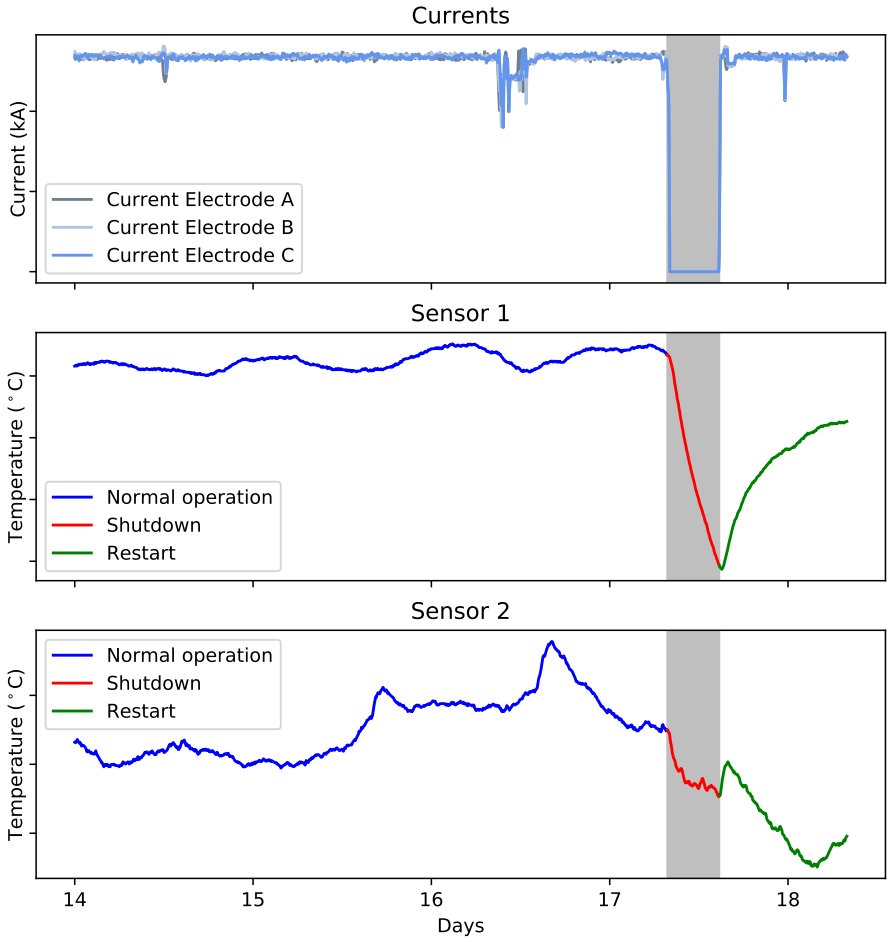

Figure 4.4: The dynamics of two temperature sensors over a period of days. Sensor 1 reacts on a shutdown of the furnace, while sensor 2 does not. The values on the y-axis are removed due to confidentiality.

4.3.2 Dynamics of the electrical phenomena

The electrical conditions have much faster dynamics than the temperatures. This is clearly seen in the Figure 4.5 where we look closer to the restart of the furnace in the time-series. All electrical variables reach the steady-state at the end of the shutdown, visualized by the grey area. Due to that the sampling rate is each fifth minute, the response of the electrical variables are not accurately shown in the figure. It is also unknown how the restart is performed. Typically, the furnace is gradually restarted and does not go directly from shutdown to full operation. This is another reason that the responses are not accurate in the plot. It should also be noted that the end of the shutdown is here defined as when the current reaches a value of full operation. Even though the responses are not believed to be accurate in the plot, the plot shows roughly the response of the variables. It can be concluded that the electrical variables use a maximum of 15 minutes to reach the steady-state at restart. The use of maximum is due to that it is unknown if the restart is gradually or not. If the furnace restarts gradually, it is assumed that the electrical variables' response will be faster.

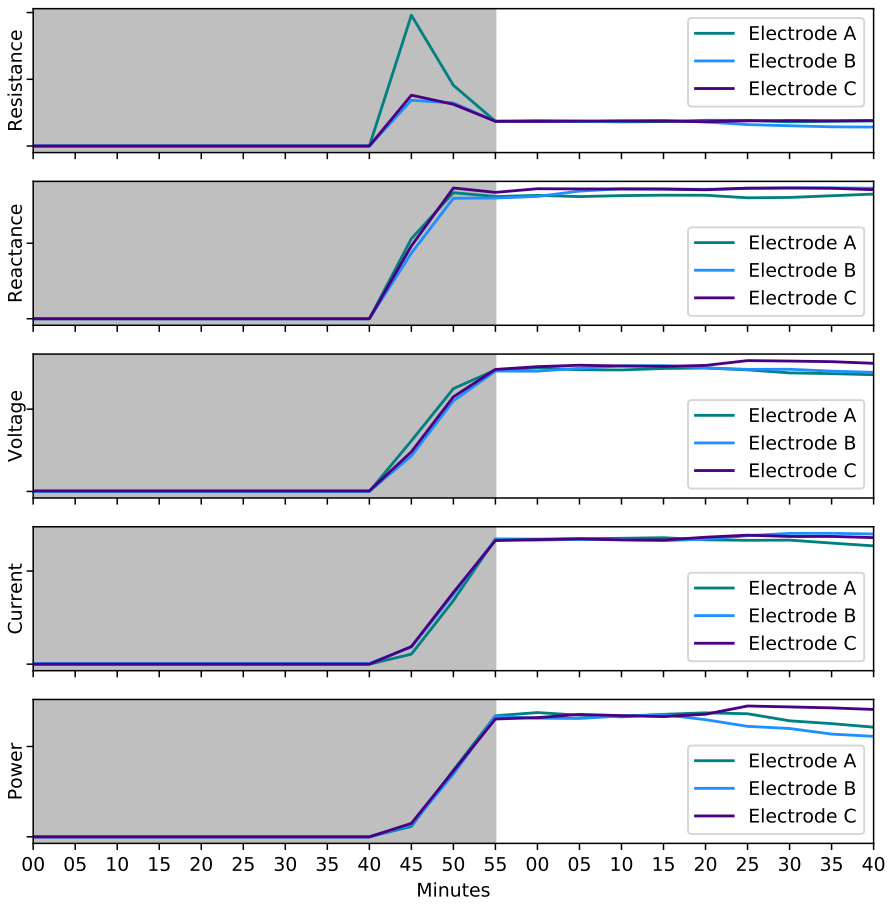

Figure 4.5: The response of the electrical conditions due to the restart of the furnace. The values on the y-axis are removed due to confidentiality.

4.4 Challenges of controlling the furnace

A detailed description of the furnace is presented in the previous sections. The main challenges are underlying in the description, but will in this section addressed. The challenges can be addressed as [11, Chap. 5.1]:

1. It is hard to know the exact condition of the furnace because of limited measurements of the furnace.
2. The processes that occur in the furnace have very long time constants. A change in the charge material takes considerable time before it affects the processes because of the large volume of masses involved.
3. There are long time delays in the system. At a change in the recipe, it takes time

before new materials are weighed out, transported to a furnace hopper, and finally reaches the top of the furnace.

4. The raw materials' properties can vary, and the materials are most often not uniformly distributed in the furnace.

It is the first addressed challenge that drives this project. Several unknown conditions of the furnace would ease the furnace's control by knowing more about the conditions. Important variables such as the electrode position, shape and conductivity of charge material and coke bed, are unknown. These variables give the resistance and conductivity in the furnace and influence the electrical conditions considerably.

A Finite Element Method (FEM) model is presented in the next chapter to gain more knowledge about the conditions of the furnace. The FEM model gives valuable relations between variables in the furnace, which can be used to gain valuable information on the furnace's unknown conditions.

Chapter 5

A Finite Element Method model of the FeMn furnace

In this chapter, a Finite Element Method (FEM) model is presented. The FEM model gives valuable relations between variables in the furnace, which is useful for gaining information about the FeMn furnace. The choice of inputs and outputs of the model are reasoned to give a good representation of the FeMn furnace. An experimental design is made and analyzed to give a representative simulations of the furnace. The database generated will be the foundation for the PLSR models that are presented later in the thesis.

5.1 A brief description of the FEM model

A 3D Finite Element Method (FEM) model was implemented in COMSOL Multiphysics 5.4 with the Magnetic and Electric Fields interface [15]. The low-frequency Maxwell equations are solved using a potential formulation for the equations. The equations are discretized with the finite-element-method using quadratic elements. The model is derived from what is presented in Herland et al. [16]. Figure 5.1 shows the FEM model of the FeMn furnace, where some parts of the model are omitted.

The model is parametrized to describe different conditions (material distributions, material properties, and electrical conditions) in the furnace. The model is static and does, therefore, not capture the transients of the variables. This means that the model, in principle, is calculating the steady-state condition of the variables.

5.1.1 Simplifications of the FeMn furnace

The real FeMn furnace is a system of various dynamics. It has electrical variables with fast dynamics and variables such as material distribution and temperature with slower dynamics. As the FEM model calculates the steady-state of the variables, it ignores how the variables reach the steady-state, it ignores the dynamics. Since most of the output

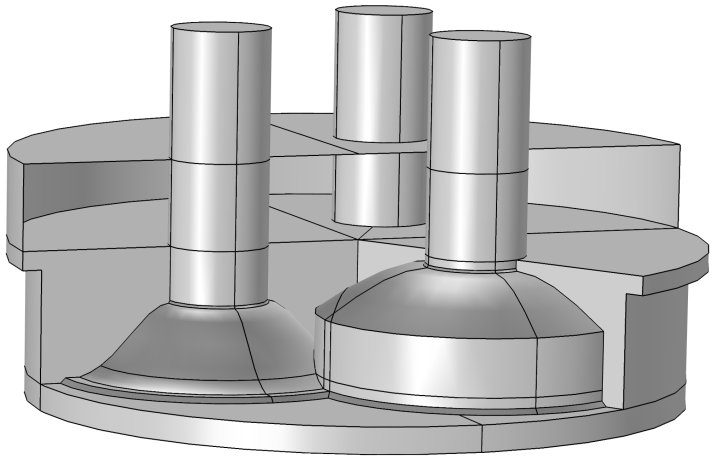

Figure 5.1: The interface of the FEM-model of a FeMn furnace. The three electrodes in the furnace are shown where some part is omitted to shows the different zones. Under the two closest electrodes, the corresponding coke beds are shown with the charge material lying on top.

variables in the FEM model are electrical and have fast dynamics, the FEM model gives a fair estimation.

The FEM model uses several simplifications and disregards many factors in the furnace that are not electrical. The FEM model disregards all thermodynamics, which plays a big part in the conditions in the furnace. For example, it disregards the distribution of materials in the furnace, chemical reactions and other processes in a real FeMn furnace. It also ignores the inputs and outputs of the FeMn furnace. The materials loaded into the furnace and the tapping of the furnace are excluded in the model.

The FEM model simplifies the shape of the furnace. For example, it is known that some lining has eroded over the years, but the model assumes no erosion. The furnace also excludes the tapping holes which influence the electrical conditions. All the simplifications mean that the FEM model is not a perfect representation of the FeMn furnace.

5.2 Digging into the details: the FEM model input

Among the many parameters that can be evaluated in the FEM model, we focused on the investigation of 12 degrees of freedom. That means that it is possible to use 12 different parameters in the calculations of the FEM model. The input parameters are chosen such that the FEM model represents a real furnace as good as possible. The inputs of the model are given in Table 5.1. The table includes 13 variables which exceeds the degrees of freedom. In reality, Shape 1 is equal to Shape 2, so the number of inputs is 12 degrees of freedom. The input parameters are visualized in Figure 5.2.

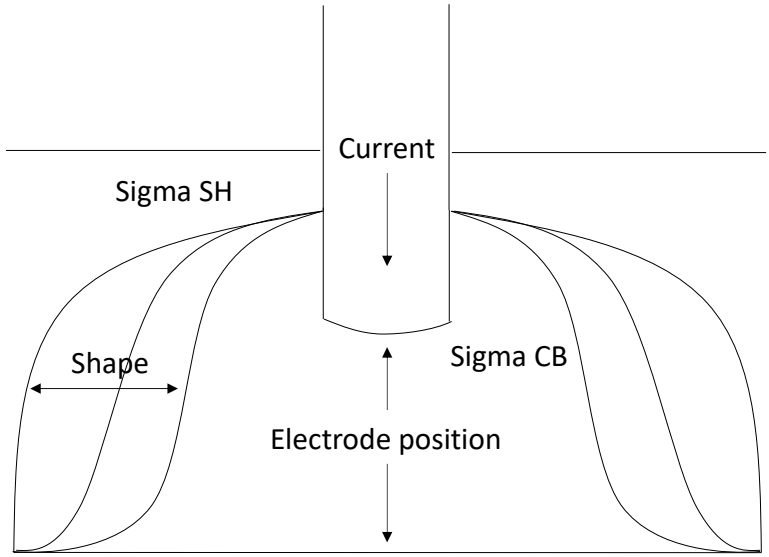

Figure 5.2: The input parameters of the FEM model connected to a electrode. The "Electrode position" gives the distance from the bottom of the furnace to the tip of the electrode. The "Shape" shows how the shape varies from narrow to broad shape. "Sigma CB" gives the conductivity in the coke bed. The current runs through the electrode. "Sigma SH" gives the conductivity in the charge material at the top of the coke bed.

Table 5.1: The input parameters of the FEM-model.

Input parameters	**Definition**
Current El 1, rms (kA)	Current in electrode 1
Current El 2, rms (kA)	Current in electrode 2
Current El 3, rms (kA)	Current in electrode 3
El 1 pos (m)	Height of the electrode 1
El 2 pos (m)	Height of the electrode 2
El 3 pos (m)	Height of the electrode 3
Sigma CB 1 (S/m)	Conductivity of the coke bed zone under electrode 1
Sigma CB 2 (S/m)	Conductivity of the coke bed zone under electrode 2
Sigma CB 3 (S/m)	Conductivity of the coke bed zone under electrode 3
Sigma SH (S/m)	Conductivity of the charge material above the coke beds
Shape 1	Broadness of the coke bed 1
Shape 2	Broadness of the coke bed 2
Shape 3	Broadness of the coke bed 3

5.2.1 Currents

The currents represent each electrode in the input space. By having three independent currents, it gives the advantage to simulate different operational zones in the furnace. In

the furnace, the current goes from one electrode to another, and chooses the path with the least resistance. This means that some of the currents go directly through the charge material, while other currents go through the coke beds, depending on the resistance in the materials.

5.2.2 Electrode positions

The electrodes are excellent conductors compared to the coke bed and the charge. Therefore, the electrode position determines the resistance in the furnace. The higher the electrode position, the larger amount of material the current must pass before reaching the metal pool.

5.2.3 Shapes of the cokebeds

The shapes of the coke beds are the last variables that affect the resistance. The shape decides the amount of coke bed and charge material the current goes through on its way, and therefore gives the resistance. There are many reasons for an uneven shape of the coke beds, for example, segregation of the incoming material, uneven activity in the zones of the coke bed, and tapping procedures.

5.2.4 Conductivity in the cokebeds

The conductivity in the coke beds determines the resistance in the furnace. A high conductivity gives lower resistance and vice versa. By dividing the coke bed into three zones connected to each electrode, it is possible to do simulations without having uniform conductivity in the whole coke bed. Since the coke bed does not have uniform conductivity in the real furnace, this gives a more realistic simulation.

5.2.5 Conductivity in the charge material

The conductivity in the charge material has less impact on the resistance than the conductivity in the coke bed. The reason for this is that the current path mostly goes through the coke beds. As for the conductivity in the coke bed, the conductivity in the charge material is not uniform. Unfortunately, due to the limited number of input parameters, the conductivity in the charge material is set as uniform.

5.3 Outputs and observables: what can we get from the analyzed FEM model?

The outputs of the FEM-model are given in Table 5.2. Most of the variables are electrical conditions, besides the volume of the coke beds that can be calculated since the shape and electrode positions are known. The variables are sectioned into zones that are corresponding to each electrode and as global variables. Electrical variables such as voltage, resistance, reactance, active power, and reactive power are directly connected to the electrode. The rest of the variables are connected to the zone connected to the given electrode.

For example, the steel shell power for electrode 1 is the power in the steel shell closest to electrode 1.

Table 5.2: Output observables of the FEM-model.

Output variables	**Definition**
Average current, rms (kA)	Average current in the electrodes
Tot Resistance (mΩ)	Total resistance
Resistance El. 1 (mΩ)	Resistance in electrode 1
Resistance El. 2 (mΩ)	Resistance in electrode 2
Resistance El. 3 (mΩ)	Resistance in electrode 3
Tot Reactance (mΩ)	Total reactance
Reactance El. 1 (mΩ)	Reactance in electrode 1
Reactance El. 2 (mΩ)	Reactance in electrode 2
Reactance El. 3 (mΩ)	Reactance in electrode 3
Reactive Power tot (MVAr)	Total reactive power below clamps
Active Power tot (MW)	Total active power below clamps
Shell Power tot (MW)	Total active power in the steel shell
Roof Power (MW)	Roof power
Active power El. 1 (MW)	Active power electrode 1
Active power El. 2 (MW)	Active power electrode 2
Active power El. 3 (MW)	Active power electrode 3
Shell power El. 1 (MW)	Active power in steel shell electrode 1
Shell power El. 2 (MW)	Active power in steel shell electrode 2
Shell power El. 3 (MW)	Active power in steel shell electrode 3
Voltage El. 1 (V)	Voltage in electrode 1
Voltage El. 2 (V)	Voltage in electrode 2
Voltage El. 3 (V)	Voltage in electrode 3
Reactive power, El. 1 (MVAr)	Reactive power electrode 1
Reactive power, El. 2 (MVAr)	Reactive power electrode 2
Reactive power, El. 3 (MVAr)	Reactive power electrode 3
Volume CB1 (m^3)	Volume of coke bed around electrode 1
Volume CB2 (m^3)	Volume of coke bed around electrode 2
Volume CB3 (m^3)	Volume of coke bed around electrode 3
Volume CB1 above El1 (m^3)	Volume of coke bed above electrode 1
Volume CB2 above El2 (m^3)	Volume of coke bed above electrode 2
Volume CB3 above El3 (m^3)	Volume of coke bed above electrode 3
Volume CB1 below El1 (m^3)	Volume of coke bed below electrode 1
Volume CB2 below El2 (m^3)	Volume of coke bed below electrode 2
Volume CB1 below El3 (m^3)	Volume of coke bed below electrode 3
Power CB1 (MW)	Power in coke bed 1
Power CB2 (MW)	Power in coke bed 2
Power CB3 (MW)	Power in coke bed 3

5.4 Simulating the system through the FEM model: considerations about the design of the experiments

The FEM model is simulated to generate a database for the data-driven models. Since the database is the "foundation" of the data-driven models, the simulations should be performed to represent the FEM model well. In this way, the data-driven models can represent the FEM model in a good way. Therefore, the experimental design is essential.

The chosen experimental design uses 12 factors at 4 possible levels [2] to cover the wide area of the operation of the furnace. In the first round of FEM calculations, a total of 128 input combinations were simulated. Using this database, PLSR models were built as a representation of the FEM model. The models were proven to be asymmetric, as the database did not give enough information to obtain symmetric models. Asymmetric models make an inaccurate model of the FEM model, which has symmetric properties. The FEM model has a perfect cylinder shell and three electrodes that are placed equidistant from the center of the furnace on an equilateral triangle. This symmetry imposes symmetry in the electrical conditions of the furnace. In the FEM model, if all the input parameters connected to the electrodes are equal, this should impose equal predictions of variables connected to each electrode. For example, the estimates of the voltages are equal if all the inputs are symmetric.

The database was extended to give the PLSR sufficient information for making a symmetric representation of the FEM model. All variables connected to one electrode in the dataset were grouped, and all global variables grouped as an individual group, which gave four groups: "Electrode 1", "Electrode 2", "Electrode 3" and "Global". As the FEM model is symmetric, it does not matter if the data connected to one electrode has the label "Electrode 1", "Electrode 2" or "Electrode 3". By changing the labels of the data connected to the electrodes, this gives 6 permutations. For the 6 permutations, the dataset was extended by 128 simulations, which gives a total of 768 simulations. In this way, symmetric information is included in the dataset, as visualized in Figure 5.3.

5.4.1 An analysis of the distribution of the simulated and the real data

The simulations in Section 5.4 obtained 768 segments of data for each input parameter and output variable. For the real furnace, not all of these parameters and variables are measured, but some are. By comparing the variables of the FEM model that are measured with the measurements available, it can give information on how the simulations cover the furnace's operational area.

The distributions for the simulated and real variables are given in Appendix A. The real variables show the values for August 2019, where all stops of the furnace are filtered out. As the distribution plots for each electrode are very similar, a summary of the distributions is given by electrode A in Figure 5.4. The figure shows that the simulations are covering the right operational area for most of the variables. Most of the simulated data have much broader distributions than the real data. This is because the simulations are designed to cover most of the furnace's operational area, and the industrial furnace is operated to stay in the optimal conditions. The figure shows that the simulated reactances do not cover the same area as the real reactances. It is expected that the simulated reactances have

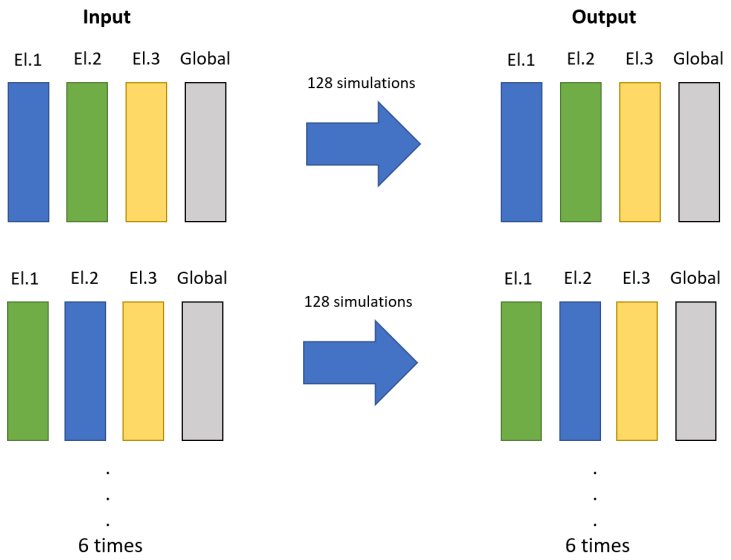

Figure 5.3: Illustration of how the data is grouped to each electrode where two groups are changed a time to make a symmetric database for the PLSR.

smaller values than the real reactances because we are ignoring all the terms coming from the part of the real world that are not covered by the model. For example, the current is modeled into the electrode as if there was a homogeneous perfect contact. In reality, current enter via some flexible copper cables with different geometries depending on the holder position. As the simulated reactances are not in the wanted operational zone for a real furnace, the FEM model can be inaccurate using data corresponding to a real furnace.

An inaccurate calculation of the reactance in the FEM model can introduce problems for the data-driven models that are made based on the simulated data in the upcoming chapters. A metamodel (an approximated model of the FEM model) will calculate the reactance wrongly relative to the real world. The problem is bigger for an inverse metamodel (a model that uses the FEM model's output to predict the input of the FEM model). An error in the reactance input will introduce an error for all estimated variables, depending on the importance of the reactance in the inverse metamodel.

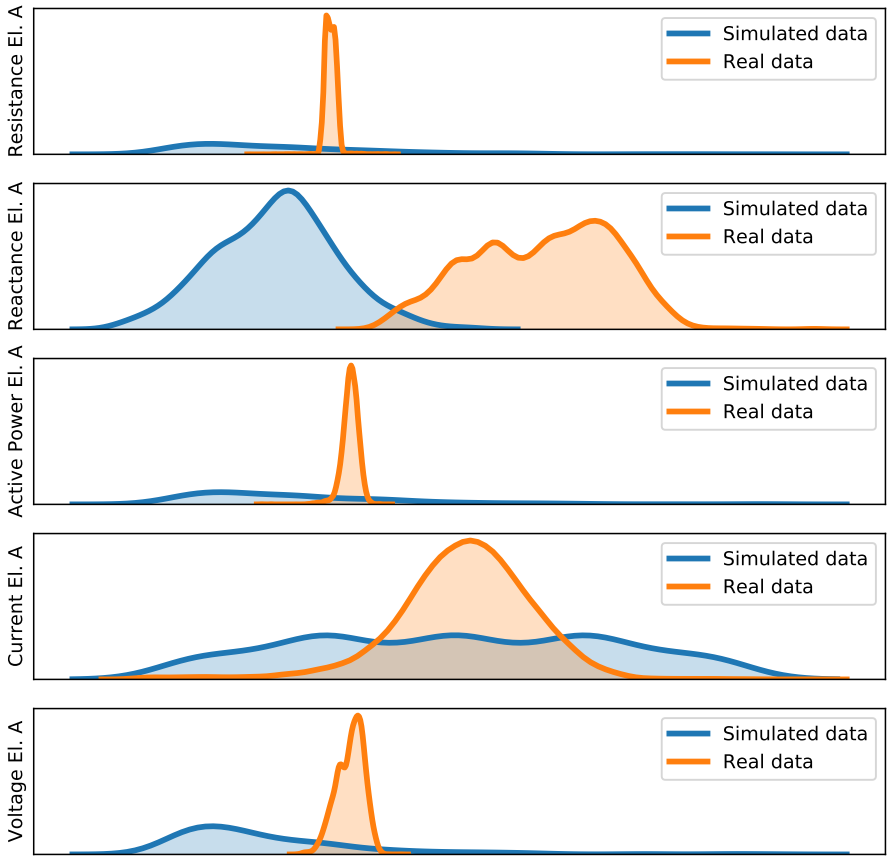

Figure 5.4: The distributions for simulated and real data for electrode A. The values on the axes are removed due to confidentiality.

Chapter 6

Modeling the FEM using a PLSR approach

It has been a goal for NORCE to build a metamodel and inverse metamodel of the FEM model. The metamodel is an estimation of the FEM model, but runs much faster than the FEM model. The inverse metamodel gives the inverse relationship between input and output, which the FEM model is unable to provide. An interface will be made for the models to make it easier for people with different backgrounds to use them. The interfaces can be used as an assistive tool for the operators when making decisions as the models gain information of the furnace. In this way, the models can be used to check if the models correspond to the operator's knowledge. The models can also be used for training purposes, to gain knowledge about the furnace.

6.1 Metamodel of the FEM model

A metamodel of the FEM model was built to obtain a faster and simplified model of the FeMn furnace. The FEM model takes approximately 40 minutes to simulate the results, while the metamodel gives the result in milliseconds. The metamodel was built on the database obtained from the experimental design, as explained in Section 5.4, using PLSR with the $\boldsymbol{X}$ variables as given in Table 5.1 and the $\boldsymbol{Y}$ variables as given in Table 5.2. Without including any extra interaction and square terms, non-linearities were observed for active power, resistance, voltage, and power in the coke bed by plotting the predicted variables against the simulated variables. The variables given for electrode 1 are representable for the other electrodes, and are shown in Figure 6.1. The plot shows that the relation between the predicted and reference is non-linear. The ideal case for the "predicted vs. reference" plots is if the points are fully aligned with the target line given in the plots. This would indeed imply a perfect representation of the data.

Interaction and square effects were added as features in the dataset to obtain a better representation of the FEM model. We recall that an interaction effect corresponds to

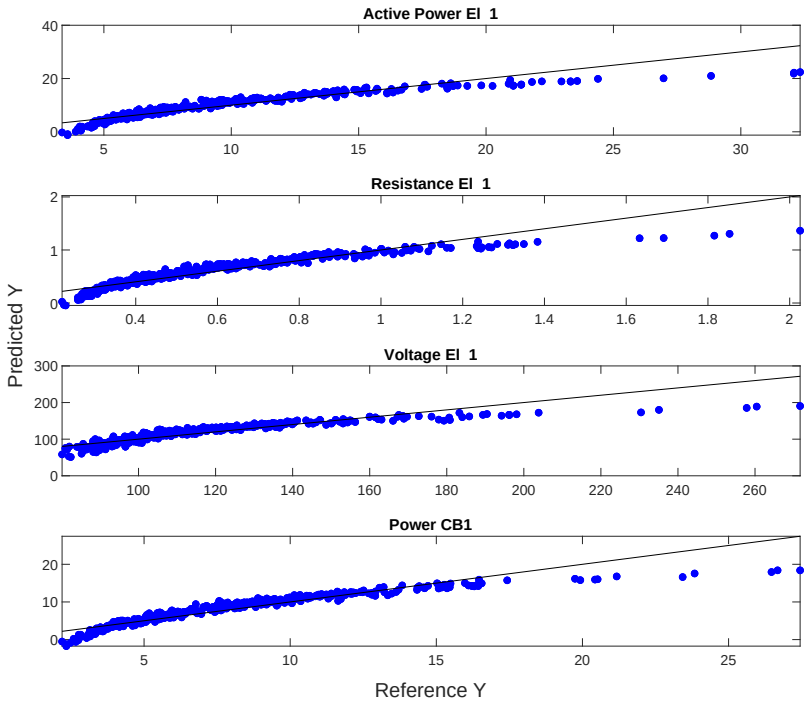

Figure 6.1: The predicted vs. reference plots with calibrated data for active power, resistance, voltage, and power in coke bed connected to electrode 1. The black line shows the target line for the regression. The plots show that the predictions are not aligned with the target line and show a non-linear relation between prediction and reference.

multiplying two variables in the set of inputs (i.e., computing new variables of the type $x_{1,2} = x_1 x_2$). Instead a square effect is an additional variable that is added that corresponds to something in the input set that gets squared (i.e., $x_{1,1} = (x_1)^2$). The interaction and square effects can contain valuable information and give a better fit of the model, especially in the presence. All the interaction and squares of nonlinearities, as we identified above, had some impact in the prediction of $\boldsymbol{Y}$, and were included in the input set. The new input set consists, therefore, of 104 inputs. This resulted in an improved predicted vs. reference plot, as seen in Figure 6.2. Compared to Figure 6.1, the relations are much more linear with the addition of interaction and square effects than without the effects.

The model was validated using leave-one-out cross-validation on the 768 segments for assessing the statistical performance the model will have on unseen data. With 17 components, the model explains 91 % of the variance, as shown in Figure 6.3. The results are given in Table 6.1 and show that the metamodel performance indexes are very good in terms of RMSE and R^2 values. The R^2 value gives a measure of how much of the variance of a variable that is explained by the model. The value ranges from 0 to 1, where

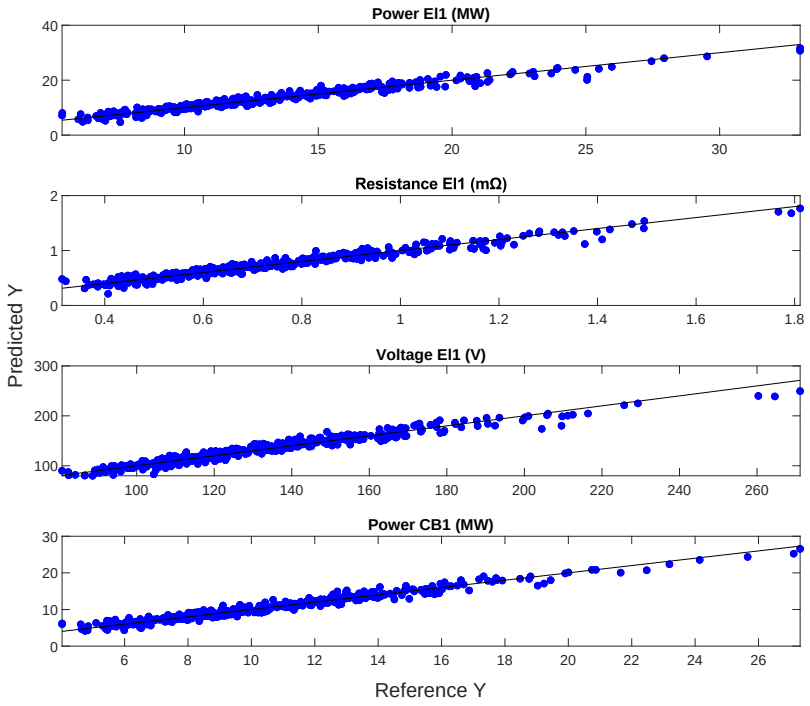

Figure 6.2: The predicted vs. reference plots with calibrated data for active power, resistance, voltage, and power in coke bed connected to electrode 1, when interaction and square effects are added in the input. The plots are aligned with the black target line.

1 is a perfect explained model. A value of R^2 over 0.85 indicates a good fit. The RMSE is the root-mean-square error between predictions by the model and real values. In this way, the measure is related to the unit of the variable, and an intuition of the variable is needed to assess the performance. As seen in Table 6.1, most of the R^2 values are given above 0.85, which indicates a good fit. The exception is the volumes above the electrodes with an R^2 value of 0.79. It could also be mentioned that the voltages have RMSE values of 7.92 $\sqrt{V}$, which is a relative big value given that the mean simulated value is 132 V. Based on the metamodel's overall performance, it can be concluded that it is a sufficiently good representation of the FEM model for our purposes.

Even though the estimator's performance is concluded to be sufficiently good based on the training set, it can be dangerous to introduce too many parameters in the model. A number of 17 components used in the model can lead to overfitting (see Section 3.3.1). Overfitting means that the model fits the training set "too good", in such a way that the model's performance is not generalizable for unseen data. In this way, the results from the training set can give a wrong indication of the model performance. For that reason, the model is tested on an independent test set to assess the performance on unseen data in

Section 6.3.

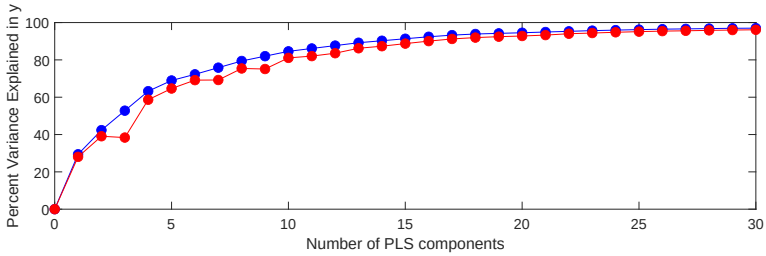

Figure 6.3: The explained variance of the model using leave-one-out cross-validation of the meta-model. The blue line shows the calibrated explained variance and the red line shows the cross-validated explained variance.

6.1.1 Regression coefficients

The weighted regression coefficients give a relative comparison of which $\boldsymbol{X}$ variables that are most important in predicting a given $\boldsymbol{Y}$ variable. High values of a regression coefficient for a given $\boldsymbol{X}$ variable imply that the variable is important in predicting the given $\boldsymbol{Y}$ variable.

The regression coefficients are difficult to visualize due to the large number of square and interaction effects added to the input. Therefore, the regression coefficients for a PLSR model with 10 components where only the squared shapes are added to the input are given in Appendix B with a 95 % confidence interval. For visualizing the concept of the regression coefficients, the regression coefficients for the roof power are given in Figure 6.4. The regression coefficients do not give the exact representation of the coefficients, but gives a representation for the most important coefficients in predicting $\boldsymbol{Y}$. In addition, interaction and square terms that are important for predicting a given $\boldsymbol{Y}$ variable will be presented in the subsections below.

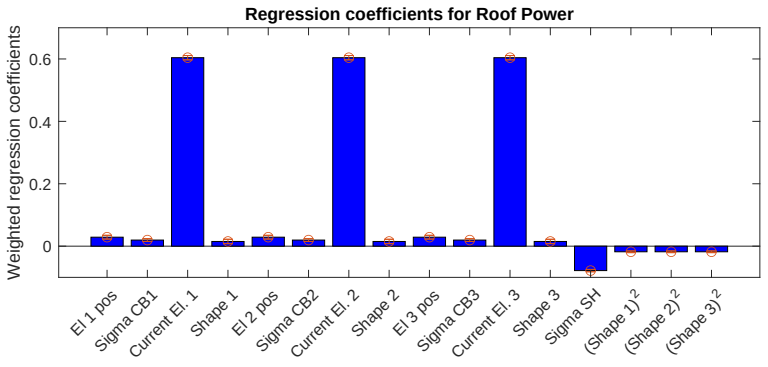

Figure 6.4: Weighted regression coefficients for total roof power. The red bars show the 95 % confidence intervals for the coefficients.

Shell and roof power

The shell and roof power are similar in the regression coefficients. Roof power, which gives the power in the roof's steel shell, is almost a direct function of the currents. The steel shell power, which gives the power in the furnace shell, is also mostly dependent on the current. This makes sense as the power in the steel shell is induced by the currents.

The interaction and square effects are less important than the original input in predicting the roof and shell power, but the sum of the effects contribute significantly. The most important effects for the prediction of shell power consist of variables that are connected to the given electrode. The most important interactions consist of electrode position, current, conductivity and shape the coke beds and conductivity in the charge material. The most important square effects are the electrode position, conductivity and shape of the coke beds for the given electrode squared. This means that all the variables in the input set is important in obtaining a prediction of the shell powers. For the roof power, the only important variables are the currents multiplied with the conductivity in the charge material. This makes sense as the coke beds should not influence the roof power.

Reactive power

The reactive power is the power generated by the magnetic field surrounding the electric current. The most important variable in defining the reactive power is the current for the given electrode. Also, the electrode position and shape of the coke bed for the given electrode have some impact. This is in line with the understanding that reactive power (and reactances) carry information about the current paths. For example, a broad coke bed with high conductivity could be able to conduct part of the currents between electrodes without the current going down into the alloy layer. This should lead to lower power and reactances.

The interaction and square effects are less important than the original input in predicting the reactive power, but the sum of the effects contribute significantly. The most important effects are mostly the variables that are connected to the given electrode. The most important interactions consist of the corresponding electrode position, conductivity and shape of the coke beds. The most important square effects are the shapes and electrodes for the given electrode.

Active power

The active power is the total power minus the power deposited on the steel shell due to induction (eddy currents). Active power depends mostly on the electrode position and the shape and conductivity of the coke bed of the given electrode. Also, the current for the given electrode has an impact on the active power. An expression of the active power can be given by:

$$P = I^2 R, \tag{6.1}$$

where P is the active power, I is the electrode current, and R is the electrode resistance. The electrode position, shape and conductivity of the coke bed give the resistance of the

current path. What is an interesting observation is that the variables that give the resistance are more important than the electrode current.

The interaction and square effects are less important than the original input in predicting the active power, but the sum of the effects contribute significantly. The most important effects are mostly the variables that are connected to the given electrode. The most important interactions consist of the corresponding electrode position, current, shape and conductivity of the coke bed and the conductivity in the charge material. The most important square effects are the electrode position, shape and conductivity of the coke bed squared. This means that all the variables in the input set is important in obtaining a prediction of the active powers.

Power in the coke bed

The weighted regression coefficients for the power in the coke bed are almost identical to the active power as one expect since most of the power is deposited into the coke beds. The coke bed depends mostly on the electrode position and the shape and conductivity of the coke bed for the given electrode. As for the active power, the power in the coke bed have interaction effects between all the original input variables corresponding to the given electrode. The most important square effects are the electrode positions, shape and the conductivity in the coke bed for the given electrode.

Resistance

The weighted regression coefficients for resistance look very similar to the weighted regression coefficients for active power, making sense since the active power is dependent on the resistance. Resistance depends mostly on the electrode position and the shape and conductivity of the coke bed of the given electrode. This can be explained by that the electrode positions give how much mass the current must go through (i.e., the resistance for the current). The shape and conductivity of the coke bed gives the resistivity of the current path.

The interaction and square effects are less important than the original input in predicting the resistance, but the sum of the effects contribute significantly. The most important effects are mostly the variables that are connected to the given electrode. The most important interactions consist of the corresponding electrode position, current, shape and conductivity of the coke bed and conductivity in the charge material. The most important squares are the electrode positions, shape and the conductivity in the coke bed squared. This means that all the variables in the input set is important in obtaining a prediction of the resistances.

Reactance

The reactance has similar regression coefficients as the reactive power. The most significant variables are the current and shape of the coke bed connected to the given electrode. Also, the electrode position for the given electrode and the currents of the two other electrodes have an impact on the reactance.

The square effects are less important than the original input, and none of the interaction effects are very important in the prediction of reactance. The most important square effects are the shapes of the coke beds and electrode positions for the given electrode squared.

Voltage

The voltage has very similar regression coefficients as the active power and resistance. The most important weighted regression coefficients for the voltage are the electrode position, shape, and conductivity of the coke bed connected to the given electrode.

The interaction and square effects are less important than the original input, but the sum of the effects contribute significantly. The most important effects are mostly the variables that are connected to the given electrode. The most important interactions consist of the corresponding electrode position, current, shape and conductivity of the coke bed and conductivity in the charge material. The most important square effects are the electrode positions, shape and the conductivity in the coke bed squared. This means that all the variables in the input set is important in obtaining a prediction of the voltages.

Volumes

The volume of the coke bed is given by the shape of the given coke bed. As the volume is divided into above and below the electrode, they become a function of the electrode position also. The interaction effects are less important than the original input, but the sum of the effects contribute significantly. The most important interactions are between the electrode positions, shapes and conductivity in the coke bed. The square effect of the shape for the given electrode has a relatively big impact on the prediction.

Table 6.1: Performance indexes for the metamodel based on leave-one-out cross-validation on the training set.

	RMSE	$\mathbf{R^2}$
Average Current (kA)	0.5293	0.9731
Active Power tot (MW)	1.7261	0.9642
Reactive Power tot (MVAr)	0.334	0.9679
Shell Power Tot (MW)	0.0058	0.9183
Roof Power (MW)	0.0049	0.7824
Tot Resistance (mΩ)	0.0965	0.9632
Total Reactance (mΩ)	0.0124	0.9465
Active Power El. 1 (MW)	1.1722	0.9388
Reactive Power El. 1 (MVAr)	0.2018	0.9444
Shell Power El. 1 (MW)	0.0025	0.8736
Resistance El. 1 (mΩ)	0.0664	0.9374
Reactance El. 1 (mΩ)	0.0103	0.9263
Voltage El. 1 (V)	7.9167	0.9365
Volume CB1 (m^3)	4.2773	0.9027
Volume CB1 above El. 1 (m^3)	2.1965	0.7919
Volume CB1 below El. 1 (m^3)	3.5279	0.8846
Power CB1 (MW)	0.9459	0.9428
Active Power El. 2 (MW)	1.1722	0.9388
Reactive Power El. 2 (MVAr)	0.2018	0.9444
Shell Power El. 2 (MW)	0.0025	0.8736
Resistance El. 2 (mΩ)	0.0664	0.9374
Reactance El. 2 (mΩ)	0.0103	0.9263
Voltage El. 2 (V)	7.9167	0.9365
Volume CB2 (m^3)	4.2773	0.9027
Volume CB2 above El. 2 (m^3)	2.1965	0.7919
Volume CB2 below El. 2 (m^3)	3.5280	0.8846
Power CB2 (MW)	0.9459	0.9428
Active Power El. 3 (MW)	1.1722	0.9388
Reactive Power El. 3 (MVAr)	0.2018	0.9444
Shell Power El. 3 (MW)	0.0025	0.8736
Resistance El. 3 (mΩ)	0.0664	0.9374
Reactance El. 3 (mΩ)	0.0103	0.9263
Voltage El. 3 (V)	7.9167	0.9365
Volume CB3 (m^3)	4.2773	0.9027
Volume CB3 above El3 (m^3)	2.1965	0.7919
Volume CB3 below El3 (m^3)	3.5279	0.8846
Power CB3 (MW)	0.9459	0.9428

6.2 Inverse metamodel of the FEM model

The inverse metamodel gives the inverse model of the FEM model, i.e., a model that uses the FEM model's output to predict the input of the FEM model. In this way, unknown internal conditions can be predicted. Some of the furnace's internal conditions are unknown and can be valuable to estimate for obtaining more knowledge of the processes occurring in the furnace. As the FEM model itself cannot be inverted, the inverse metamodel can give valuable information about the FEM model's input. The inverse metamodel was built using PLSR with the output given in Table 5.2 as $\boldsymbol{X}$ variables and the input given in Table 5.1 as $\boldsymbol{Y}$ variables. As for the metamodel, the database given in Section 5.4 was used. The model is validated using leave-one-out cross-validation on the 768 segments for assessing the statistical performance that the model would have on unseen data. With 23 components, the model explains 92 % of the variance, as shown in Figure 6.5. Square effects of the coke bed's volume below and above the electrodes and the coke bed's total volume were added to the input set to obtain a better fit for the model. Other square terms had little impact on the prediction, and by leaving them out, a better fit was obtained for the model. The interaction effects were excluded because of the large number of interactions, and the loss of interpretability by using the interaction effects.

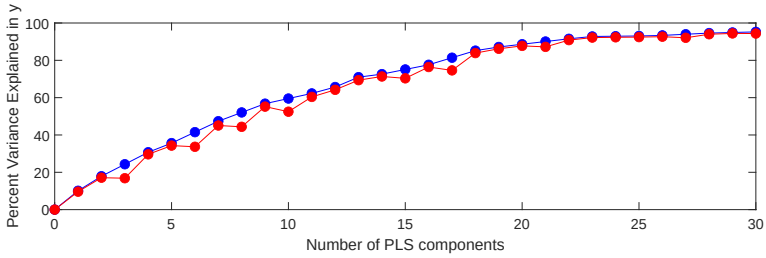

Figure 6.5: The explained variance of the inverse metamodel using leave-one-out cross-validation of the PLSR model. The blue line shows the calibrated explained variance, and the red line shows the cross-validated explained variance.

Figure 6.6 gives the calibrated predicted vs. reference plots for the variables connected to electrode 1 and the conductivity in the charge material. The variables connected to electrode 1 are representable for the two other electrodes. The plot visualizes the fit of the model, and shows that the points are fairly aligned with the black target line. It also shows that there is a small amount of reference values due to the experimental design. This can make it more challenging to obtain a good fit for the variables.

Table 6.2 shows the performance of the inverse metamodel is given by the performance indexes RMSE and R^2. The R^2 gives a measure of the fit and ranges from 0 to 1, where 1 is a perfect fit by the model. The RMSE gives the root-mean-square error between the model and the real values and is related to the unit of the variables. The performance indexes are given in Table 6.2 and show generally good results for the different variables. All the variables have an R^2 value above 0.80, which is a good fit. The best predicted variables are the currents and shape of the coke beds with a R^2 value close to 1.

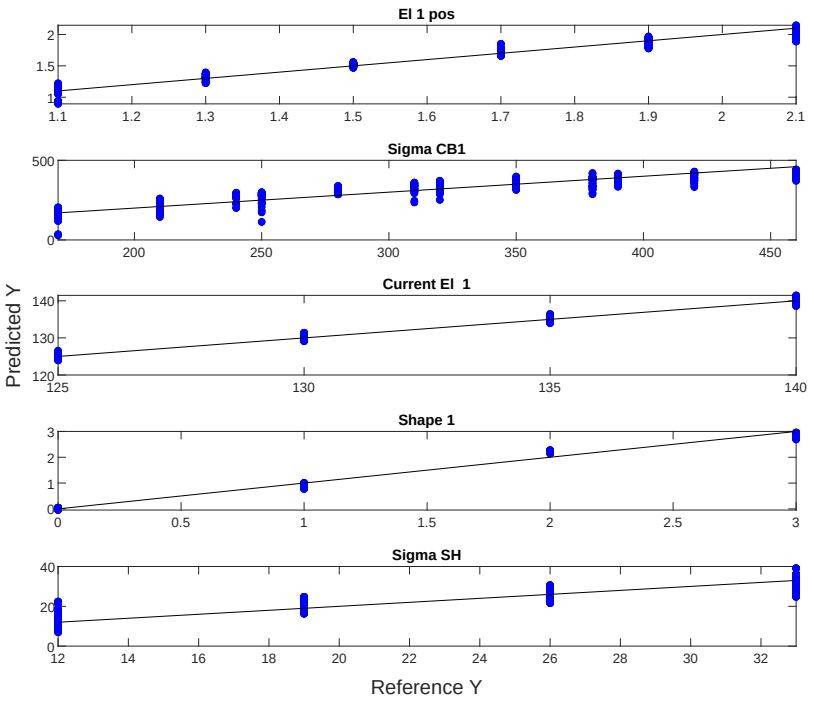

Figure 6.6: Predicted vs. reference plots with calibrated data for electrode position, conductivity in the coke bed, current and shape of the coke bed connected to electrode 1, and conductivity in the charge material when square effects are added in the input. The plots are aligned with the black target line.

6.2.1 Regression coefficients

The weighted regression coefficients for the inverse metamodel are given in Appendix C with a 95 % confidence interval. The weighted regression coefficients show the relative importance of the $\boldsymbol{X}$ variables in predicting a given $\boldsymbol{Y}$ variable.

Electrode position

The most important weighted regression coefficients in predicting electrode position are the volume below and above the electrode position. This makes sense as it is the electrode position that splits the volume into the volumes below and above the electrode. The added square effects of the volume variables connected to the given electrode have also a big impact on the prediction. Unfortunately this relation is not useful in the real world as it unveil only a trivial relation imposed by construction.

Table 6.2: Performance indexes for the inverse metamodel based on leave-one-out cross-validation on the training set.

	RMSE	$\mathbf{R^2}$
El 1 pos (m)	0.0604	0.9468
Sigma CB1 (S/m)	38.0333	0.7989
Current El. 1 (kA)	0.5541	0.9902
Shape 1	0.1469	0.9827
El 2 pos (m)	0.0604	0.9468
Sigma CB2 (S/m)	38.0333	0.7989
Current El. 2 (kA)	0.5541	0.9902
Shape 2	0.1469	0.9827
El 3 pos (m)	0.0604	0.9468
Sigma CB3 (S/m)	38.0333	0.7989
Current El. 3 (kA)	0.5541	0.9902
Shape 3	0.1469	0.9827
Sigma SH (S/m)	3.2407	0.8285

Conductivity in the coke bed

The coke bed's conductivity depends mostly on the volume above and below the given electrode and the electrical variables as active power, resistance, reactance, voltages, and power in the coke bed connected to the given electrode. The added square effects of the volume variables connected to the given electrode also have big impact on the prediction.

Current

The current depends on most of the electrical variables in the furnace, where the most important variables are the reactive power and the reactance for the given electrode.

Shape of coke bed

The weighted regression coefficients show that the shape is given by the three volume variables, total volume, and the volume below and above the electrode. The square terms of the volume variables connected to the given electrode have also a big impact on the prediction.

Conductivity in the charge material

The conductivity in the charge material is given by all variables except the active power, resistance, and shell power. The most important variable is the total reactance. That the active power and resistance have little impact on the conductivity in the charge material is most likely due to the current mostly goes through the coke bed and not the charge material.

6.2.2 Problem with the dynamics

Section 5.1.1 explains that the FEM model disregards the dynamics of the FeMn furnace as the FEM model is static and only calculates the steady-state of the furnace. Further, it was explained that it is a fair approximation since the FEM model's outputs have fast dynamics. In the case of the inverse metamodel, the output, $\boldsymbol{Y}$, represents the input of the FEM model given in Table 5.1, and the input of the FEM model, $\boldsymbol{X}$, is the output of the FEM model in Table 5.2. This means that the FEM model has different output variables than the inverse metamodel, which introduces a problem. The dynamics of the output of the inverse metamodel contains variables that have slower dynamics than the output of the FEM model. For example, the electrode's consumption, the conductivity and shape of the coke beds are believed to have slower dynamics than the electrical variables. Also, the electrode positions have limitations in the change of holder position and slipping rate. This means that the static inverse metamodel may have a problem in estimating the output variables accurately as the inverse metamodel does not describe how the variables reach the steady-state; it just provides the steady-state value. If the input is changed rapidly before a variable has reached a steady-state, the estimation will be off.

Figure 6.7 illustrates the problem with a static model. When the input is changed at $t = 0$, the static estimator immediately goes to steady-state on the change of input. A real first-order response will, though, react much slower and take longer to reach the steady-state. This approximation is dependent on the units of the time-axis. If the unit is given in seconds, this can be a fair approximation, while the approximation will be worse if the units are given in hours. Section 4.3 shows that the electrical variables used a maximum of 15 minutes to reach the steady-state, while a case for a temperature variable used 16 hours and 50 minutes to reach the steady-state. Most of the inverse metamodel's outputs are believed to have time constants somewhere near the temperature variables. The only variables that have fast dynamics are the currents. Therefore, the estimation can be off for conductivity of coke beds and charge material, shapes of the coke beds, and electrode position. For the currents, the estimation is believed to be more accurate.

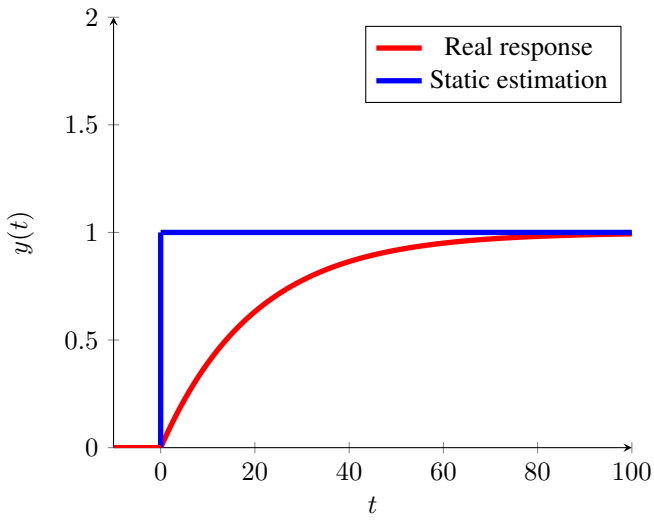

Figure 6.7: The response of a static model and a dynamic 1. order system where a step function is given as input.

6.3 Assessing the performance of the metamodel and inverse metamodel using unseen data

The model orders of the metamodel and inverse metamodel were chosen based on leave-one-out cross-validation. The performance indexes from the cross-validation indicates the statistical performance on new unseen data. New data have been simulated to make a stronger assessment of the models. The simulations are performed using the same design of experiment as given in Section 5.4. New combinations of the input data are used to obtain new simulated data that have not been used in training. Still, the same four levels for the input parameters are used. In this way, the models can be evaluated on new unseen data in the same range as they have been trained on. 32 simulations were performed, where the dataset was extended symmetrically, to obtain 192 samples.

6.3.1 Results from assessing the metamodel on unseen data

To assess how the metamodel selected in Section 6.1 perform on new unseen data, the model has been tested on a test set. The test set contains 192 samples, which have not been used in the training of the model. The same performance indexes as in Section 6.1, R^2 and RMSE, are used to have a comparable result. The performance of the metamodel on the test set can be seen in Table 6.3. Comparing with the cross-validated result in Table 6.1, the performance drops some, but not significantly. A reason why the model performance is better on the training set than on the test set, can be due to that the model is overfitted to the training set. Overfitting can be explained by that the model is describing the limited number of training samples very well, but the fit is not generalizable for other

data points. To avoid overfitting, the number of components used in the model can be reduced. It is tough expected that the performance will be slightly better for the training set. As for this case, the reduction in performance is not very big, and the model can be concluded to perform well on unseen data.

Figure 6.8 shows the simulated $\boldsymbol{Y}$ (reference Y) from the test set plotted against the predicted $\boldsymbol{Y}$ using the metamodel obtained in Section 6.1 for the variables connected to electrode 1. As the test set is symmetric, the corresponding plots for electrode 2 and 3 will be the same. Most of the variables are fairly aligned with the optimal target line, which indicates a good fit. To have a perfect fit, all the points should be on the target line. For shell power and the volume of the coke beds variables, there is a deviation from the target line. This corresponds with the performance indexes in Table 6.3, where the same variables have the lowest performance indexes. This means that the prediction of these variables is more uncertain than the other variables.

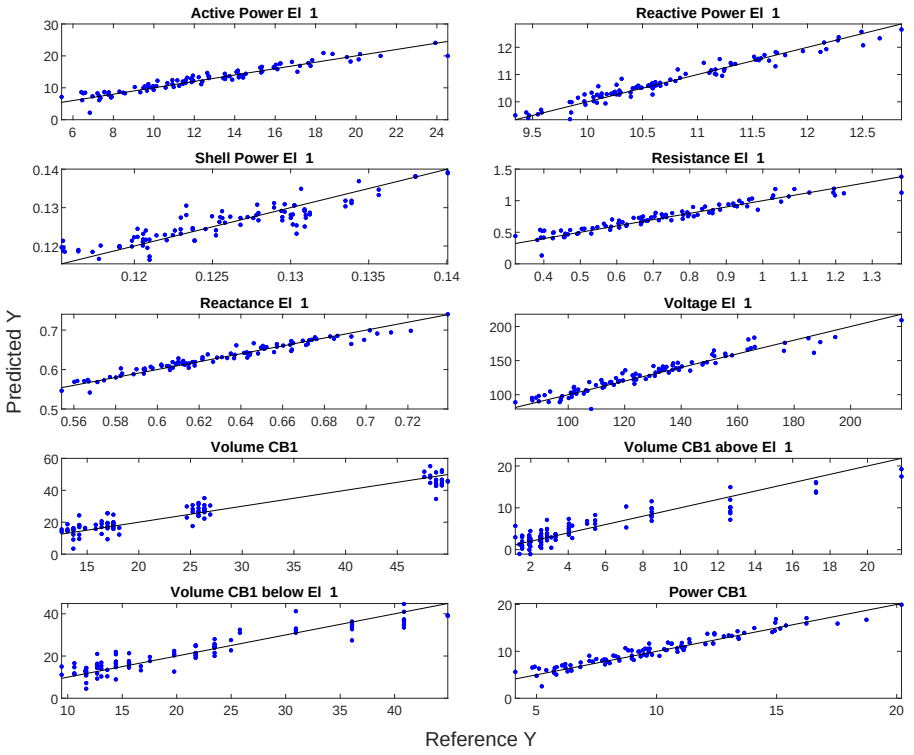

Figure 6.8: The reference vs. predicted plots for variables connected to electrode 1 using the metamodel on the test set.

6.3.2 Results from assessing the inverse metamodel on unseen data

As for the metamodel, the inverse metamodel performance is assessed on the same test set. The test set contains 192 samples, which have not been used in the training of the model. The same performance indexes as in Section 6.2, R^2 and RMSE, are used to have a comparable result. The performance of the inverse metamodel on the test set can be seen in Table 6.4. Comparing with the cross-validated result in Table 6.2, the performance for most of the variables are improved. This indicates that the model order is well selected for the inverse metamodel. The model is therefore proven to be generalizable for unseen data points without loss of accuracy.

Figure 6.9 shows the real $\boldsymbol{Y}$ (reference Y) from the test set plotted against the predicted $\boldsymbol{Y}$ using the inverse metamodel obtained in Section 6.2 for the variables connected to electrode 1 and the conductivity in the charge material. As the test set is symmetric, the corresponding plots for electrode 2 and 3 will be the same. The plot looks very similar to the Figure 6.6, which gives the reference vs. predicted plot for the training set. This indicates a good performance, and is in line with that the performance indexes of the test set, given in Table 6.4, are much the same as the performance indexes obtained in training, given in Table 6.2.

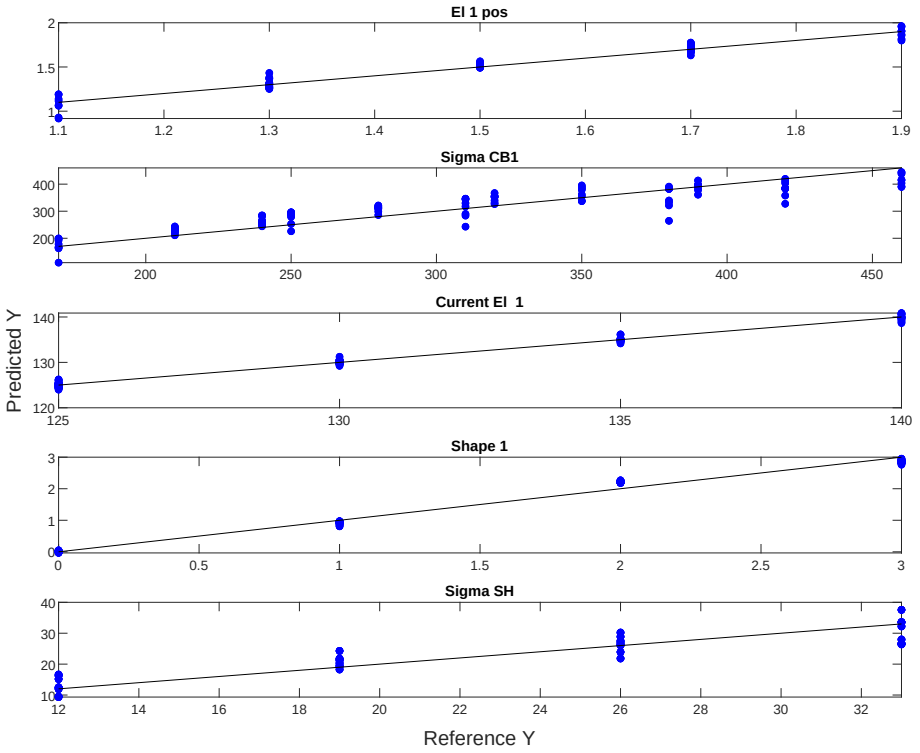

Figure 6.9: The reference vs. predicted plots for variables connected to electrode 1 using the inverse metamodel on the test set.

Table 6.3: Performance indexes for the metamodel on the test set.

	RMSE	$\mathbf{R^2}$
Average Current (kA)	0.6882	0.9328
Active Power tot (MW)	1.7749	0.9485
Reactive Power tot (MVAr)	0.2958	0.9643
Shell Power Tot (MW)	0.0063	0.8599
Roof Power (MW)	0.0049	0.7086
Tot Resistance (mΩ)	0.0951	0.9547
Total Reactance (mΩ)	0.0104	0.9645
Active Power El. 1 (MW)	1.1964	0.9145
Reactive Power El. 1 (MVAr)	0.1788	0.9511
Shell Power El. 1 (MW)	0.0026	0.8115
Resistance El. 1 (mΩ)	0.0689	0.9155
Reactance El. 1 (mΩ)	0.0094	0.9454
Voltage El. 1 (V)	7.4541	0.9248
Volume CB1 (m^3)	4.2519	0.9039
Volume CB1 above El. 1 (m^3)	1.8704	0.8470
Volume CB1 below El. 1 (m^3)	3.5698	0.8747
Power CB1 (MW)	0.9239	0.9231
Active Power El. 2 (MW)	1.1964	0.9145
Reactive Power El. 2 (MVAr)	0.1788	0.9511
Shell Power El. 2 (MW)	0.0026	0.8115
Resistance El. 2 (mΩ)	0.0689	0.9155
Reactance El. 2 (mΩ)	0.0094	0.9454
Voltage El. 2 (V)	7.4541	0.9248
Volume CB2 (m^3)	4.2519	0.9039
Volume CB2 above El. 2 (m^3)	1.8704	0.8470
Volume CB2 below El. 2 (m^3)	3.5698	0.8747
Power CB2 (MW)	0.9239	0.9231
Active Power El. 3 (MW)	1.1964	0.9145
Reactive Power El. 3 (MVAr)	0.1788	0.9511
Shell Power El. 3 (MW)	0.0026	0.8115
Resistance El. 3 (mΩ)	0.0689	0.9155
Reactance El. 3 (mΩ)	0.0094	0.9454
Voltage El. 3 (V)	7.4541	0.9248
Volume CB3 (m^3)	4.2519	0.9039
Volume CB3 above El3 (m^3)	1.8704	0.8470
Volume CB3 below El3 (m^3)	3.5698	0.8747
Power CB3 (MW)	0.9239	0.9231

Table 6.4: Performance indexes for the inverse metamodel on the test set.

	RMSE	$\mathbf{R^2}$
El 1 pos (m)	0.0472	0.9512
Sigma CB1 (S/m)	34.6859	0.8327
Current El. 1 (kA)	0.5201	0.9910
Shape 1	0.1393	0.9845
El 2 pos (m)	0.0472	0.9512
Sigma CB2 (S/m)	34.6859	0.8327
Current El. 2 (kA)	0.5201	0.9910
Shape 2	0.1393	0.9845
El 3 pos (m)	0.0472	0.9512
Sigma CB3 (S/m)	34.6859	0.8327
Current El. 3 (kA)	0.5201	0.9910
Shape 3	0.1393	0.9845
Sigma SH (S/m)	3.2393	0.8287

6.4 Interfaces

An interface has been implemented in Microsoft Excel to make it easier to use the metamodel and the inverse metamodel. Since the models gain information regarding the furnace, it can be used as an assistive tool for the operators when making decisions. In this way, the models can be used to check if the models correspond to the operators' knowledge. The models can also be used for training purposes, for exploring and gaining knowledge about the furnace.

An estimation of the $\boldsymbol{Y}$ variables is automatically generated by inserting values for the $\boldsymbol{X}$ variables. A prediction interval with a 95 % confidence level is included in the interface. The prediction interval is given by the Equation 3.11 and gives a measure of the quality of the prediction and gives an intuition of how reliable the prediction is.

Metamodel								
Input								
Variables	**El. 1**		**El. 2**		**El. 3**		**Global**	
Position	1,30		1,30		1,30		-	
Sigma CB	260		260		260		-	
Shape CB	1,9		1,9		1,9		-	
Current	103 %		103 %		103 %		-	
Sigma SH	-		-		-		19	
Output								
Variables	**El. 1**		**El. 2**		**El. 3**		**Global**	
	Prediction	**(+/-) 95 % PI**	**Prediction**	**(+/-) 95 % PI**	**Prediction**	**(+/-) 95 % PI**	**Prediction**	**(+/-) 95 % PI**
Power (MW)	111 %	3 %	111 %	3 %	111 %	3 %	111 %	1 %
Reactive Power (MW)	105 %	1 %	105 %	1 %	105 %	1 %	105 %	0 %
Shell Power (MW)	0,13	0,00	0,13	0,00	0,13	0,00	0,40	0,00
Roof Power (MW)	-	-	-	-	-	-	0,20	0,00
Resistance (mΩ)	108 %	3 %	108 %	3 %	108 %	3 %	108 %	1 %
Reactance (mΩ)	99 %	1 %	99 %	1 %	99 %	1 %	99 %	0 %
Voltage (V)	97 %	2 %	97 %	2 %	97 %	2 %	-	-
Volume CB (m^3)	16,59	2,26	16,59	2,26	16,59	2,26	-	-
Volume CB above (m^3)	1,94	1,82	1,94	1,82	1,94	1,82	-	-
Volume CB below (m^3)	14,65	2,05	14,65	2,05	14,65	2,05	-	-
Power CB (MW)	11,31	0,34	11,31	0,34	11,31	0,34	-	-

Figure 6.10: The interface for the metamodel. The input and output variables are grouped to the belonging electrode and global. The predictions are given with a 95 % prediction interval. Some of the values are given as a percentage of a not given reference value due to that the information is classified.

Inverse Metamodel

Input

Variables	El. 1	El. 2	El. 3	Global
Average Current (kA)	-	-	-	103 %
Power (MW)	102 %	102 %	102 %	102 %
Reactive Power (MW)	104 %	104 %	104 %	104 %
Shell Power (MW)	0,13	0,13	0,13	0,4
Roof Power (MW)	-	-	-	0,2
Resistance (mΩ)	100 %	100 %	100 %	100 %
Reactance (mΩ)	100 %	100 %	100 %	99 %
Voltage (V)	91 %	132,4	132,4	-
Volume CB (m^3)	16,9	16,9	16,9	-
Volume CB above (m^3)	3,4	3,4	3,4	-
Volume CB below (m^3)	13,5	13,5	13,5	-
Power CB (MW)	10,7	10,7	10,7	-

Output

Variables	El. 1		El. 2		El. 3		Global	
	Prediction	(+/-) 95 % PI	Prediction	(+/-) 95 % PI	Prediction	(+/-) 95 % PI	Prediction	(+/-) 95 % PI
Position	1,31	0,03	1,31	0,03	1,31	0,03	-	-
Sigma CB	296,04	32,96	296,04	32,96	296,04	32,96	-	-
Current	102 %	0 %	102 %	0 %	102 %	0 %	-	-
Shape CB	2,14	0,04	2,14	0,04	2,14	0,04	-	-
Sigma SH	-	-	-	-	-	-	20,45	2,62

Figure 6.11: The interface for the inverse metamodel. The input and output variables are grouped to the belonging electrode and global. The predictions are given with a 95 % prediction interval. Some of the values are given as a percentage of a not given reference value due to that the information is classified.

6.5 Numerical examples of the metamodel and inverse metamodel

For demonstrating the performance of the metamodel and inverse metamodel one case of input parameters as given in Table 6.5, was simulated by the FEM model and the metamodel. The models have not seen the data before, and can be seen as a simple validation of the models. A more thorough validation has been done in section 6.3, where a larger amount of data was used. It should be noted that this is only one case, and one should be careful not to over-analyze the results from one simulation.

Table 6.5: Input case for simulation. The current is given as a percentage of a not given reference value due to that the information is classified.

Input	Case 1		
	El. 1	El. 2	El. 3
Current	103 %	103 %	103 %
Electrode position (m)	1.30	1.30	1.30
Sigma CB (S/m)	260	260	260
Shape	1.9	1.9	1.9
Sigma SH (S/m)		19	

The results from simulating the Case 1 in Table 6.5 for the FEM model and the metamodel are shown in Table 6.6. The overall estimation of the case is generally good, with some deviations on some of the variables. It is important to see the error in estimation with respect to the real value. For example, the error on the active power for the electrodes is 9.85 %, while the error on the voltage for the electrodes is 5.82 % with respect to the real values. From the results in Table 6.1 and 6.3, it is known that the shell powers are one of the variables that have the lowest performance indexes. Nevertheless, as the value of the shell powers are low and show only two decimals, the result seems perfect.

Table 6.6: Comparing the FEM model and the direct Metamodel results. Some of the values are given as a percentage of a not given reference value due to classified information.

	Case 1					
	FEM model			**Metamodel**		
Average current (kA)	103 %			103 %		
Total Active Power (MW)	102 %			111 %		
Total Reactive Power (MW)	105 %			105 %		
Total Shell Power (MW)	0.40			0.40		
Total Roof Power (MW)	0.20			0.20		
Total Resistance (mΩ)	100 %			108 %		
Total Reactance (mΩ)	99 %			99 %		
	El. 1	El. 2	El. 3	El. 1	El. 2	El. 3
Active Power (MW)	102 %	102 %	102 %	112 %	112 %	112 %
Reactive Power (MW)	104 %	104 %	104 %	105 %	105 %	105 %
Shell Power (MW)	0.13	0.13	0.13	0.13	0.13	0.13
Resistance (mΩ)	100 %	100 %	100 %	108 %	108 %	108 %
Reactance (mΩ)	100 %	100 %	100 %	98 %	98 %	98 %
Voltage	91 %	91 %	91 %	97 %	97 %	97 %
Volume CB (m^3)	16.9	16.9	16.9	16.6	16.6	16.6
Volume CB above (m^3)	3.4	3.4	3.4	1.9	1.9	1.9
Volume CB below (m^3)	13.5	13.5	13.5	14.7	14.7	14.7
Power CB (MW)	10.7	10.7	10.7	11.3	11.3	11.3

The results from simulating the output of the FEM given in Table 6.6 with the inverse metamodel compared with the input of the FEM model are given in Table 6.7. As given by the performance indexes in Table 6.2, it is the conductivity in the coke bed that is the most uncertain prediction. The rest of the prediction are relatively good.

Table 6.7: Comparing the FEM model and Direct Metamodel results. Some of the values are given as a percentage of a not given reference value due to classified information.

	Case 1					
	Real input			**Inverse metamodel**		
	El. 1	El. 2	El. 3	El. 1	El. 2	El. 3
Current (kA)	103 %	103 %	103 %	102 %	102 %	102 %
Electrode position (m)	1.3	1.3	1.3	1.29	1.29	1.29
Sigma CB (S/m)	260	260	260	284.2	284.2	284.2
Shape	1.9	1.9	1.9	1.9	1.9	1.9
Sigma SH (S/m)		19			19.9	

6.6 Suggested improvement for the metamodel and inverse metamodel

The are other measures that can be done in order to possibly improve the metamodel and inverse metamodel. The first thing, is that the $\boldsymbol{Y}$ variables can be modeled independently, a method called PLS1. In our case, the $\boldsymbol{Y}$ variables have been modeled all together, also called PLS2. By using the PLS1 approach, the model may give a better fit, but the PLS2 approach is much more practical when there is a lot of $\boldsymbol{Y}$ variables, as in this thesis. By using the PLS1 approach gives the opportunity to use a different number of components, and use different interaction and square effects for each $\boldsymbol{Y}$ variable.

In Section 6.3, the models have been assessed using a test set. This set has not been used in the training of the models, and therefore indicates the performance of the models on unseen data. This test set can also be used to get a better fit of the model. By selecting all the points in the test set that the model predicts poorly, and adding them to the training set, the performance of the models can be improved in this area. This can be done iteratively with different test sets to obtain a better model.

Chapter 7

Modeling the FEM model using a PLSR approach with a limited number of variables

In this chapter, an estimator of unknown internal conditions is made based on the simulations from the FEM-model using PLSR. In this case, only variables that are measured are used as inputs of the estimator. This is to obtain an estimator that predicts in real-time using purely measured variables and not any parameters. In this way, a prediction of unknown variables can be obtained at each sampling instant. An accurate estimator can be used as an assistive tool for the operators, and possibly be implemented in the control system for better control of the furnace. In this chapter, we will no longer link input to the output and vice versa, as in a metamodel and inverse metamodel. We will look into interesting measurements independent of if the variables are in the input or output space in the FEM model. That is why we will now call the PLSR model for an estimator and not metamodel or inverse metamodel.

7.1 Building an estimator based on only available measurements as input

This section will use only available measurements as the $\boldsymbol{X}$ variables to build an estimator using PLSR. The reason for using only available measurements as the inputs is to do real-time estimations using real data. In this way, it is possible to see how a model based on the FEM model performs on real data. $\boldsymbol{X}$ and $\boldsymbol{Y}$ variables are selected, and the performance of the estimator is analyzed.

7.1.1 Variable selection for the estimator

The FEM model has a defined input space (Table 5.1) and an output space (Table 5.2) generated from simulations. The input space consists of variables that are valuable to estimate. However, in the output space, some variables are also valuable to estimate – volume and power in the coke beds and the electrode voltages. The voltages are valuable to estimate in the sense that the voltage measurement is regarded as an inaccurate measurement. This introduces the idea to use all variables that are valuable to estimate in the $\boldsymbol{Y}$ set of PLSR model. The variables in $\boldsymbol{Y}$ can be found in Table 7.1.

Table 7.1: $\boldsymbol{Y}$ variables of the estimator.

Variables	**Definition**
El 1 pos (m)	Height of the electrode 1
El 2 pos (m)	Height of the electrode 2
El 3 pos (m)	Height of the electrode 3
Sigma CB 1 (S/m)	Conductivity of the coke bed zone under electrode 1
Sigma CB 2 (S/m)	Conductivity of the coke bed zone under electrode 2
Sigma CB 3 (S/m)	Conductivity of the coke bed zone under electrode 3
Sigma SH (S/m)	Conductivity of the charge material above the coke beds
Shape 1	Broadness of the coke bed 1
Shape 2	Broadness of the coke bed 2
Shape 3	Broadness of the coke bed 3
Steel Shell Power (MW)	Total steel shell power
Shell Power El. 1 (MW)	Steel shell power in the zone around electrode 1
Shell Power El. 2 (MW)	Steel shell power in the zone around electrode 2
Shell Power El. 3 (MW)	Steel shell power in the zone around electrode 3
Volume below El. 1 (m^3)	Volume of coke bed zone around electrode 1
Volume below El. 2 (m^3)	Volume of coke bed zone around electrode 2
Volume below El. 3 (m^3)	Volume of coke bed zone around electrode 3
Power CB1 (MW)	Power in the coke bed zone around electrode 1
Power CB2 (MW)	Power in the coke bed zone around electrode 2
Power CB3 (MW)	Power in the coke bed zone around electrode 3
Voltage (V)	Voltage in electrode 1
Voltage (V)	Voltage in electrode 2
Voltage (V)	Voltage in electrode 3

For the estimation of the $\boldsymbol{Y}$ variables, it is needed to select variables in the $\boldsymbol{X}$ set in the PLSR. Today, the variables in Table 5.2 that are available in a real furnace are resistance, reactance, active power, voltage, and current. Since the voltage is known to be an inaccurate measurement in a real furnace, the voltage is excluded in the $\boldsymbol{X}$ set. This is leading to the $\boldsymbol{X}$ variables given in Table 7.2.

Table 7.2: $\boldsymbol{X}$ variables of the estimator.

Variables	Definition
Resistance El. 1 (mΩ)	Resistance in electrode 1
Resistance El. 2 (mΩ	Resistance in electrode 2
Resistance El. 3 (mΩ)	Resistance in electrode 3
Reactance El. 1 (mΩ)	Reactance in electrode 1
Reactance El. 2 (mΩ)	Reactance in electrode 2
Reactance El. 3 (mΩ)	Reactance in electrode 3
Active power El. 1 (MW)	Active power electrode 1
Active power El. 2 (MW)	Active power electrode 2
Active power El. 3 (MW)	Active power electrode 3
Current El. 1 (kA)	Electrode 1 current
Current El. 2 (kA)	Electrode 2 current
Current El. 3 (kA)	Electrode 3 current

7.1.2 Modeling the estimator

A new estimator has been built using PLSR with the variables in Table 7.2 as $\boldsymbol{X}$, and the variables in Table 7.1 as $\boldsymbol{Y}$. The model is validated using leave-one-out cross-validation on the 768 segments for assessing the statistical performance that the model would have on unseen data. With 9 components, the model covers 75 % of the variance, as seen in Figure 7.1. Interaction and square effects were tested without any significant improvements in the performance indexes.

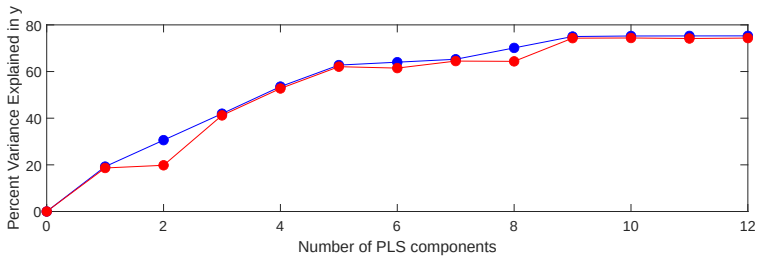

Figure 7.1: Explained variance using leave-one-out cross-validation of the PLSR model built with $\boldsymbol{X}$ variables from the FEM model that is also available in for the real furnace. The $\boldsymbol{Y}$ variables are chosen to be variables in the FEM model that is valuable to estimate. The blue line shows the calibrated explained variance, and the red line shows the cross-validated explained variance.

The results are given in Table 7.3, and it is used the same performance indexes as for the metamodel and inverse metamodel – R^2 and RMSE. The R^2 gives a measure of the fit for the model, where 1 is a perfect fit. The RMSE gives the root-mean-squared error, which is related to the unit of the variables. Generally, an R^2 value over 0.85 indicates a good fit. The conductivity of the coke beds and charge material have very low R^2 value and are therefore very poorly predicted. The electrode positions have some better performance indexes but are not very well predicted either. Further, the shape and volume of the coke

beds have a decent fit with R^2 values of 0.77 and 0.84, respectively. The shell powers have a good fit, good R^2 value and low RMSE. The voltages and power in the coke beds are close to a perfect fit with an R^2 value close to 1.

Table 7.3: Performance indexes for the estimator using leave-one-out cross-validation.

	RMSE	$\mathbf{R^2}$
El 1 pos (m)	0.3024	0.5615
El 2 pos (m)	0.3024	0.5615
El 3 pos (m)	0.3024	0.5615
Sigma CB1 (S/m)	83.686	0.3261
Sigma CB2 (S/m)	83.686	0.3261
Sigma CB3 (S/m)	83.686	0.3261
Sigma SH (S/m)	7.471	0.0887
Shape 1	0.5326	0.7730
Shape 2	0.5326	0.7730
Shape 3	0.5326	0.7730
Steel Shell Power (MW)	0.0032	0.9591
Shell Power El. 1 (MW)	0.0021	0.8701
Shell Power El. 2 (MW)	0.0021	0.8701
Shell Power El. 3 (MW)	0.0021	0.8701
Volume below El. 1 (m^3)	5.4932	0.8414
Volume below El. 2 (m^3)	5.4932	0.8414
Volume below El. 3 (m^3)	5.4932	0.8414
Power CB1 (MW)	0.4767	0.9877
Power CB2 (MW)	0.4767	0.9877
Power CB3 (MW)	0.4767	0.9877
Voltage El1 (V)	3.2071	0.9879
Voltage El2 (V)	3.2071	0.9879
Voltage El3 (V)	3.2071	0.9879

7.1.3 Regression coefficients

The weighted regression coefficients plots for the estimator can be found in Appendix D. The weighted regression coefficients are the β's found for a single $\boldsymbol{Y}$ variable when performing PLSR on normalized data. The weighted regression coefficients are given with a 95 % CI calculated by using Equation 3.9. The plots give an overview of which variable that is most important in predicting a $\boldsymbol{Y}$ variable relatively.

Electrode positions

The weighted regression coefficients for the electrode positions are given in Figure D.1, D.2 and D.3. They show that the variables connected to the given electrode is the most important. Amongst them, especially current and reactance, are the most important variables.

Conductivity in the coke beds

The weighted regression coefficients for the conductivity in the coke bed are given in Figure D.4, D.5 and D.6. They show that the variables connected to the given electrode is the most important. Amongst them, especially active power and resistance are the most important variables.

Conductivity charge material

The weighted regression coefficients for the conductivity in the charge material are given in Figure D.7. The plot shows that all the coefficients have low weight, and that the variables connected to each electrode are weighted equally. That the coefficients are low-weighted matches with the fact that the conductivity in the charge material is hard to predict.

Shapes of coke beds

The weighted regression coefficients for the shapes of the coke beds are given in Figure D.8, D.9 and D.10. They show that the variables connected to the given electrode is the most important. Amongst them, especially reactance and current, are the most important variables.

Total steel shell power

The weighted regression coefficients for the total steel shell power are given in Figure D.11. The plot shows that the variables connected to each electrode are weighted equally. The currents are the most important variables in predicting the total steel shell power.

Steel shell power for zones

The weighted regression coefficients for the steel shell power for each zone are given in Figure D.12, D.13 and D.14. They show that the variables connected to the given electrode is the most important. Of all variables, the currents are the most important, even the currents connected to different zones.

Volume of the coke beds below the electrode positions

The weighted regression coefficients for the volumes of the coke beds below the electrode positions are given in Figure D.15, D.16 and D.17. They show that the variables connected to the given electrode is the most important. Amongst them, especially reactance and current, are the most important variables.

Power in the coke beds

The weighted regression coefficients for the power in the coke beds are given in Figure D.18, D.19 and D.20. They show that the variables connected to the given electrode is the most important. Amongst them, especially resistance and active power are the most important variables.

Voltage

The weighted regression coefficients for the voltage in the electrodes are given in Figure D.21, D.22 and D.23. They show that the variables connected to the given electrode is the most important. Amongst them, especially resistance and active power are the most important variables.

7.1.4 Tuning the model by implementing an reactance bias

In Section 5.4.1, it was explained that the simulations of the FEM model do not represent the reactances well. To make the model compatible with real data, a bias term must be implemented on the model's reactance. The metamodel in Section 6.1 was used for that purpose. The model's current input was chosen to be the average operational values of the current given in Table 7.4. The rest of the input variables were tuned to give approximately the values of the resistances and active powers given in Table 7.4 as output of the metamodel. In this way, it was obtained estimated values for the reactances. By subtracting the average operational reactances by the estimated reactances, a bias of 0.15 $m\Omega$ was found for each of the reactances.

The bias is constant and may not be the best approximation as the real furnace's reactance depends on the holder position. The flexible cables connecting the transformer to the electrode bends in different ways depending on the holder positions. Since the reactance depends on the currents' path, the change in the arrangement of the flexibles changes the contribution of reactance. A more accurate approximation is to find a bias that is depending on the holder position.

Table 7.4: The average of real operational variables in August compared to the average of the simulated data in the FEM model. The values are given as a percentage of a not given reference value due to that the information is classified.

Variables	Average operational value	Average simulated value
Resistance El. A (mΩ)	99 %	80 %
Resistance El. B (mΩ)	100 %	80 %
Resistance El. C (mΩ)	99 %	80 %
Reactance El. A (mΩ)	123 %	98 %
Reactance El. B (mΩ)	115 %	98 %
Reactance El. C (mΩ)	120 %	98 %
Active Power El. A (MW)	97 %	77 %
Active Power El. B (MW)	100 %	77 %
Active Power El. C (MW)	93 %	77 %
Current El. A (kA)	100 %	100 %
Current El. B (kA)	101 %	100 %
Current El. C (kA)	98 %	100 %

7.1.5 Assessing the performance of the estimator

In this section, the estimator's performance is assessed using real data as input to the estimator. The estimator must be accurate for using the estimator as an assistive tool or as a part of the control system. The assessment provides how good the estimator is and state to what extent the estimator can be used on the real furnace. It is not trivial how to assess the estimator's performance as there are no real measurements of most of the predicted variables. If the estimator gives values in a range that the FEM model would also produce, it gives an indication of the estimator's performance. Figure 7.2 shows a segment of predictions in January 2019. All variables are in realistic ranges, which is a positive sign for the estimator.

Since the estimator is static and ignores the dynamics of the furnace, it is believed that the estimator estimates the variables with fast dynamics the best. The variables with fast dynamics are shell power, power in coke beds, and voltages. The rest of the variables have slower dynamics and are more inaccurate in the prediction since the static model does not take into account the dynamics of the variables.

Electrode position

What might be the most interesting prediction is the electrode position. The electrode position in the real system is a function of the holder position, the slipping rate, and the electrode's consumption rate. During tapping, the conductivity is decreasing, and to maintain the reference on the resistance, the electrodes drop. The intuition is, therefore, that also the estimates of the electrode positions should drop during the tapping cycles. Figure 7.3 shows a segment of data in January 2019 with holder positions and estimated electrode positions. The gray areas visualize the tapping cycles. The plot shows that the holder position drops during the tapping cycles, while the electrode position's estimates seem to be unaffected by the tapping cycles. This gives a bad estimate of the electrode positions. The reason why the electrode position's estimation does not drop during the tapping cycles is most likely because the input of the estimator is based only on electrical conditions, and the electrical conditions are not affected by the tapping cycles due to the constant electrical references. The normalized correlation between the estimation of the electrode position and the holder position is given by -0.2877, -0.2477 and -0.1960 for electrode A, B and C, respectively. The normalized cross correlation varies from -1 to 1. A value of 1 is a perfect correlation, while -1 are two opposite signals. This means that there is no correlation between the estimation of the electrode position and the holder position.

The variables that are known to drop during tapping is the conductivity of the coke bed. Introducing the coke bed's conductivity to the input of the estimator might make the estimator respond to the tapping cycles. The problem is – there is no measurement of the conductivity in the coke bed. Though, an approximation of the loss in conductivity can be made based on the amount of slag and metal tapped over a given time.

Conductivity in the coke bed

As explained in the previous section, the conductivity in the coke bed is believed to correlate with the tapping cycles. Before tapping, the coke bed contains slag, which makes the

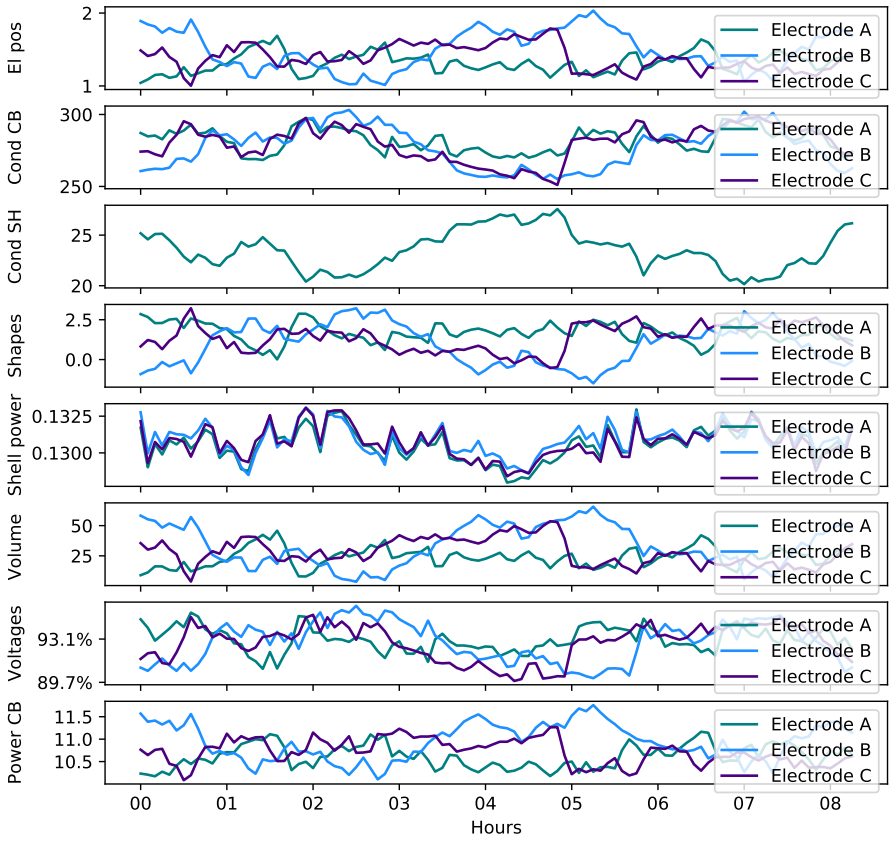

Figure 7.2: The results from estimating variables based on a segment of real data in January 2019. The voltages are given as a percentage of a not given reference value due to that the information is classified.

coke bed conductive. Hence, it is believed that the conductivity drops during tapping and increases between the taps. Figure 7.4 gives the predictions of the conductivity in the three coke beds for the same data segment as in Figure 7.2. The tapping cycles are visualized by the gray area. The conductivity in the coke bed does not seem to be much influenced by the tapping cycles. The reason for that is probably, as stated in the previous section, that the input of the estimator is only electrical variables that do not change much during tapping. The predictions do have large prediction intervals, and it is hard to conclude based on the predictions.

Sigma SH

Sigma SH has very low performance indexes as given in Table 7.3, and is therefore unlikely to be estimated well. The regression coefficients also show that the most important variables are the reactances, and therefore will the prediction be influenced by the inaccu-

rate reactance bias imposed in Section 7.1.3. This indicates that there is a poor estimation of Sigma SH.

Shapes

The shapes have good performance indexes given in Table 7.3, which indicates that it should represent the FEM model well. The biggest problem with the estimation is that the inaccurate reactance bias profoundly influences it. As seen in Figure 7.2, the shapes sometimes have values below 0 for electrode B, which is a value that is not valid as the shapes do only vary from 0 to 3 in the FEM model. This is most likely due to the reactance bias, which shifts the estimation due to a linear model.

Shell powers

Since this is an electrical variable with fast dynamics, it should be estimated well by the static estimator. The performance indexes in Table 7.3 also indicates that the variables should represent the FEM model well. As given in Section 7.1.3, the regression coefficients in the prediction should be mostly dependent on the currents, which is the most reliable measurement in the furnace. It is though hard to assess the prediction of the shell powers compared to real data as there are no measurements of the shell powers.

Volumes

The volume variables give the volume below the electrode tips and have, therefore, regression coefficients similar to the electrode positions regression coefficients. This is also seen in Figure 7.2, as the volumes and electrode positions are varying very similarly. The volumes have good performance indexes, as shown in Table 7.3 and represent the FEM model well. The volumes are also affected by the inaccurate reactance bias as the reactance has a big influence according to the regression coefficients given in Section 7.1.3. It is hard to assess the prediction of the volumes compared to real data as there are no measurements available.

Voltage

Voltage is the only estimated variable that is measured. By comparing the voltage prediction with the voltage measurement, the estimator performance of the estimation of voltage can be assessed. The MSE between the prediction of the voltages and the real voltages are given by 6.9 %, 7.4 % and 6.9 % for electrode A, B and C, respectively. Figure 7.5 gives the comparison between measured and predicted voltage. The plot shows that there is a bias between the voltage prediction and measurement. The voltages have very good performance indexes based on the training set of the FEM model given in Table 7.3, which should indicate that the estimator recreated the FEM model well.

It is not easy to say what is the reason for the bias between measurement and prediction. One could believe introducing bias in reactance in Section 7.1.4 could be the reason for the bias in voltage. However, the regression coefficients plots in Figure D.21, D.22 and D.23 show that the influence from reactances are rather small and are therefore unlikely

to influence the estimate of voltage much. Therefore, the bad prediction can be due to an inaccurate FEM model, as the estimator recreates the FEM model in the prediction of voltage very well. The most likely reason for the bias in the voltage predictions is caused by measurement error. As explained in Section 4.2.6, the voltage measurements are inaccurate. The input of the estimator are resistance, reactance, active power and currents. In the regression coefficients, resistance and active power are the most important variables. Since both of them are calculated using voltage measurements, they will most likely give an error in the estimates. This means that the prediction of the voltages is given indirectly by the voltage measurements, making the prediction not valid.

Power in the coke beds

Since this is an electrical variable with fast dynamics, it should be estimated well by the static estimator. The performance indexes in Table 7.3 also indicate that the variables should represent the FEM model very well. As given by the regression coefficients in Section 7.1.3, the prediction should be mostly dependent on the resistances and the active powers. It should not be influenced much by the reactance bias given in Section 7.1.4. However, the power in the coke bed is hard to assess as there are no measurements available.

7.1.6 Preliminary conclusions about the assessment of the performance of the estimator

The assessment of the estimator can be summed up as:

1. The electrode positions and conductivity in the coke beds do not correspond to the tapping cycles, and are therefore bad predictions. In addition, the conductivity is so uncertain in the prediction that even if the conductivity was following the tapping cycles to some degree, it is difficult to trust the prediction.

2. Voltages are influenced by the voltage measurement and give, therefore, an invalid estimation.

3. The rest of the variables are hard to assess due to no measurements and little information regarding the variables are known.

This means that the estimator in this stage is not very reliable. Practically speaking, this means that the estimator cannot be used as any part of a control system, but some variables might be used as an assistive tool for the operators. As the tapping cycles play a big role in the furnace operation, the variables that should correspond to the tapping cycles must do so. Therefore, the electrode positions and conductivity cannot be used as part of the control system or as an assistive tool at this stage.

Since the estimation of voltage is dependent on the voltage measurement, there is not much use of the voltage prediction. If the estimation of the voltage were independent of the voltage measurement, it could be used to check if the voltage measurement drifts away and detect the need for calibration. As the voltage estimation is dependent on the voltage measurement, the estimation is also believed to drift off in the same way as the voltage

measurement. Anyways, as the voltage prediction is recreating the voltage measurement well, this can indicate that the FEM model is a good representation of the voltage.

As the other variables are hard to assess, they cannot be seen as reliable. They might be used as an assistive tool to check if the operator's knowledge of the furnace corresponds with the estimation. Anyhow, it has to be kept in mind that the predictions of these variables are not validated for a real furnace.

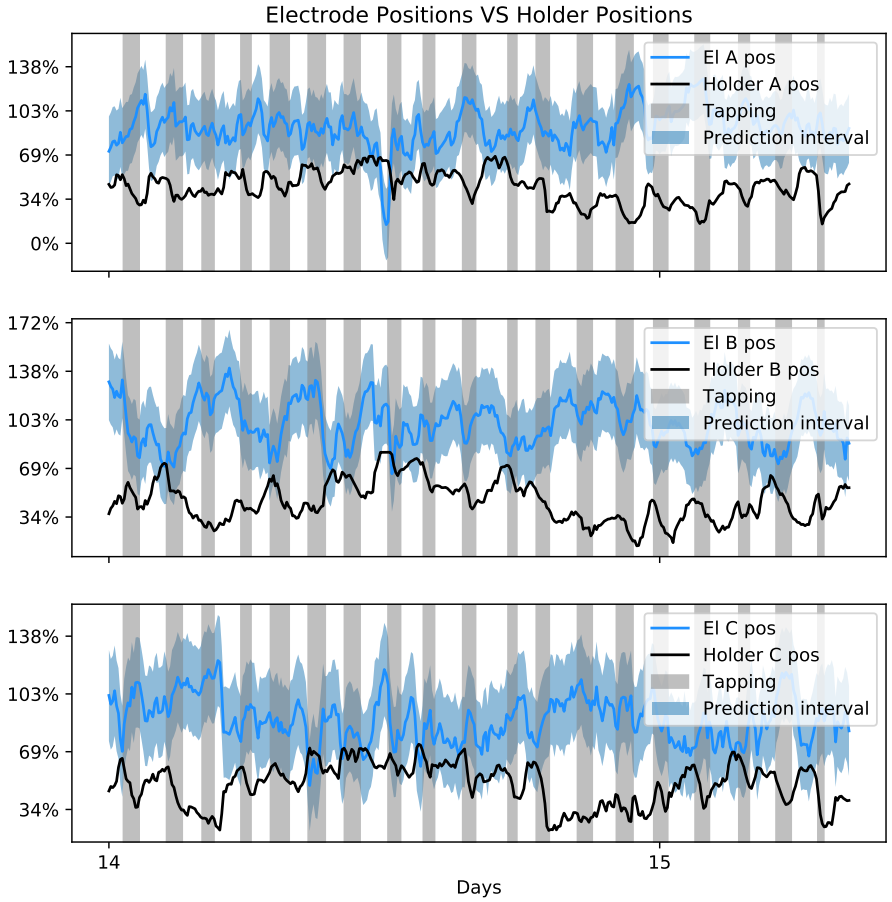

Figure 7.3: The estimated electrode positions with a 95 % PI using a segment of real data in January 2019 compared with the holder positions. The gray areas show the tapping cycles. The values on the y-axis are given as a percentage of a not given reference value due to that the information is classified.

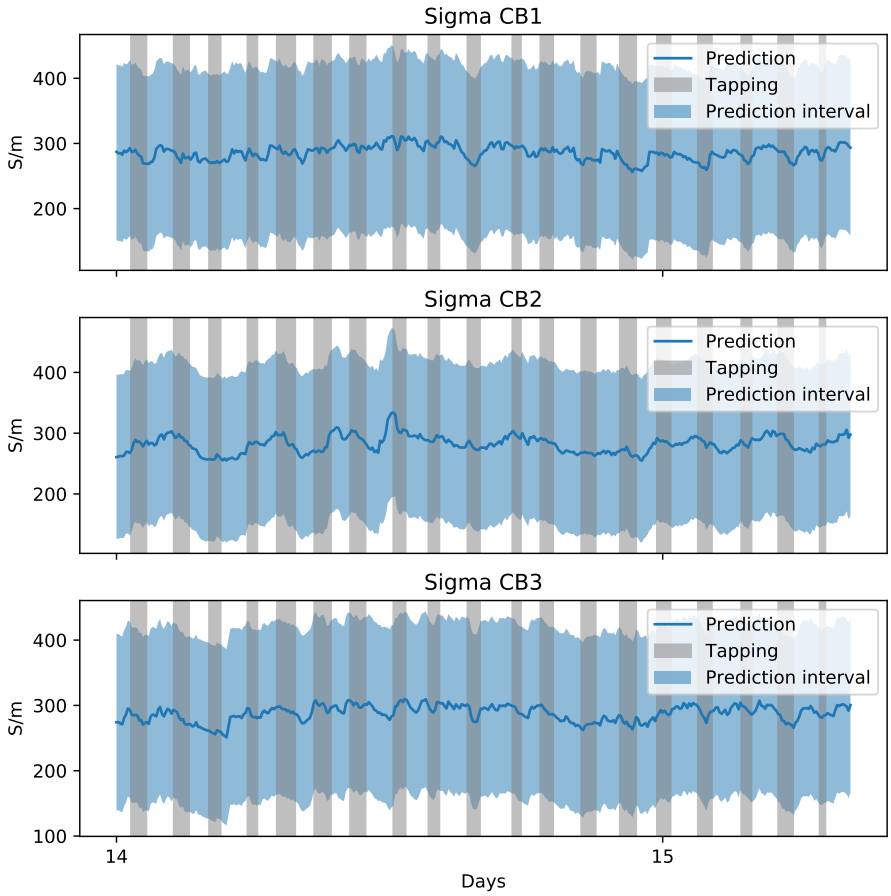

Figure 7.4: The estimation of the conductivity in the coke beds with a 95 % PI using a segment of real data in January 2019 compared with the holder position. The gray areas show the tapping cycles.

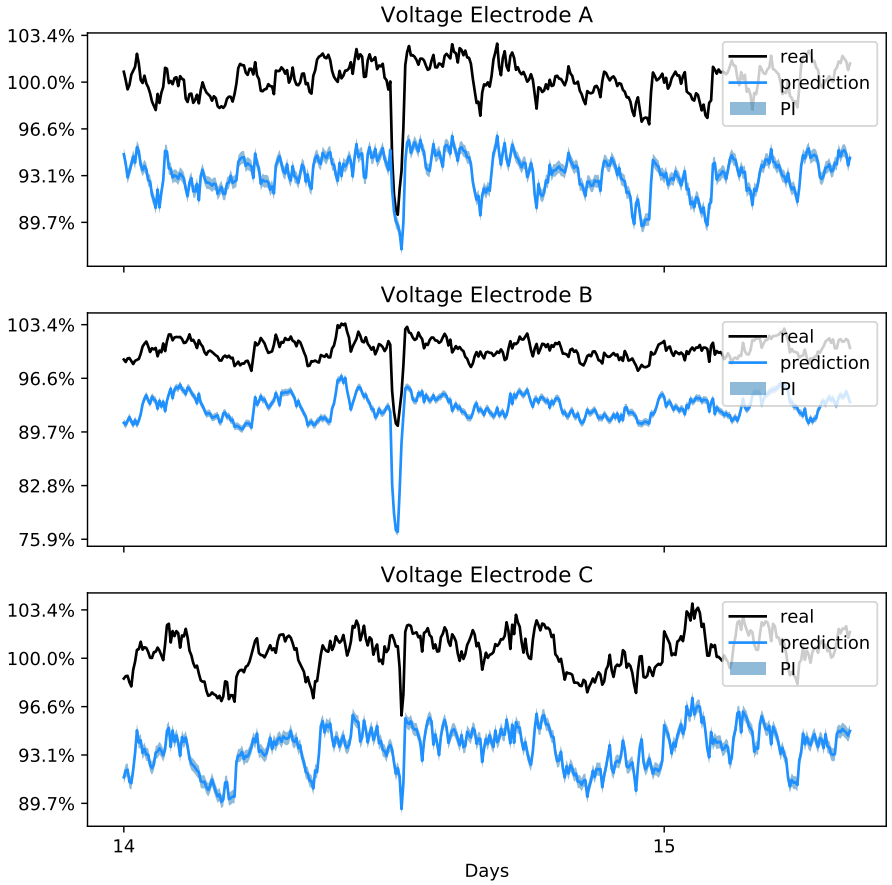

Figure 7.5: The figure shows the estimation of the electrode voltages using a segment of real data in January 2019 compared with the measured electrode voltages. The values on the y-axis are given as a percentage of a not given reference value due to that the information is classified.

7.2 Building an estimator based on available measurements and coke bed properties

For the estimator in Section 7.1, it was proven that the electrode positions' estimation did not correspond to the tapping cycles, and there was no correlation between the electrode positions and the holder positions. Therefore, a new estimator was built by including conductivity and shape of the coke beds, and the conductivity in the charge material to see if the estimation corresponds to the tapping cycles. Approximations of these quantities will be used to estimate the electrode position based on real data.

7.2.1 Variable selection for the estimator

Section 7.1.5 explains that the voltage predictions are not valid since they indirectly rely on the voltage measurements. The other variables are difficult to assess because there are no measurements available to assess the predictions. Also, it was showed that the electrode position did not respond to the tapping cycles. To have the estimations of electrode positions respond on the tapping, Sigma CB's, Sigma SH, and the Shapes are included in the $\boldsymbol{X}$ set. The only $\boldsymbol{Y}$ variables are the electrode positions. The $\boldsymbol{X}$ and $\boldsymbol{Y}$ variables are given in Table 7.5 and 7.6, respectively.

Table 7.5: $\boldsymbol{X}$ variables of the estimator for predicting electrode position including properties for the coke beds and charge material.

Variables	Definition
Resistance El. 1 (mΩ)	Resistance in electrode 1
Resistance El. 2 (mΩ)	Resistance in electrode 2
Resistance El. 3 (mΩ)	Resistance in electrode 3
Reactance El. 1 (mΩ)	Reactance in electrode 1
Reactance El. 2 (mΩ)	Reactance in electrode 2
Reactance El. 3 (mΩ)	Reactance in electrode 3
Active power El. 1 (MW)	Active power electrode 1
Active power El. 2 (MW)	Active power electrode 2
Active power El. 3 (MW)	Active power electrode 3
Current El. 1 (kA)	Electrode 1 current
Current El. 2 (kA)	Electrode 2 current
Current El. 3 (kA)	Electrode 3 current
Sigma CB 1 (S/m)	Conductivity in the coke bed under electrode 1
Sigma CB 2 (S/m)	Conductivity in the coke bed under electrode 2
Sigma CB 3 (S/m)	Conductivity in the coke bed under electrode 3
Sigma SH (S/m)	Conductitvity in the charge material above the coke beds
Shape 1	Broadness of the coke bed 1
Shape 2	Broadness of the coke bed 2
Shape 3	Broadness of the coke bed 3

Table 7.6: $\boldsymbol{Y}$ variables of the estimator for predicting electrode position.

Variables	Definition
El 1 pos (m)	Height of the electrode 1
El 2 pos (m)	Height of the electrode 2
El 3 pos (m)	Height of the electrode 3

7.2.2 Modelling the estimator

A new estimator was built using PLSR with the variables given in Table 7.5 as $\boldsymbol{X}$ and the variables given in 7.6 as $\boldsymbol{Y}$. The model was validated using leave-one-out cross-validation on the 768 segments for assessing the statistical performance that the model would have on unseen data. With 8 factors, the model covers 79 % of the variance, as seen in Figure 7.6. This means that the explained variance has increased by 4 % with one less component from the estimator based on only electrical variables in Section 7.1. The results given in Table 7.7 also shows that the extended set of variables in the $\boldsymbol{X}$ set gives better results than in the previous estimator for electrode position given in Table 7.3. The R^2 value for the electrode positions has increased from 0.56 to 0.79, and the RMSE has decreased from 0.30 to 0.21. This means that the electrode positions' estimation has been improved by extending the $\boldsymbol{X}$ set. The reactance bias found in Section 7.1.4 was also implemented for this model to compensate for the difference in reactance between simulation and real data.

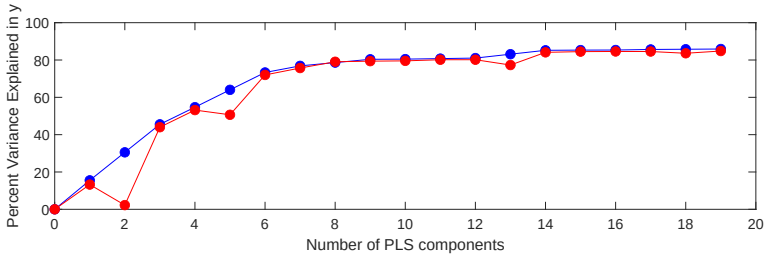

Figure 7.6: Explained variance of the leave-one-out cross-validated estimator done with $\boldsymbol{X}$ as the variables given in Table 7.5 and $\boldsymbol{Y}$ as variables given in Table 7.6. The blue line shows the calibrated explained variance, and the red line shows the cross-validated explained variance.

Table 7.7: Performance indexes for the estimator predicting electrode positions using leave-one-out cross-validation.

	RMSE	$\mathbf{R^2}$
El. 1 pos (m)	0.209	0.7906
El. 2 pos (m)	0.209	0.7906
El. 3 pos (m)	0.209	0.7906

7.2.3 Regression coefficients

Figure 7.7 shows that the most important variables are the resistances, reactances, active power and conductivity connected to the given electrode for predicting the electrode position. The shape of the coke bed connected to the given electrode also has some impact.

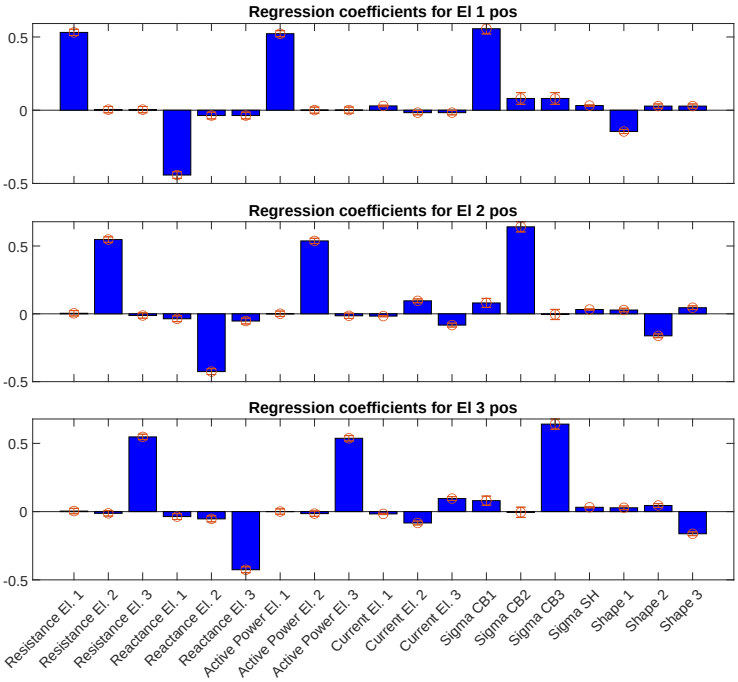

Figure 7.7: Weighted regression coefficients for electrode positions. The red bar show the 95 % confidence interval for the coefficients.

7.2.4 Assessing the performance of the estimator

The estimator's clear disadvantage is that it is based on estimations on the shapes and conductivity of the coke beds and the conductivity in the charge material since there are no measurements of these quantities. How the shape and conductivity change during tapping is not known. It is anyways wanted to make the best estimation possible to see how the electrode position reacts to the new included $\boldsymbol{X}$ variables. As explained in Section 7.2.3, the conductivity in the zone around the electrode will have the biggest impact on the estimation. This means that the electrodes will most likely react to change in the conductivity in the coke bed. But, the change in conductivity in the coke bed will also be the biggest cause of error in the estimated electrode positions if the coke bed's estimation is wrong.

The intuition is that the coke bed, before tapping, contains slag and is conductive. During tapping the slag is tapped and the conductivity drops. Since this changes the resistance in the furnace, the electrode position should go down during tapping to maintain the reference on resistance. The holder position is known to drop during tapping, and by finding a correlation between holder position and estimated electrode position can mean that the estimated electrode position correspond to the tapping cycles. To see how the electrode positions react to the change of Sigma CB's, shapes and Sigma SH an experiment has been set up in the following way:

1. The Sigma SH was set constant at 22 S/m.
2. The Shapes were set constant at 1.5.
3. The Sigma CB's are set to increase from a minimum value ($Sigma_{min}$) to a maximum value ($Sigma_{max}$) when not tapping, and decrease from the $Sigma_{max}$ to the $Sigma_{min}$ when tapping. Thus, we can define $Sigma_{delta} = Sigma_{max} - Sigma_{min}$.

It is wanted to find a possible correlation between the holder positions and the estimated electrode positions. A correlation indicates that the electrode positions react to the tapping cycles. As the holder positions don't give the exact electrode position, there is not expected a maximum correlation. However, it is expected some correlation as the holder position reacts on the tapping cycles.

Since the estimator is linear, an equal shift in $Sigma_{max}$ and $Sigma_{min}$ gives a shift in the prediction of the electrode positions. However, it will not interfere with the correlation between the estimated electrode positions and the holder positions. Therefore, the $Sigma_{delta}$ was changed to see if that changes the correlation. The $Sigma_{min}$ was set constant at 200 S/m, which means that only $Sigma_{max}$ was changed according to the changes in $Sigma_{delta}$. The different $Sigma_{delta}$ were given as 0 S/m, 50 S/m, 100 S/m, 150 S/m, 200 S/m and 250 S/m. For a data segment in January 2019, the estimations are given in Figure 7.8 using the different $Sigma_{delta}$. The plot shows the mean-centered predictions of the electrodes with the mean-centered holder position. In the plot, there is no clear correlation between the estimates of the electrode positions and the holder positions. To assess the correlation, the normalized cross correlation has been calculated between the electrode positions and the holder position at zero lag given in Table 7.8. The normalized cross correlation varies from -1 to 1. A value of 1 is a perfect correlation, while -1 are two opposite signals. As the electrode positions and holder positions are expected to decrease during tapping and increase in between tapping, the correlation should be positive. The results show a negative correlation for most of the different $Sigma_{delta}$. Thus, there is no correlation between the measures. Even though the correlation becomes less negative with bigger values of $Sigma_{delta}$, there seems to be no correlation between the measures.

7.2.5 Preliminary conclusions about the assessment of the performance of the estimator

The imposed change in conductivity during tapping and in between tapping makes the estimation of the electrode positions a function of the tapping intervals. This makes sense

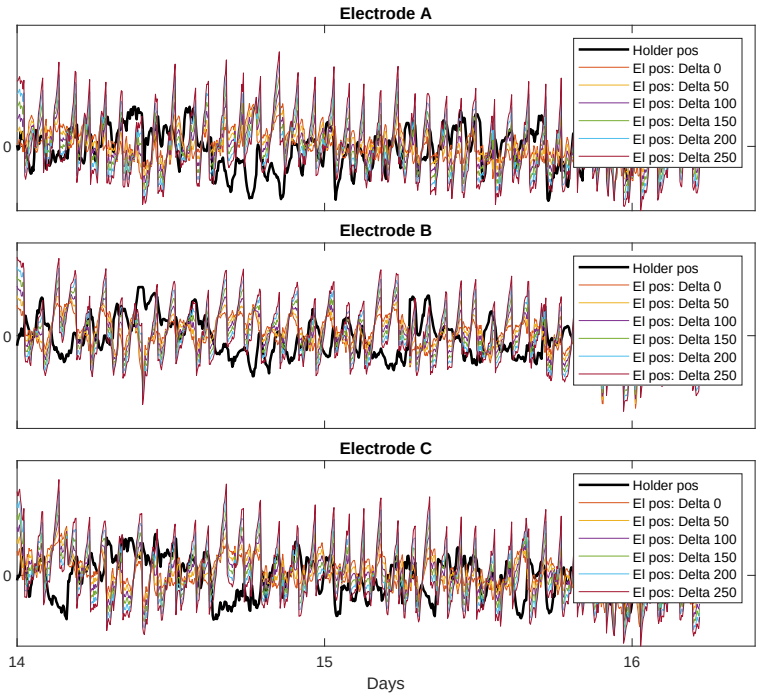

Figure 7.8: The colored lines show the different estimations of electrode position for each electrode using different delta in the conductivity in the coke bed. The black, highlighted line shows the measured holder position. Both holder and electrode positions are mean-centered. Only the zero is given on the y-axis due to that the information is classified.

from a theoretical perspective. Anyways, the electrode positions' estimation does not correlate much with the holder positions, which makes the estimation unreliable. As the conductivity in the coke bed at any time is unknown, it is difficult to use the conductivity as an input of the estimator. To get a better assessment of the electrode position estimation, more information should be extracted from the system. The slipping rate is known in the system, and the consumption of the electrode can be estimated. An alternative estimation of the electrode position is provided by extracting this information in addition to the holder position. If the alternative estimation of the electrode position correlates with the estimation of the electrode position, it gives a better assessment of the estimation of electrode position.

By the assessment done so far on the electrode position by including the conductivity in the coke bed, it can be concluded that the estimation does not seem to be promising. As there are no measurements available for the conductivity's and the shapes for the input of the estimator, the estimation becomes unreliable. In this way, the estimator cannot be used in the control system or as an assistive tool for the operators at this stage.

Table 7.8: The normalized cross correlation between each of the electrode positions and the holder positions at zero lag for different changes in conductivity in the coke bed.

Delta	Electrode A	Electrode B	Electrode C
0 (S/m)	-0.5333	-0.6604	-0.6079
50 (S/m)	-0.3559	-0.5583	-0.4868
100 (S/m)	-0.1577	-0.4312	-0.3202
150 (S/m)	-0.0202	-0.3155	-0.1819
200 (S/m)	0.0661	-0.2232	-0.0847
250 (S/m)	0.1218	-0.1525	-0.0175

7.3 Building an estimator based on available measurements and electrode positions

The prediction of the conductivity in the coke bed in Section 7.1 showed that the predictions did not correspond to the tapping cycles as wanted. Since the electrode positions are believed to correspond to the tapping cycles, it is included in the input of the model. As there are no measurements of the electrode position, the electrode positions are approximated by using the holder positions.

7.3.1 Variable selection for the estimator

Section 7.1 shows that the estimation of the conductivity in the coke beds are not affected by the tapping cycles. The intuition is that the conductivity in the coke beds are expected to be influenced by the tapping intervals. Therefore, the electrode positions have been included in the $\boldsymbol{X}$ set. The holder positions will be used as an estimate for the electrode positions since the electrode positions are unknown. It has been shown that the electrode positions are functions of the holder positions. The problem with the experiment is that the holder positions does not represent the electrode positions, but it should be correlated with the electrode positions. The $\boldsymbol{X}$ and $\boldsymbol{Y}$ variables are given in Table 7.9 and 7.10, respectively.

7.3.2 Modelling the estimator

The new estimator was built using PLSR with the variables given in Table 7.9 as $\boldsymbol{X}$ and the variables given in Table 7.10 as $\boldsymbol{Y}$. The model was validated using leave-one-out cross-validation on the 768 segments. With 12 factors, the model explains 82 % of the variance, as shown in Figure 7.9. This means that the inclusion of the electrode positions has made an increase of 3 components and 7 % higher explained variance compared to the estimator in Section 7.1.2. The reactance bias found in Section 7.1.4, was implemented for tuning the model to real data.

Table 7.11 shows the results from leave-out-out cross-validation on the training data. Comparing the results with the results of the estimator with only available measurements as input in Table 7.3, we can see that the performance indexes have been improved. The RMSE has been lowered from 83.7 to 52.7, and the R^2 has been increased from 0.33

Table 7.9: $\boldsymbol{X}$ variables of the estimator for predicting conductivity's in the coke beds including electrode positions.

Variables	**Definition**
Resistance El. 1 (mΩ)	Resistance in electrode 1
Resistance El. 2 (mΩ)	Resistance in electrode 2
Resistance El. 3 (mΩ)	Resistance in electrode 3
Reactance El. 1 (mΩ)	Reactance in electrode 1
Reactance El. 2 (mΩ)	Reactance in electrode 2
Reactance El. 3 (mΩ)	Reactance in electrode 3
Active power El. 1 (MW)	Active power electrode 1
Active power El. 2 (MW)	Active power electrode 2
Active power El. 3 (MW)	Active power electrode 3
Current El. 1 (kA)	Electrode 1 current
Current El. 2 (kA)	Electrode 2 current
Current El. 3 (kA)	Electrode 3 current
El. 1 pos (m)	Electrode 1 height
El. 2 pos (m)	Electrode 2 height
El. 3 pos (m)	Electrode 3 height

Table 7.10: $\boldsymbol{Y}$ variables of the estimator for predicting the conductivity's in the coke beds including electrode positions.

Variables	**Definition**
Sigma CB 1 (S/m)	Conductivity in the coke bed under electrode 1
Sigma CB 2 (S/m)	Conductivity in the coke bed under electrode 2
Sigma CB 3 (S/m)	Conductivity in the coke bed under electrode 3

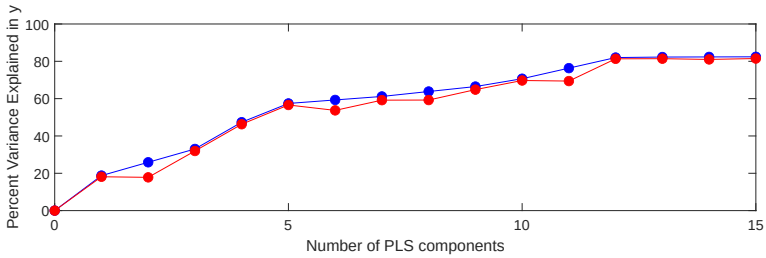

Figure 7.9: Explained variance of the estimator for predicting conductivity's in the coke beds using leave-one-out cross-validation. The blue line shows the calibrated explained variance and the red line shows the cross-validated explained variance.

to 0.73. This means that the coke bed conductivity estimation has been improved by including electrode positions in the $\boldsymbol{X}$ set.

Table 7.11: Performance indexes for the estimator for predicting conductivity in the coke bed by using leave-one-out cross-validation.

	RMSE	**R^2**
Sigma CB1 (S/m)	52.695	0.73279
Sigma CB2 (S/m)	52.695	0.73279
Sigma CB3 (S/m)	52.695	0.73279

7.3.3 Regression coefficients

Figure 7.10 shows that the most important variables are the resistances, reactances, active power, current, and electrode position connected to the given electrode. The importance of the electrode positions in predicting the conductivity was expected due to the increase in explained variance, and improved performance indexes compared to the model in Section 7.1.

7.3.4 Assessing the performance of the estimator

Figure 7.11 shows the prediction of Sigma CB1, Sigma CB2, and Sigma CB3 for a segment of data in January 2019 using holder position as an estimate of the electrode position. The plot shows that the estimation is sometimes negative, which is not a possible measure for the conductivity. That is due to that the holder positions move in a different span than what the electrode positions do in the FEM model. Figure 7.3 shows the electrode positions' estimation compared to the holder position using the same time-series with the model made in Section 7.1. Thus, if a positive shift in the holder positions is introduced, the values are more representative for the electrode position. The shift also gives a positive shift in the estimation of the conductivity.

Comparing with Figure 7.4, it is seen that the Sigma CB's are varying a lot more now when the electrode positions are included in the $\boldsymbol{X}$ set. Comparing the prediction inter-

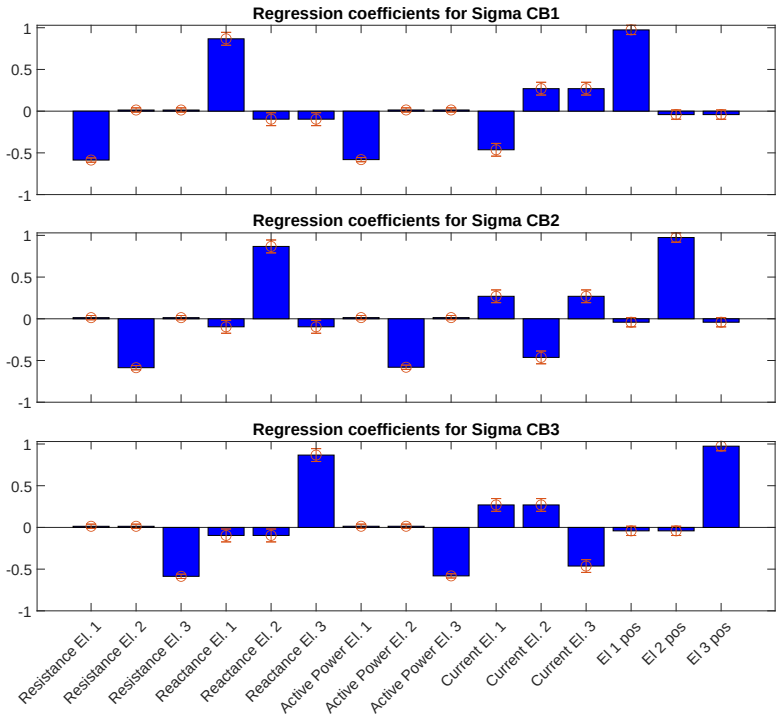

Figure 7.10: Weighted Regression Coefficients for the conductivity's in the coke bed by including electrode position in the $\boldsymbol{X}$ set. The red bar show the 95 % confidence interval for the coefficients.

vals, the estimations are also more confident now. This can be explained by the model's increased explained variance and improved performance indexes by the inclusion of electrode position in the $\boldsymbol{X}$ set.

The experiment was done to see if the Sigma CB's varied according to the tapping cycles, that the conductivity drops during tapping and increases in between tapping. The average drop in conductivity during tapping (for the tapping cycles shown in the figure) for coke bed 1, 2, and 3 are given by 43, 43, and 57 S/m, respectively. This doesn't paint the whole picture as it is not known if the drop in conductivity is due to just tapping, but at least there seems to be some correlation between the tapping cycles and drop in conductivity.

According to Eidem [17], the difference in conductivity between a coke bed with slag and a dry coke bed can be between 22 and 41 % depending on the material composition. As seen for the second tap for coke bed 2 in Figure 7.11, the conductivity drops by approximately 300 S/m. This indicates that the estimations may have too big drops. It is known that the reference value on the y-axis is wrong, but it is needed a starting value of 732 S/m for the percentage drop to be less than 41 %, which is a very high conductivity. Anyways, most of the drops are smaller than 300 S/m.

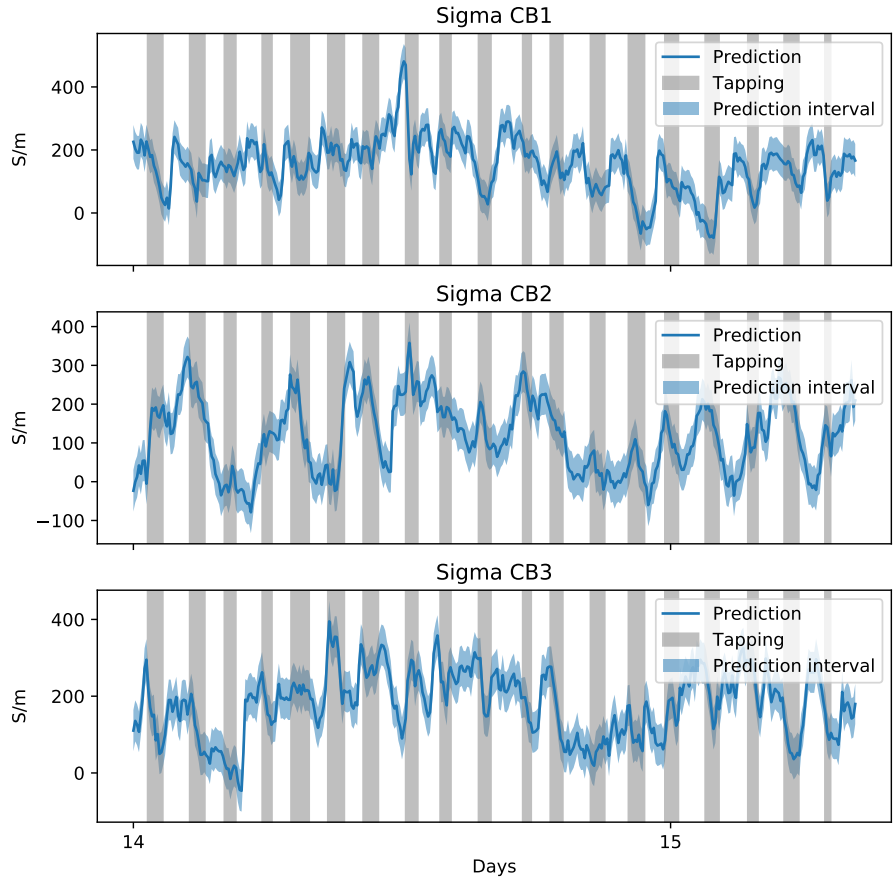

Figure 7.11: The prediction of the conductivity's in for a data segment in January 2019 using holder positions as approximations of the electrode positions.

7.3.5 Preliminary conclusions about the assessment of the performance of the estimator

Using the holder positions as the electrode positions are very rough estimations as the electrode position is a function of the holder position, slipping rate, and consumption rate. It is known that the operators have information regarding the slipping rate and an estimation of the consumption. By collecting this information, a more exact estimation of the electrode position can be done, and thus more accurate results.

An experiment should be set up to get a better assessment of the estimation of the coke beds' conductivity. The model excludes variables such as shapes of the coke beds and conductivity of the charge material. In an ideal experiment, all other factors than the tapping should be as constant as possible. For example, should the shapes of the coke beds and the conductivity in the charge material be as constant as possible so they do not

interfere with the process. By holding the variables constant, it gives more definite answers on how the conductivity in the coked beds changes.

Also, more information and understanding can be gathered if one looks into the difference of each tap. The tapping occurs on two sides, A and C, which may change the conductivity more on the tapping side than on the other. The taps also change in time and the amount of slag and metal tapped each time. Utilizing this data can give a deeper insight into how the tapping cycles change the coke bed's conductivity.

Even though it is a very rough estimation by using the holder positions as the electrode positions, it seems that the estimator gives a correlation between tapping cycles and the conductivity. A more robust experiment, as explained above, should be performed to gather more exact results.

As for now, the conductivity estimation by using the holder position as the electrode position can be used to see how the conductivity changes. Since the holder position does not provide an accurate estimation of the electrode position, the estimated value of conductivity is wrong. However, it can be used to approximate how much the conductivity drops during tapping.

7.4 Assumptions of using models based on the FEM model on real data

All PLSR models presented in the thesis are based on the FEM model and are thereby an estimation of the FEM model. This means in practice that the PLSR models are models of the FEM model, which again is a model of the FeMn furnace. This implies that all assumptions done in the FEM model becomes assumptions for the PLSR models in estimating the FeMn furnace. The assumptions of the FEM model can be found in Section 5.1.1. In theory, if the FEM model is a perfect FeMn furnace model, the PLSR models can be seen as a direct model of the FeMn furnace.

Firstly, the assumption that the PLSR does is to assume the FEM model to be linear. This assumption has varying effects depending on both the input and output of the PLSR model. Generally, the assumption is good as the performance indexes are good. For variables with worse performance indexes, the linear assumption may be the reason for the performance indexes. Another reason could also be that the data is not giving enough information to give an accurate estimation.

When using the PLSR models on real data as done in Chapter 7, one assumption in the FEM model becomes very important, which is the assumption of a static furnace. As explained in Section 5.1.1, the assumption is good when using slow dynamic variables as input and predicting fast dynamic variables as output. In Chapter 7, the tables have turned, the fast dynamic variables are predicting slow dynamic variables. If the input is changed rapidly or more precisely, if the input changes faster than the time constants of the output variables, the estimator has a problem in estimating the variables. A natural question is then – how fast is the dynamics of the output variables? By knowing the dynamics of the output variables, one can assess the validity of the prediction as the input is known. Though, the dynamics of the output variables are not known. For some variables, it is possible to model the dynamics of the output variables. By doing this, it gives a better

understanding of the process.

Another assumption that becomes important when predicting the furnace's internal conditions is everything that is disregarded in the model. For example, when predicting the conductivity of the charge material, the models do not take into account the material fed into the furnace. A change in the material composition loaded into the furnace have an impact on the conductivity in firstly the charge material and then later in the coke beds. How the material flows around in the furnace is also not taken into consideration.

Chapter 8

Further work

PLSR is not the unique way of creating data-driven metamodels of the considered FEM model. Other methods can be used, and can possibly make a better fit for the data. Indeed – and this is an important point – the PLSR approach is linear in the considered features of the data. Even if simple static nonlinearities may be introduced by opportunely feature-engineering the data (namely, by introducing squared and interaction effects), other nonlinear methods have more powerful capabilities in handling nonlinearities. This means that there may exist better representations of the FEM model than the one considered in this thesis. (At the same time, we consider that PLSR provides intuitive results, and has high explainability properties, qualities that are appreciated when dealing with needs for interpretability.)

As the modeling choice in this thesis is PLSR, we shall also report how we tried to improve the modeling by opportunely tailoring our PLSR approach. We thus note that, in this thesis, all $\boldsymbol{Y}$ variables have been modeled together - this is also called a PLS2 approach. Indeed it is possible to model the $\boldsymbol{Y}$ variables independently (something that is called a PLS1 approach). Despite by using the PLS1 approach, the model may give a better fit, to the best of our knowledge the PLS2 approach is much more practical when there are several $\boldsymbol{Y}$ variables, as in this thesis, since potential correlations among these variables are then captured and used for modelling approaches – in other words, in a PLS2 approach also the interactions among the $\boldsymbol{Y}$'s are used to create the overall model. At the same time, using the PLS1 approach would give the additional opportunity of using a different number of components, and different interaction and square effects for each $\boldsymbol{Y}$ variable. Despite this, our overarching choice has in any case been to go for a full PLS2 effect, given its increased capability of modeling joint effects.

Besides the modeling aspects above, we also mention that to understand the processes in the furnace, and model the furnace in the best way, all the data that could be collectible from the FEM model should hypothetically be gathered and analyzed. In other words, collecting more data from more experiments from the FEM model may give more information about the process at a low cost. At the same time, one may not run the FEM model for the eternity – in this thesis we thus considered running the FEM as much as feasible,

and draw our conclusions based on a (in our intuitions) sufficiently rich dataset. Despite this, more data may lead to better results.

Also, some data sources were available but not used in this thesis. For example measurements of pressure, temperatures and other things such as data about the tapping cycles, the amount of slag and metal tapped, duration of the taps and which side the tapping occurred: all this information may hypothetically be utilized to gain a deeper understanding of the conductivity in the furnace, and general information about the tapping.

More information should also be extracted from the system to assess the electrode position estimation better. The slipping rate is known in the system, and the consumption of the electrode can be estimated. An alternative estimation of the electrode is provided by extracting this information in addition to the holder position. If the alternative estimation of the electrode position correlates with the estimation of the electrode position, it gives a better assessment of the estimation of electrode position.

We mention that there exists the possibility of setting up experiments to get a better assessment of the estimation of the coke beds' conductivity. Our models exclude variables such as shapes of the coke beds and conductivity of the charge material. In an ideal experiment, all other factors than the tapping should be as constant as possible. For example, the shapes of the coke beds and the conductivity in the charge material should be kept as constant as possible, so they don't interfere with the process. By holding the variables constant, this would give more definite answers on how the conductivity in the coked beds changes. At the same time, performing this type of experiment is definitely not easy, and well beyond the scope of this work.

Finally, we explained in section 7.4 the problems associated to disregarding the dynamics of the plant when using static models. To make a better model of the FeMn furnace, we should consider its dynamics. It is possible to use Prediction Error Methods (PEM) to model some variables in the system; however, the problem with using PEM approaches is that one needs data of the variables to be predicted to recreate the variables. And as before, we have been in this thesis in the situation where the most interesting variables that should be estimated in the furnace are so that we do not have any measurements of them. This makes it somehow a non-sense to use PEM to predict these variables, since we would not be able to assess the effectiveness of the estimates. Another way to capture the dynamics of the furnace is to make a physical model of the furnace using known physics equations. Combining the static PLSR model with a physical model can indeed give a more accurate model of the furnace. Also this, though, is beyond the scope of the thesis and should be considered a potential further work.

Chapter 9

Conclusion

The thesis builds on the question: *What is happening inside a ferromanganese (FeMn) furnace?* Before answering this, it is essential to understand how a FeMn furnace works. Therefore the thesis starts with a thorough evaluation of the known characteristics of such furnaces. An evaluation that somehow motivates the question itself, since it highlights the challenge of measuring the furnace's internal conditions, since the typical measurement systems provided in this type of plants provide limited information about the furnace behavior.

To gain information regarding this behavior and complement the experimentally available data, NORCE has developed a finite element method (FEM) model that describes the electrical conditions of such furnaces. This FEM model includes properties of the coke beds and electrode positions (information that is typically not known for real furnaces, and that is thus deemed as useful by the plant operators). Such FEM model comes though with a disadvantage: it is indeed complex to use and time-consuming to run, making its usage impractical for a rapidly changing furnace. To obtain a significantly faster and more practical representation of such FEM model, the thesis explored the topic creating a metamodel (i.e., a model of the FEM model) using data-driven methods. More precisely, we provided a data foundation for data-driven modeling by simulating the FEM model using an experimental design approach that was built to cover the most of the furnace operational area. In more detail, the first data-driven models were proved to lead to a metamodel with asymmetric properties, while the FEM model is perfectly symmetric. This made us realize the need for including in the experiment design methodology strategies that preserve symmetricity assumptions. This was obtained by grouping all variables connected to each electrode and extending the dataset by swapping the data for two electrodes a time; with this discovered approach, symmetry was imposed on the dataset - and on the metamodels obtainable from this dataset.

The final metamodel, whose purpose is to work as a computationally-efficient approximation of the FEM model, was then built using a PLSR approach. Leave-one-out cross-validation was used to assess its generalization capabilities, and the results showed that the metamodel captures the FEM model well, except for the voltages and the volume of the

coke bed below and above the electrodes, which were decent fits.

In addition to the metamodel above, the thesis also produced an inverse metamodel, that was built to compute the inverse relationship between the inputs and outputs. In other words, the FEM model cannot be used to solve the problem: *"consider this output. Which input produced it?"* In other words, this inverse metamodel has been built to be able to compute an estimate of which plant input (and thus also internal condition) leads to a specific plant output (i.e., set of measurements from the plant sensors). To validate the accuracy of such an inverse metamodel in estimating the inputs, leave-one-out cross-validation was used in this case as well. The assessment showed varying results: currents were estimated well; electrode positions, shapes of the coke beds and conductivity in the charge material were estimated decently; the conductivity in the coke beds was proven to be difficult to estimate.

Note though, that not all of the inputs of the metamodels are measured in the plant. Therefore we also considered building an estimator that uses only the variables that are actually physically measured to compute, as outputs, variables that are unknown to the operators. In this way, the estimator can quickly estimate unknown conditions in real-time. Such an estimator was validated using leave-one-out cross-validation too, and the results showed that the conductivity in the coke beds and charge material, and electrode positions are all hard to estimate. The shapes of the coke beds, steel shell powers, and volume of the coke beds below the electrode positions are instead estimated well. The voltages and power in coke beds are, in their turn, estimated *very* well. It was shown that the electrical variables for the given electrode are the most important in estimating such variables. For the conductivity in the coke beds and charge material, and electrode positions, the most important variables in estimation are reactance and current. For the voltages and power in coke beds, the resistance and active power are the variables most influencing this estimation step.

Such estimator was also tested on real data to assess the performance on real situations. The assessment concluded that the electrode position and conductivity in the coke beds do not correspond to the tapping cycles and lead, therefore, too bad estimation results. The voltage measurement is used to calculate the electrical variables used in the input of the voltage estimation, making the estimation of the voltage invalid. The rest of the estimated variables are hard to assess as there are no measurements available, and little information is known about them. Summarizing, the electrode position and coke bed are not behaving as expected, the voltage estimation is influenced by the voltage measurement, and the rest of the variables are hard to assess. In such conditions the estimator at this stage is not reliable. Practically speaking, this means that the estimator cannot be used as any part of a control system, even if some of the variables that are estimated with the produced tool might be used as assistive information by the operators.

Since the electrode positions' estimation did not correspond to the tapping cycles, a new estimator was built, including conductivity, shape of the coke beds, and conductivity in the charge material (information that is typically not measured) as additional inputs for the estimator. This was done to check how much such additional information would improve the electrode positions' estimator – in a sense, an operation that has the meaning of assessing the benefits of having such measurements for estimation purposes. The results from leave-out-out cross-validation led to record improvements with respect to the first es-

timator, since the electrode positions were now decently estimated. However, since there exist no real-life measurements of such conductivities and shapes, experimental values could not be used to assess the value of these variables in real-life conditions. Moreover, in our experiments the shapes of the coke beds and the conductivity of the charge material values were set constant, and the values for the coke beds' conductivity was decreased linearly during tapping, and increased linearly in between tapping. Since the holder positions correspond to the tapping intervals, the wanted result was to find a correlation between the electrode position and the holder position. The results showed no correlation for different cases of change in the conductivity of the coke beds. This means that the estimation of the electrode position is actually unreliable.

Further, the coke beds' conductivity was also proved to be not corresponding to the tapping intervals in the furnace for the first estimator. Therefore we built another estimator by including the electrodes positions to the set of electrical variables working as inputs of the model for estimating the conductivity in the coke beds. Since the electrode positions are believed to correspond to the tapping cycles, it was wanted to see if the electrode position's change makes the estimated conductivity in the coke bed correspond to the tapping cycles. The estimator was validated using leave-one-out cross-validation, and the results were significantly increased, giving a decent estimation of the conductivity in coke beds. As there is no measurement of the electrode positions, the holder positions are roughly approximated as the electrode positions. The results using real data and approximated electrode position showed that the conductivity in the coke bed corresponds with the tapping intervals.

To sum up, the metamodel is successfully representing the original FEM model. The inverse metamodel represents the inverse of the FEM model with varying accuracy in estimating the various variables. For the subsequent estimators, improvements in the work can be made; suggestions are elaborated under the dedicated further work section. For now, it is not possible to use any of the estimators in a control system, since the results are deemed to be not accurate enough for the purpose. In our opinion, though, information and knowledge can be generated from these estimators, and be used as a supportive tool in understanding the behavior of the furnace in real-life conditions.

Bibliography

[1] K. Stråbø, "Metamodeling of large ferromanganese furnaces," 2019.

[2] K. Tøndel and H. Martens, "Analyzing complex mathematical model behavior by partial least squares regression-based multivariate metamodeling," *WIREs Comput Stat*, vol. 6, pp. 440–475, 2014.

[3] S. Wold, M. Sjostrom, and L. Eriksson, "PLS-regression: a basic tool for chemometrics," *Chemometrics and Intelligent Laboratory Systems*, vol. 58, pp. 109–130, 2001.

[4] B. K. Alsberg, *Chemometrics*. xxxx.

[5] S. de Jong, "SIMPLS: An alternative approach to partial least squares regression," *Chemometrics and Intelligent Laboratory Systems*, vol. 18, pp. 251–263, 1993.

[6] B. Lambert, "Using spectroscopy and machine learning to estimate mosquito lifespans." `https://ben-lambert.com/2016/02/19/using-spectroscopy-and-machine-learning-to-estimate-mosquito-lifespans/`. (Accessed Jun 9, 2020).

[7] F. Dekking, C. Kraaikamp, H. P. Lopuhaä, and L. Meester, *A modern introduction to probability and statistics : understanding why and how*. Springer-Verlag London, 2005.

[8] P. Nomikos and J. F. MacGregor, "Multi-way partial least squares in monitoring batch processes," *Chemometrics and intelligent laboratory systems*, vol. 30, pp. 97–108, 1995.

[9] J. Friedman, T. Hastie, and R. Tibshirani, *The elements of statistical learning: Data Mining, Inference, and Prediction (2nd ed.)*. Springer series in statistics New York, 2001.

[10] K. P. Burnham and D. R. Anderson, *Model Selection and Multimodel Inference (2nd ed.)*. Springer-Verlag New York, Inc, 2002.

[11] B. Asphaug, “FeMn Production,” 1997.

[12] K. Stråbø, “Report - Visiting the plant in Sauda,” 2019.

[13] R. F. Schulte and C. A. Tuck, “Ferroalloys,” *USGS 2016 Minerals Yearbook*, 2020.

[14] M. Sparta, “Temperature profiles during shutdown,” 2019.

[15] Comsol, “COMSOL Multiphysics,” 2020.

[16] E. V. Herland, M. Sparta, and S. A. Halvorsen, “3D models of proximity effects in large FeSi and FeMn furnaces.,” *J. S. Afr. Inst. Min. Metall.*, vol. 118, no. 6, pp. 607–618, 2018.

[17] P. A. Eidem, *Electrical Resistivity of Coke Beds*. PhD thesis, NTNU, 7491 Trondheim, 2008.

Appendix

Appendix A

Distributions of simulated data and real data

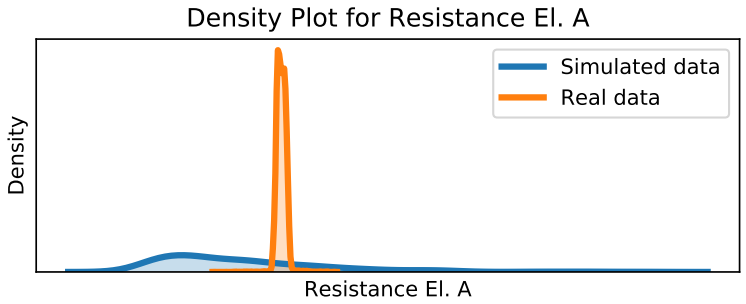

Figure A.1: Density plot for resistance El. A for real operational data and simulated data.

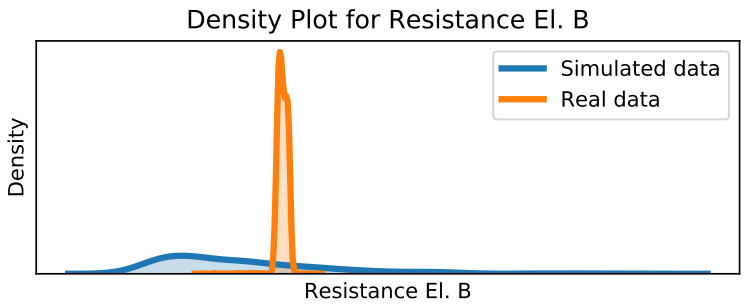

Figure A.2: Density plot for resistance El. B for real operational data and simulated data.

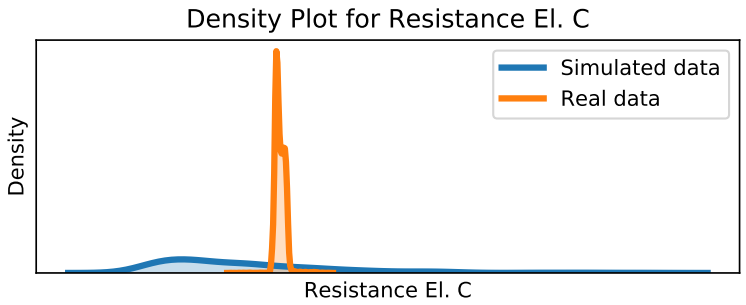

Figure A.3: Density plot for resistance El. C for real operational data and simulated data.

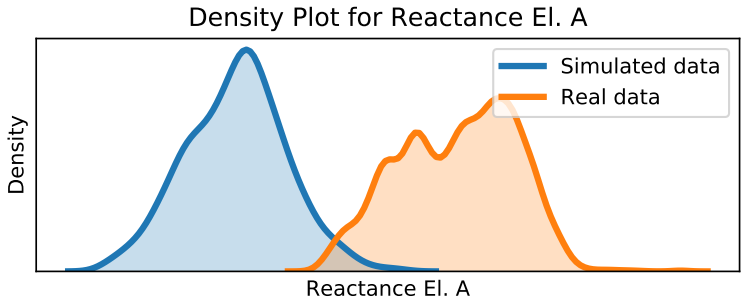

Figure A.4: Density plot for reactance El. A for real operational data and simulated data.

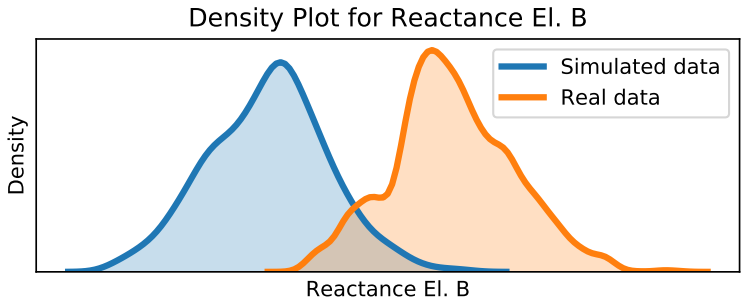

Figure A.5: Density plot for reactance El. B for real operational data and simulated data.

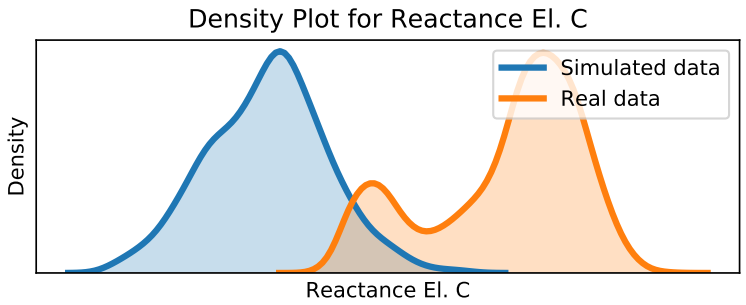

Figure A.6: Density plot for reactance El. C for real operational data and simulated data.

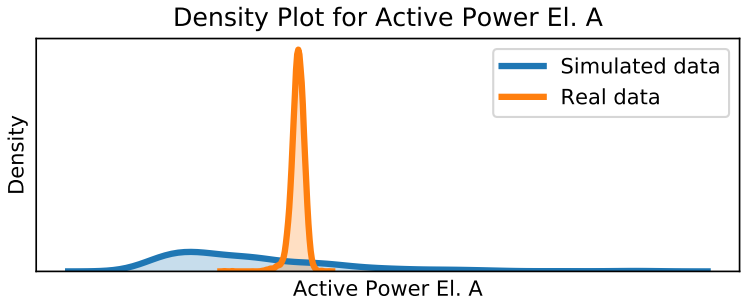

Figure A.7: Density plot for active power El. A for real operational data and simulated data.

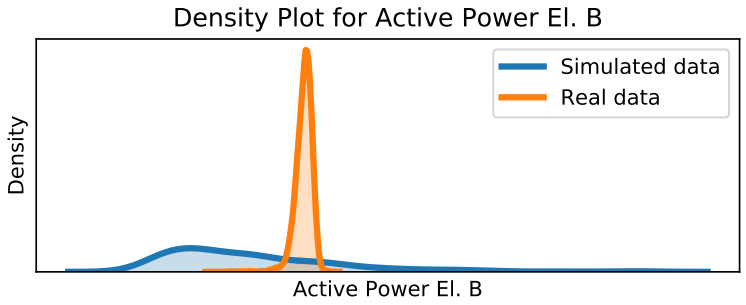

Figure A.8: Density plot for active power El. B for real operational data and simulated data.

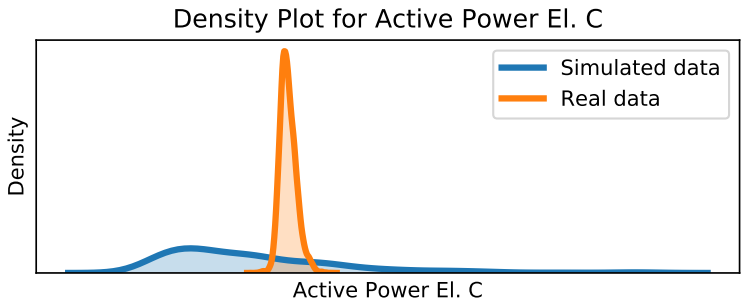

Figure A.9: Density plot for active power El. C for real operational data and simulated data.

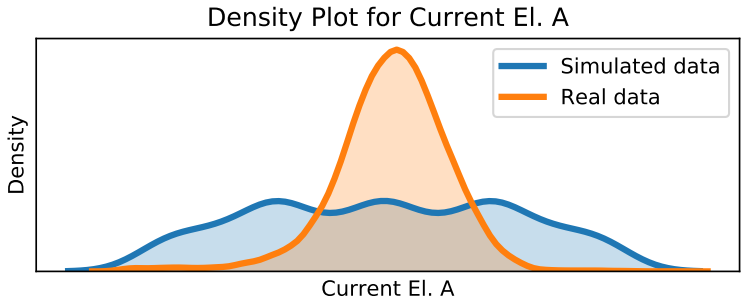

Figure A.10: Density plot for current El. A for real operational data and simulated data.

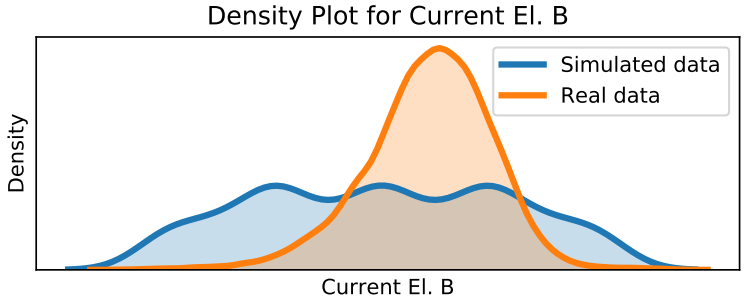

Figure A.11: Density plot for current El. B for real operational data and simulated data.

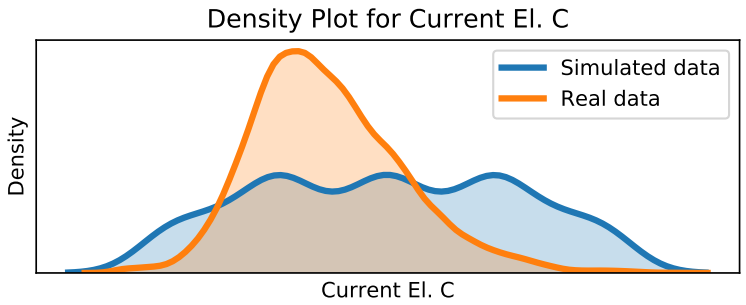

Figure A.12: Density plot for current El. C for real operational data and simulated data.

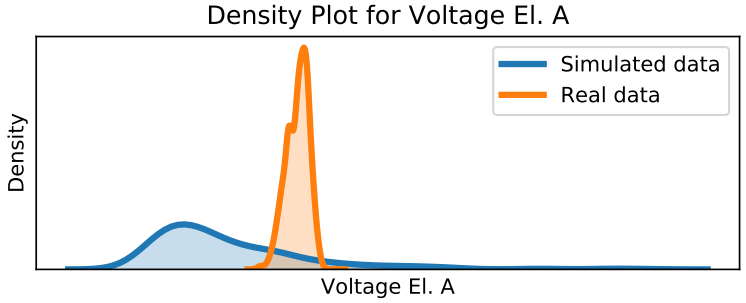

Figure A.13: Density plot for current El. A for real operational data and simulated data.

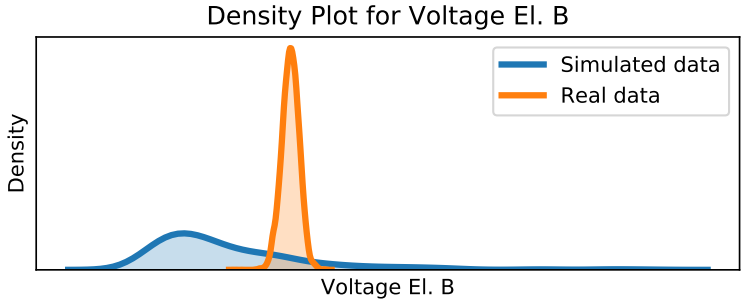

Figure A.14: Density plot for current El. B for real operational data and simulated data.

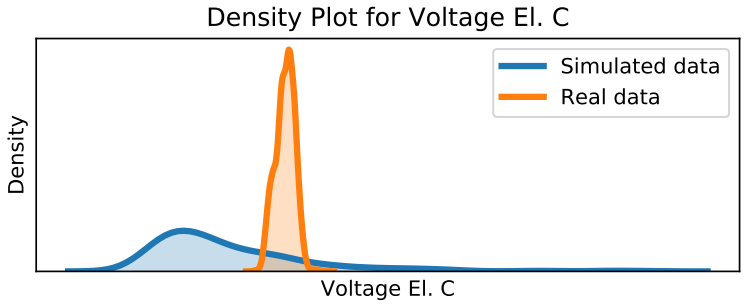

Figure A.15: Density plot for current El. C for real operational data and simulated data.

Appendix B

Weighted regression coefficients for metamodel

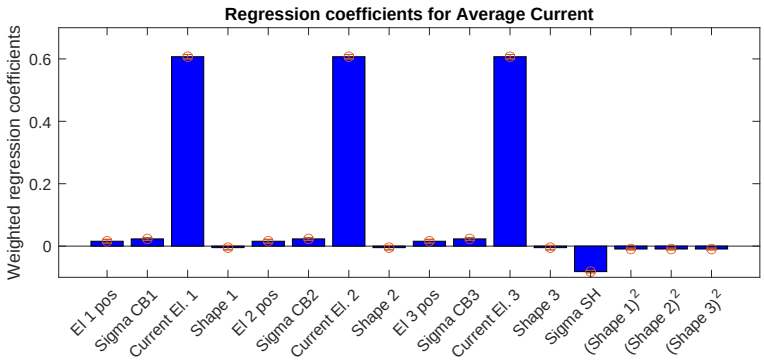

Figure B.1: Weighted regression coefficients for average current.

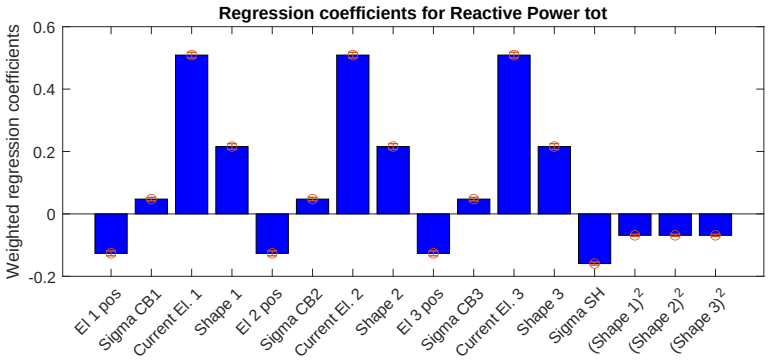

Figure B.2: Weighted regression coefficients for total reactive power.

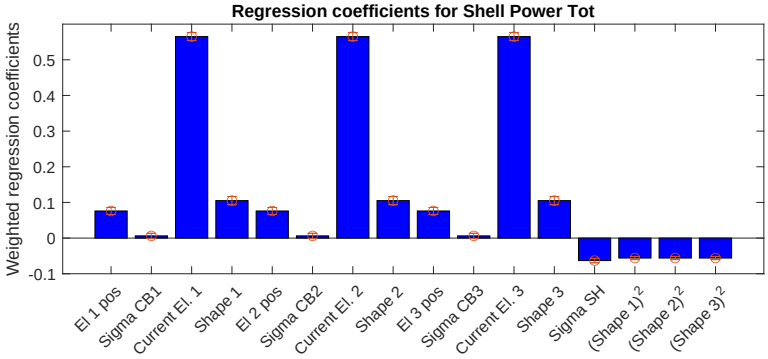

Figure B.3: Weighted regression coefficients for total shell power.

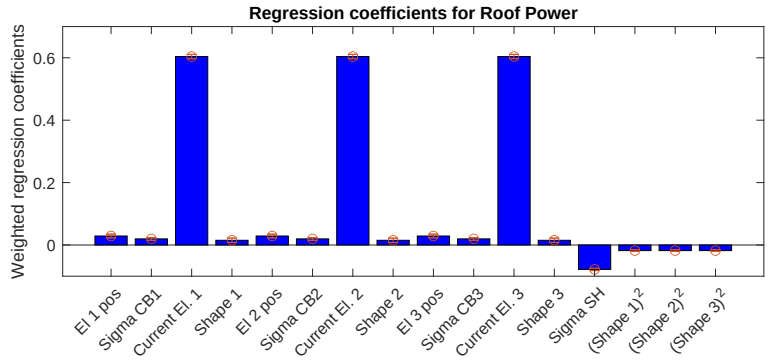

Figure B.4: Weighted regression coefficients for total roof power

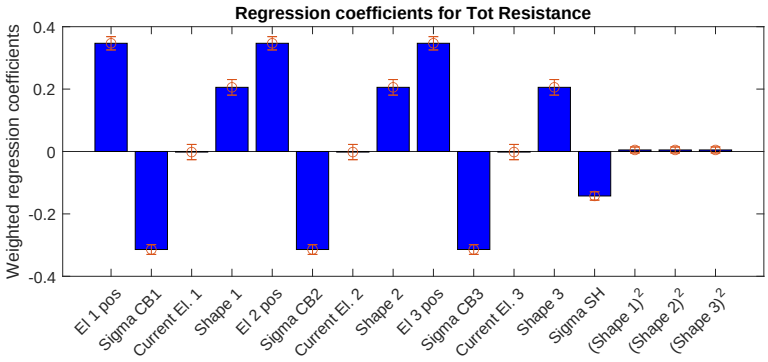

Figure B.5: Weighted regression coefficients for total resistance

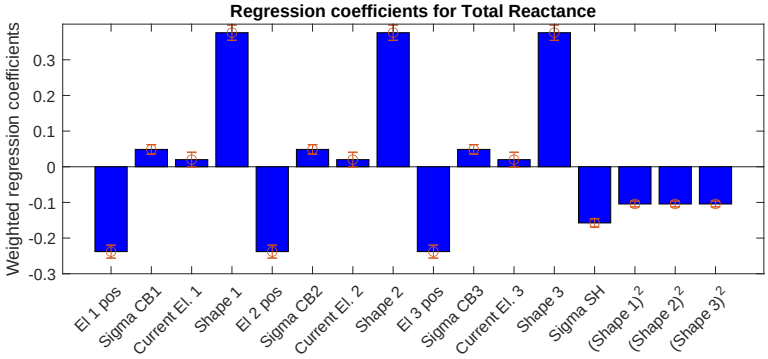

Figure B.6: Weighted regression coefficients for total reactance

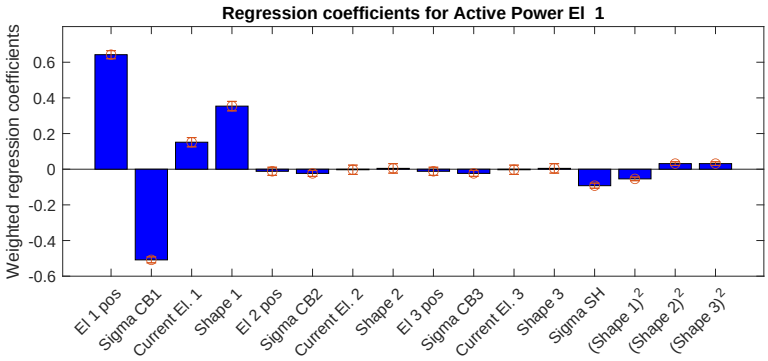

Figure B.7: Weighted regression coefficients for active power El. 1.

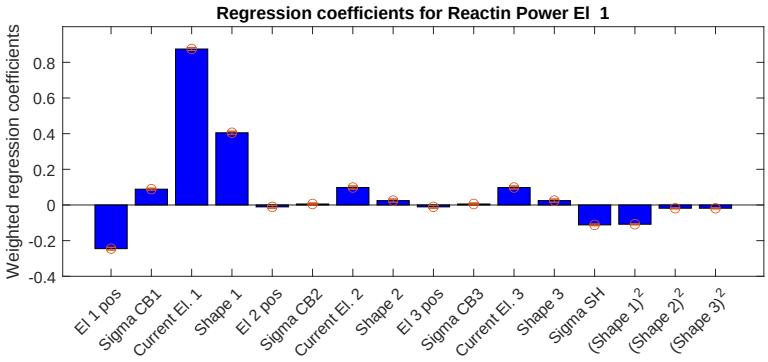

Figure B.8: Weighted regression coefficients for reactive power El. 1.

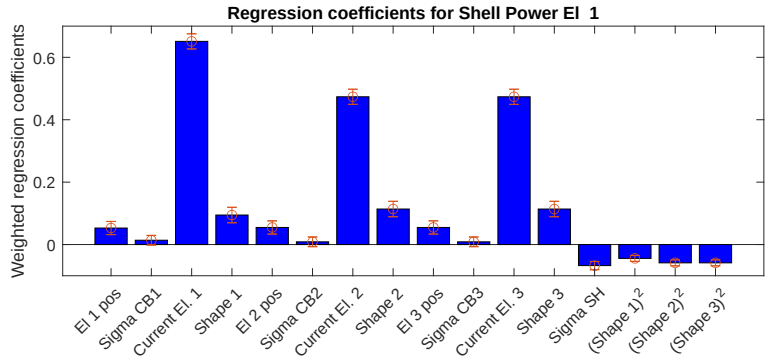

Figure B.9: Weighted regression coefficients for shell power El. 1.

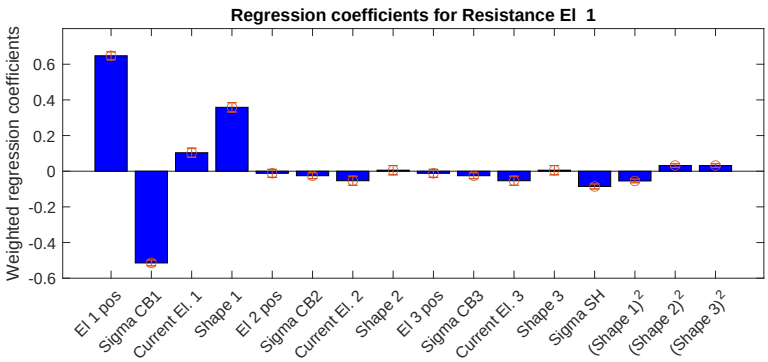

Figure B.10: Weighted regression coefficients for resistance El. 1.

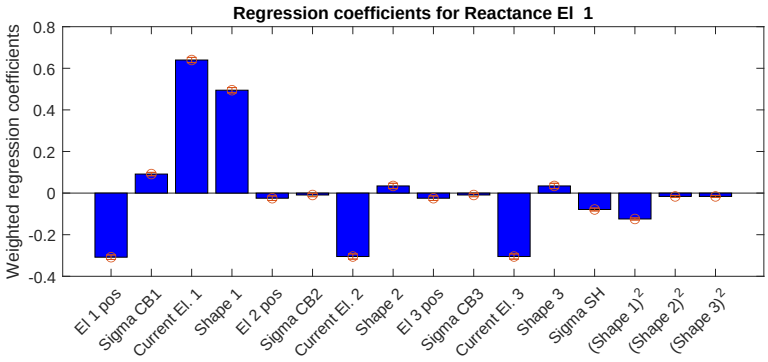

Figure B.11: Weighted regression coefficients for reactance El. 1.

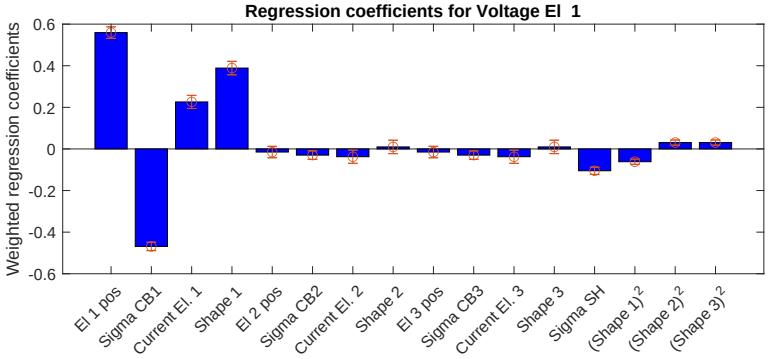

Figure B.12: Weighted regression coefficients for voltage El. 1.

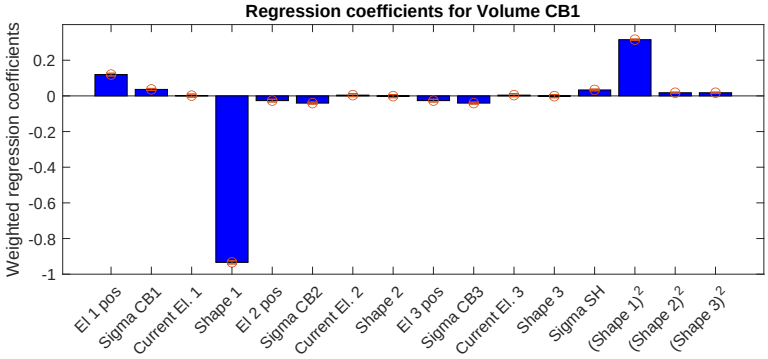

Figure B.13: Weighted regression coefficients for volume CB1.

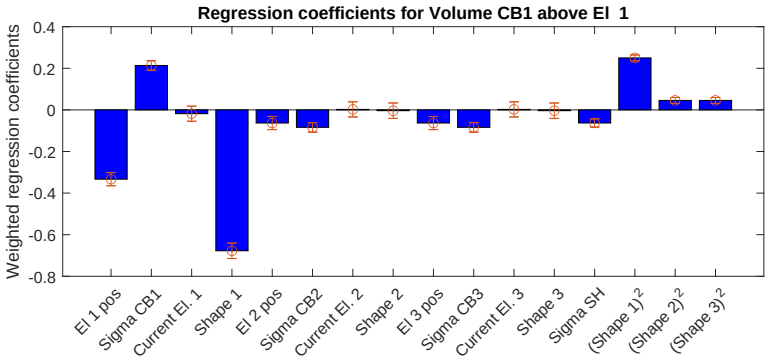

Figure B.14: Weighted regression coefficients for volume CB1 above El. 1.

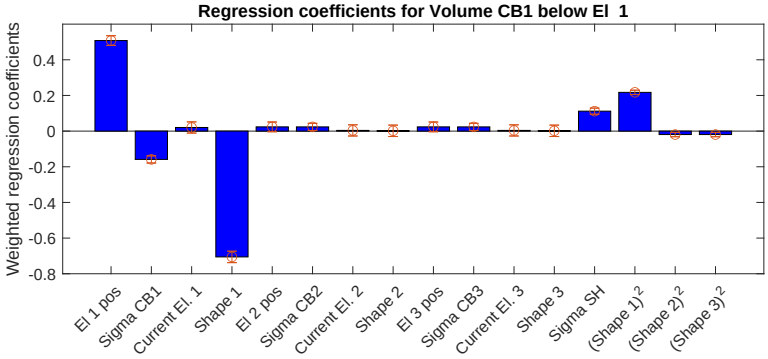

Figure B.15: Weighted regression coefficients for volume CB1 below El. 1.

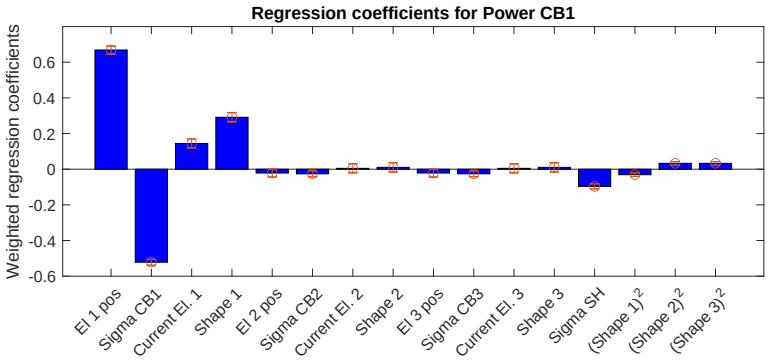

Figure B.16: Weighted regression coefficients for power CB.

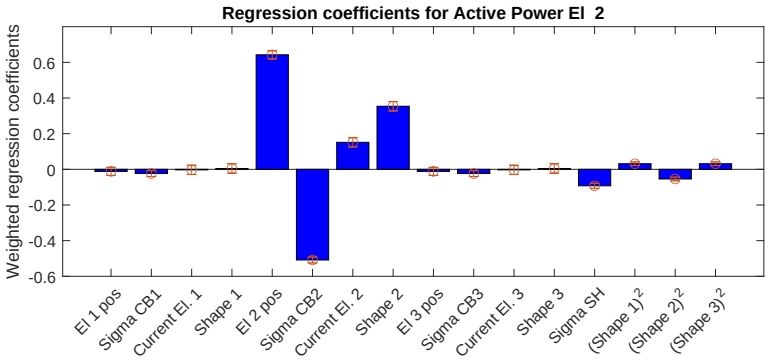

Figure B.17: Weighted regression coefficients for power El. 2.

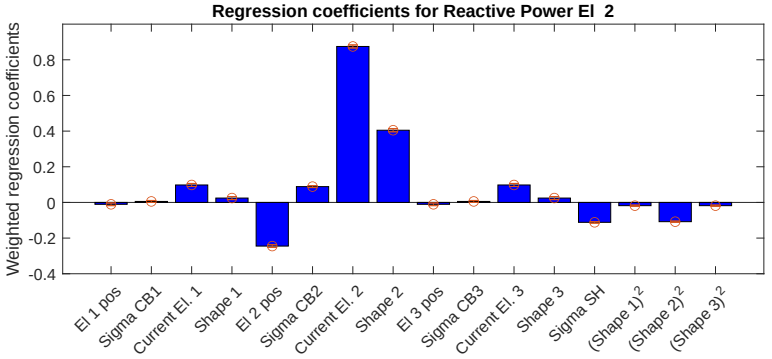

Figure B.18: Weighted regression coefficients for reactive Power El2

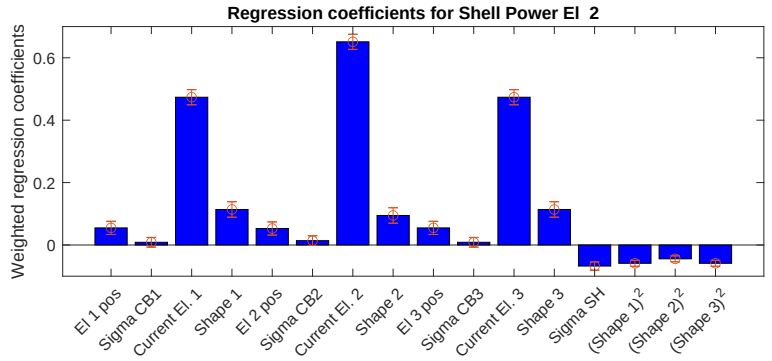

Figure B.19: Weighted regression coefficients for shell power El. 2.

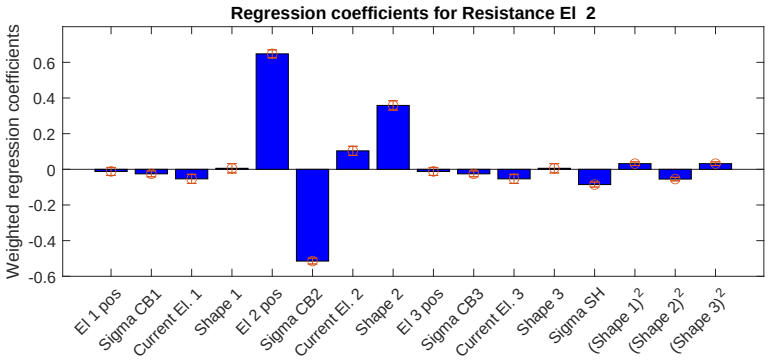

Figure B.20: Weighted regression coefficients for resistance El. 2.

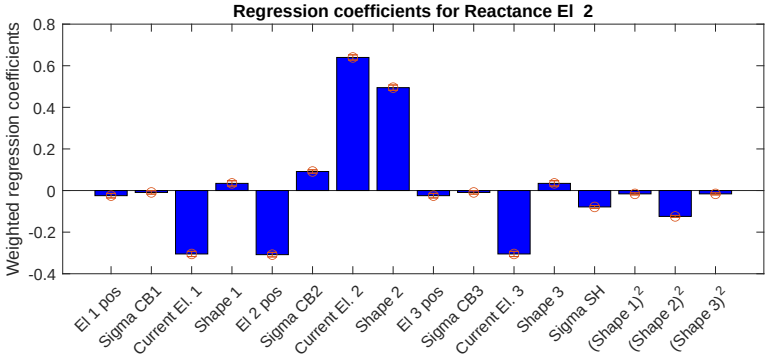

Figure B.21: Weighted regression coefficients for reactance El. 2.

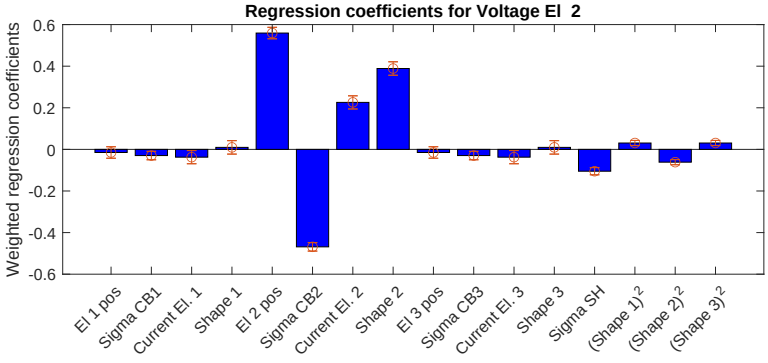

Figure B.22: Weighted regression coefficients for voltage El. 2.

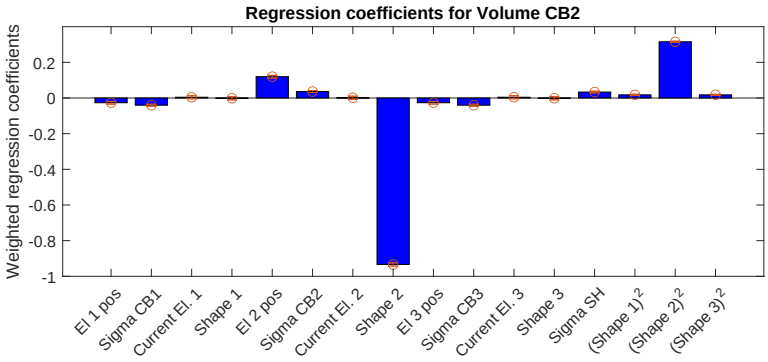

Figure B.23: Weighted regression coefficients for volume CB2.

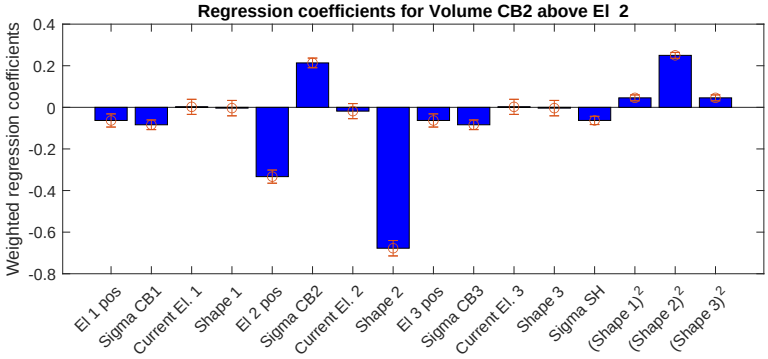

Figure B.24: Weighted regression coefficients for volume CB2 above El. 2.

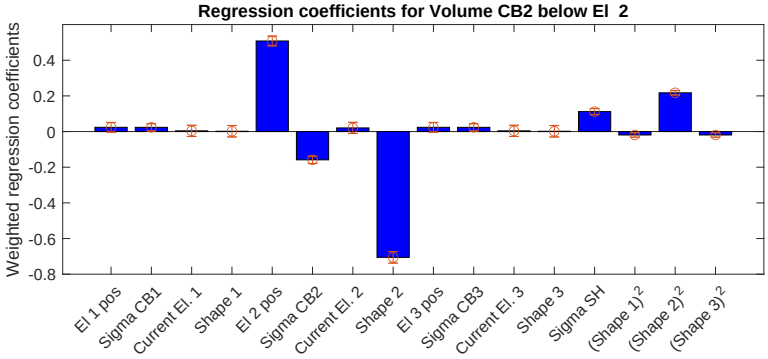

Figure B.25: Weighted regression coefficients for volume CB2 below El. 2.

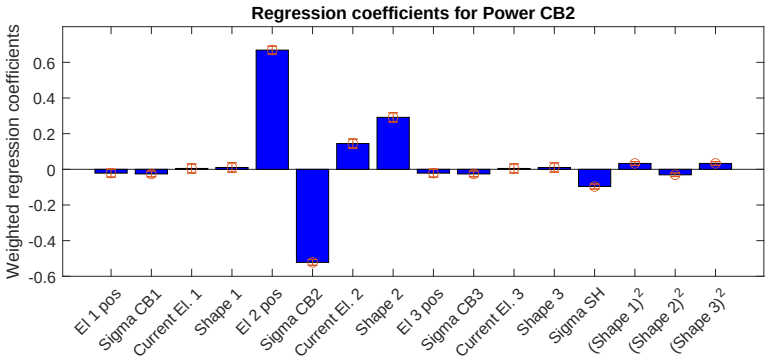

Figure B.26: Weighted regression coefficients for power CB2.

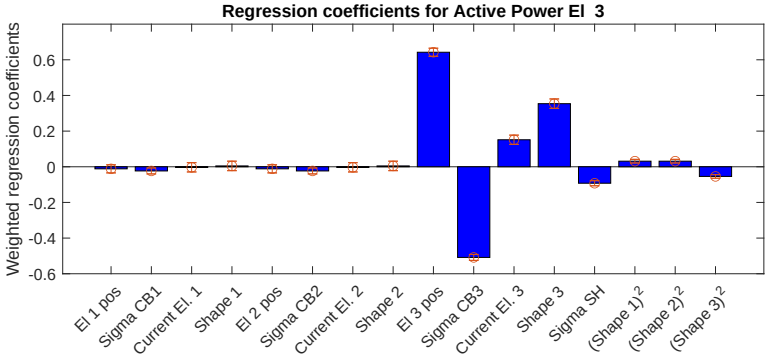

Figure B.27: Weighted regression coefficients for power El. 3.

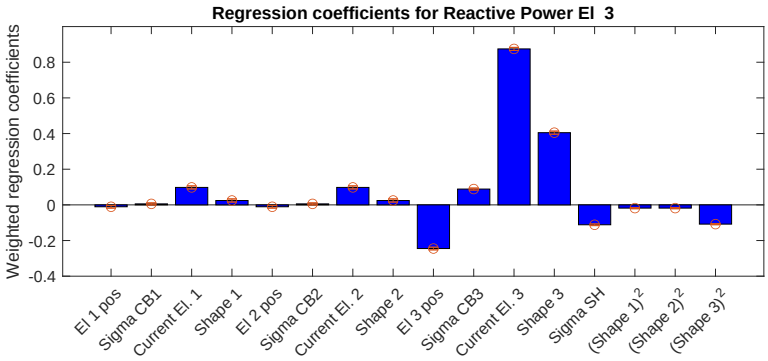

Figure B.28: Weighted regression coefficients for reactive power El. 3.

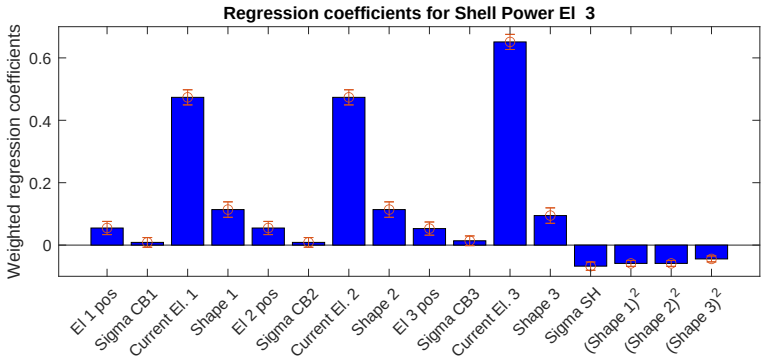

Figure B.29: Weighted regression coefficients for shell power El. 3.

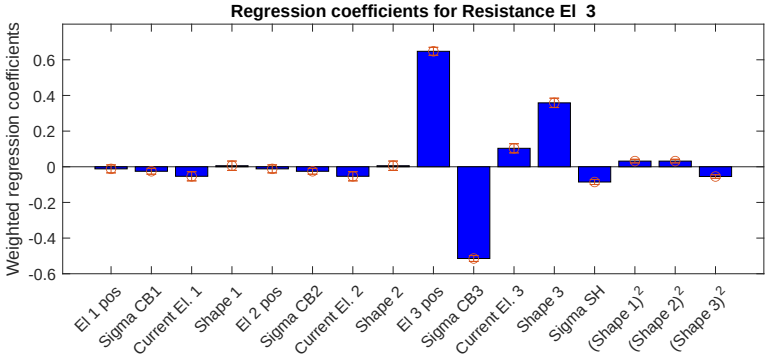

Figure B.30: Weighted regression coefficients for resistance El. 3.

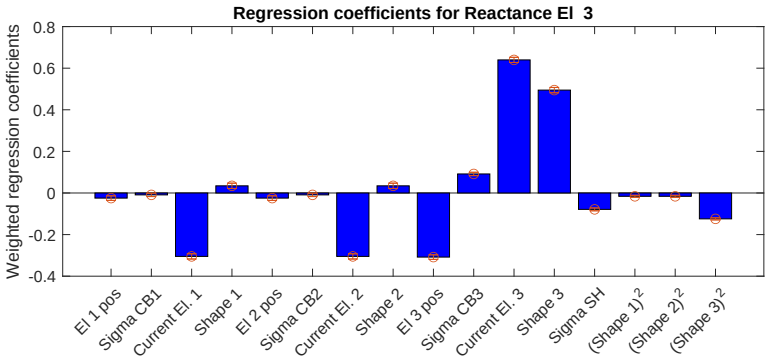

Figure B.31: Weighted regression coefficients for reactance El. 3.

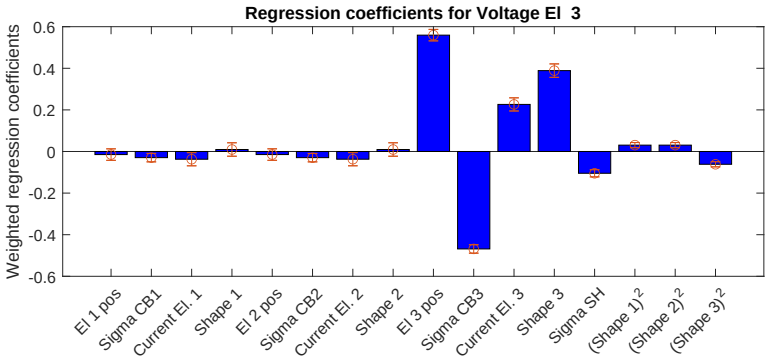

Figure B.32: Weighted regression coefficients for voltage El. 3.

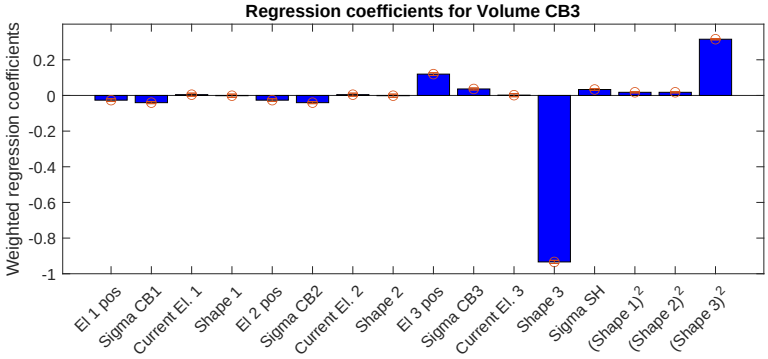

Figure B.33: Weighted regression coefficients for volume CB3.

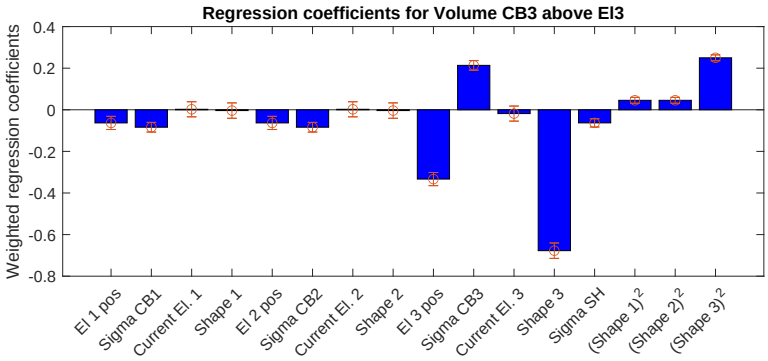

Figure B.34: Weighted regression coefficients for volume CB3 above El. 3.

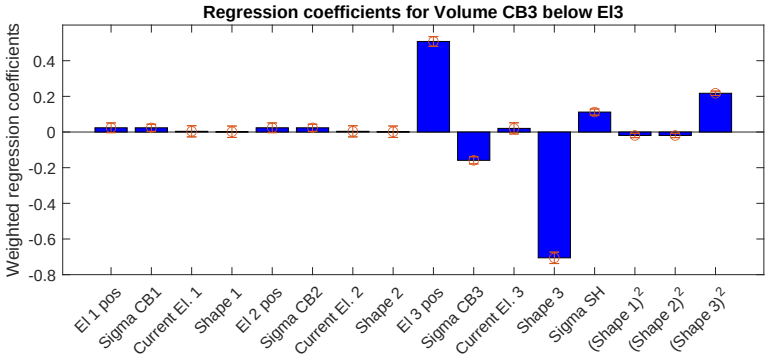

Figure B.35: Weighted regression coefficients for volume CB3 below El. 3

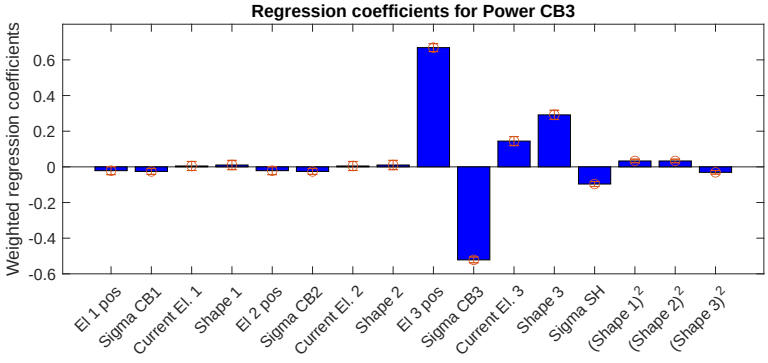

Figure B.36: Weighted regression coefficients for power CB3.

Appendix C

Weighted regression coefficients for inverse metamodel

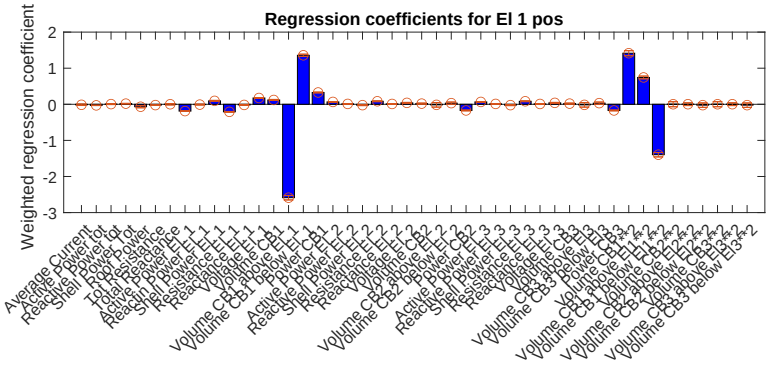

Figure C.1: Weighted regression coefficients for El. 1 pos.

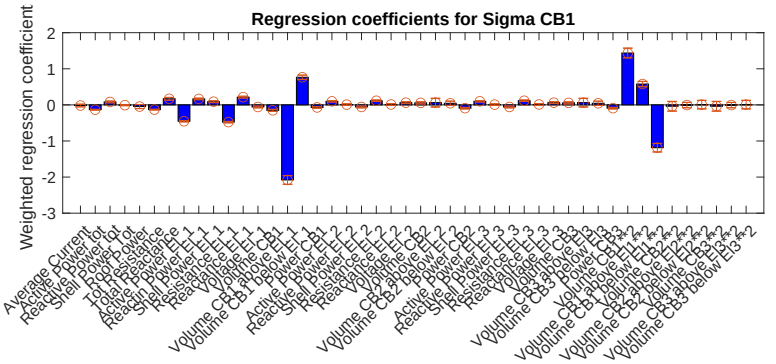

Figure C.2: Weighted regression coefficients for Sigma CB1.

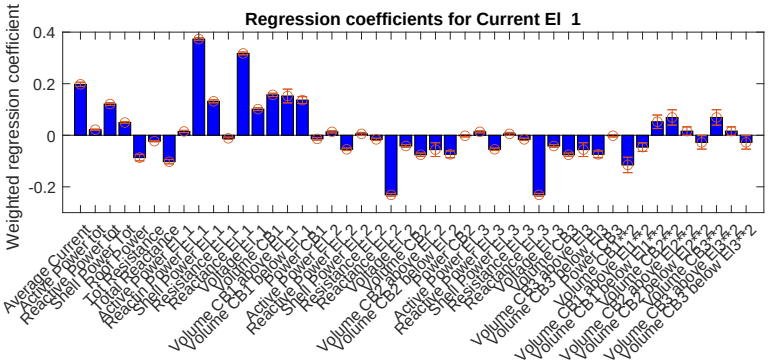

Figure C.3: Weighted regression coefficients for Current El. 1.

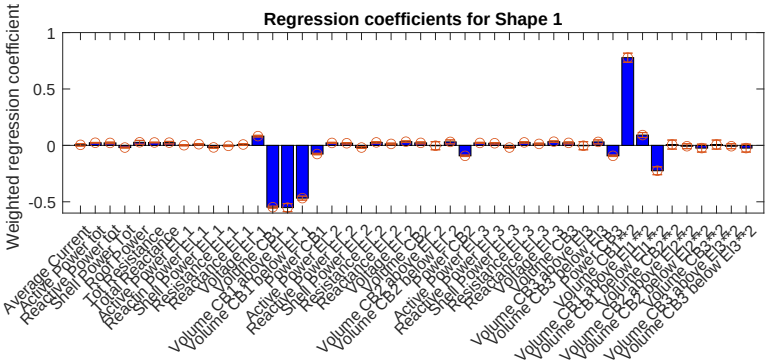

Figure C.4: Weighted regression coefficients for Shape 1.

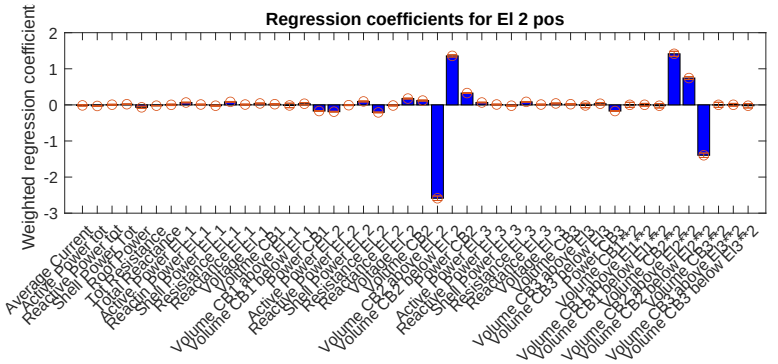

Figure C.5: Weighted regression coefficients for El. 2 pos.

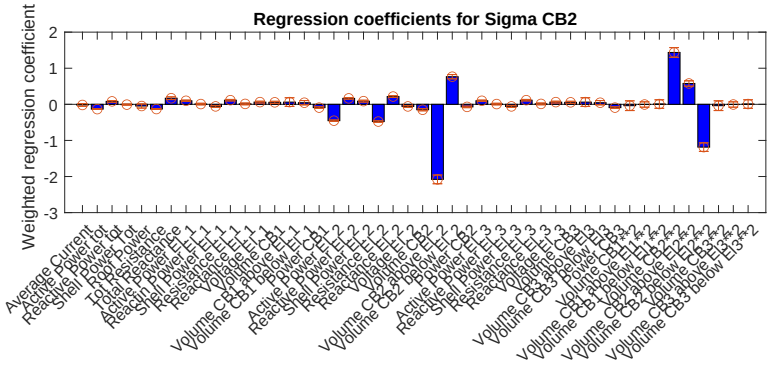

Figure C.6: Weighted regression coefficients for Sigma CB2.

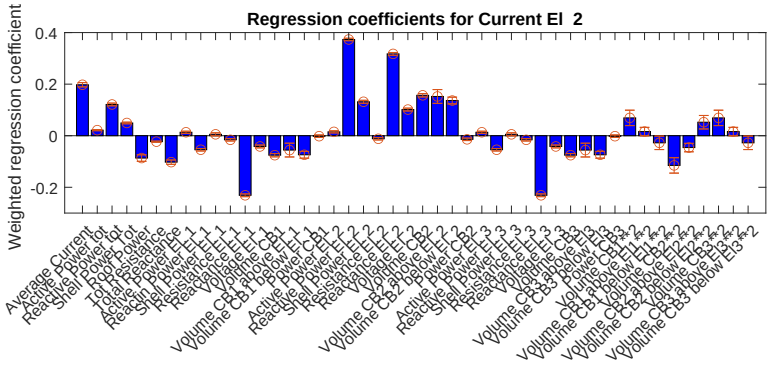

Figure C.7: Weighted regression coefficients for Current El. 2.

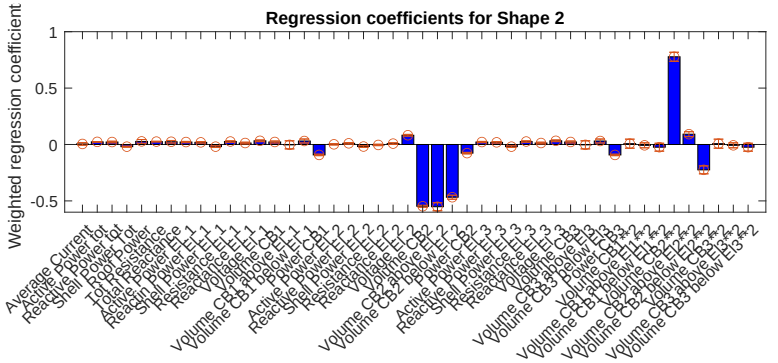

Figure C.8: Weighted regression coefficients for Shape 2.

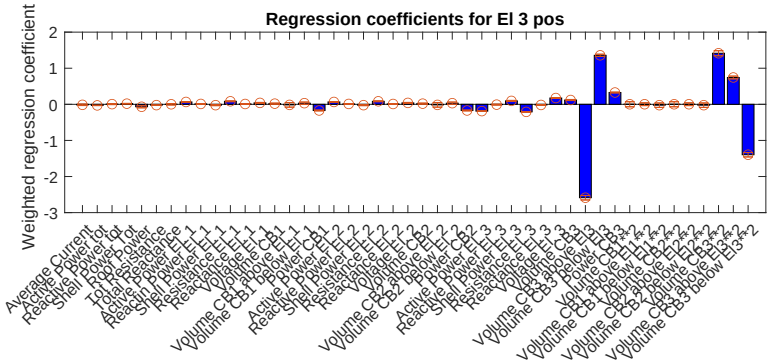

Figure C.9: Weighted regression coefficients for El. 3 pos.

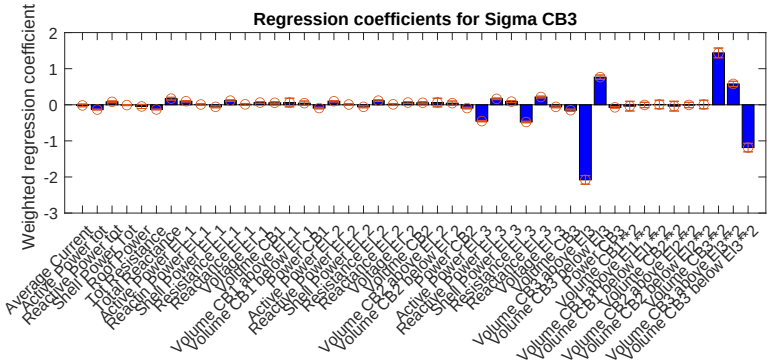

Figure C.10: Weighted regression coefficients for Sigma CB3.

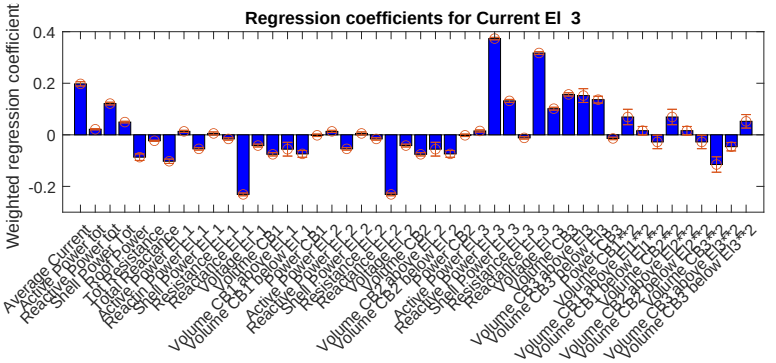

Figure C.11: Weighted regression coefficients for Current El. 3.

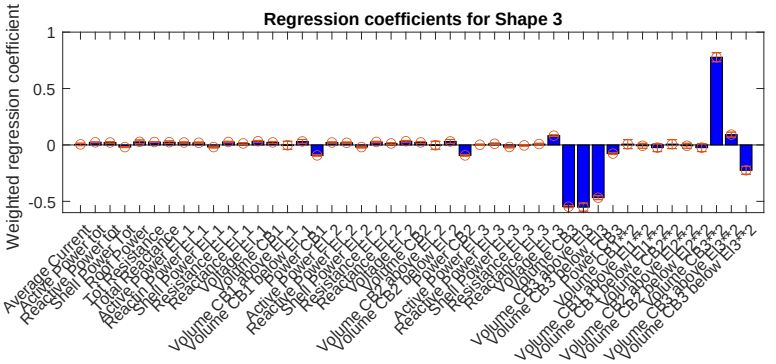

Figure C.12: Weighted regression coefficients for Shape 3.

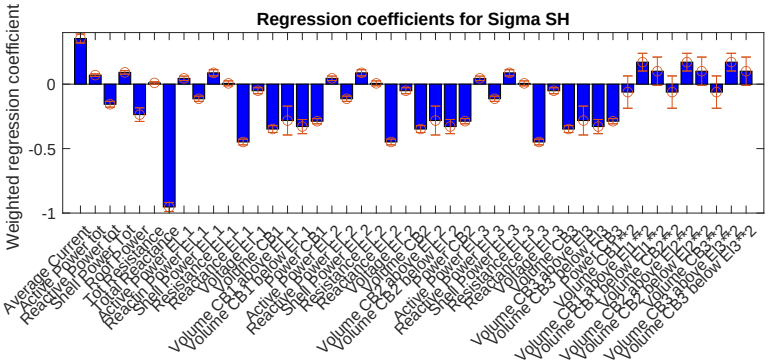

Figure C.13: Weighted regression coefficients for Sigma SH.

Appendix D

Weighted regression coefficients coefficients for the estimator

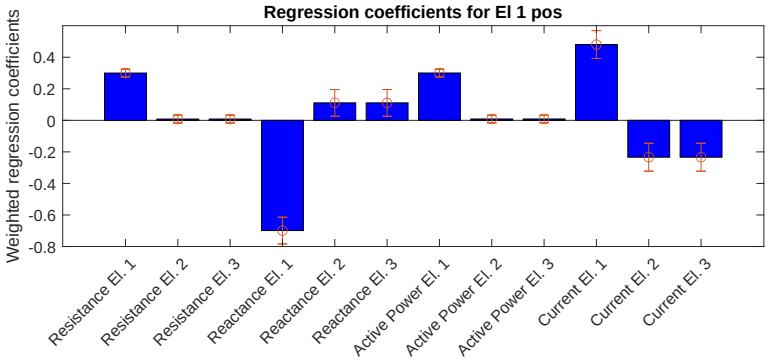

Figure D.1: Weighted regression coefficients for El. 1 pos.

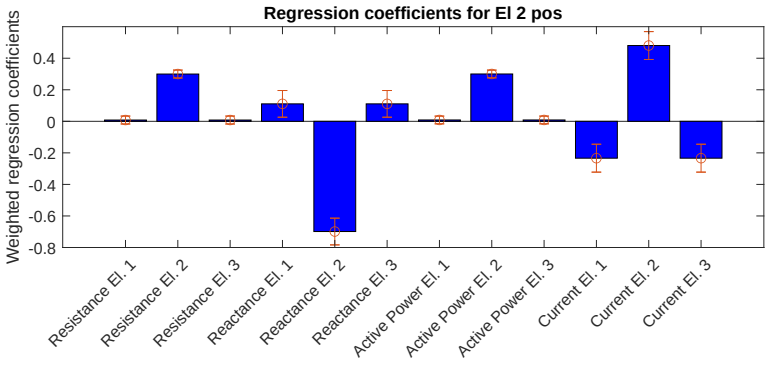

Figure D.2: Weighted regression coefficients for El. 2 pos.

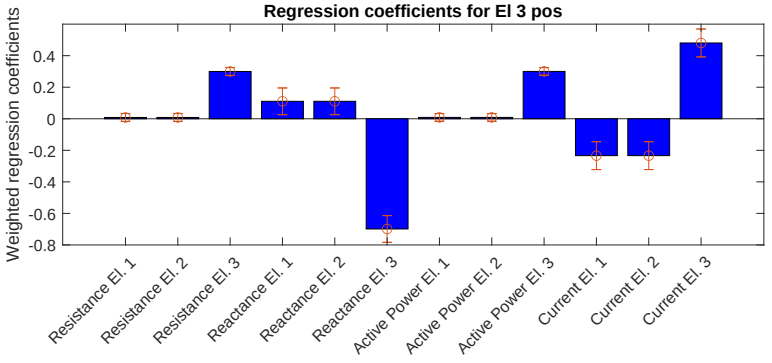

Figure D.3: Weighted regression coefficients for El. 3 pos.

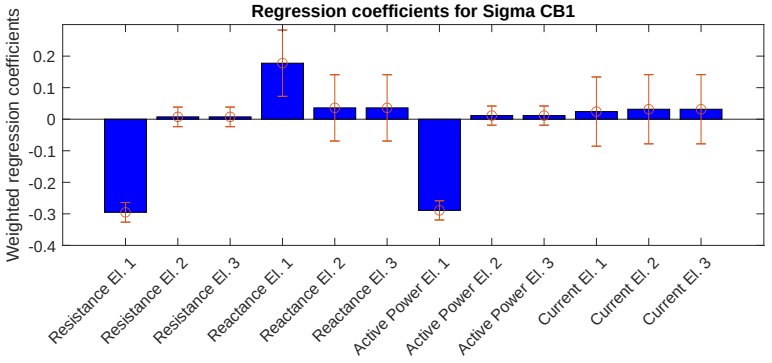

Figure D.4: Weighted regression coefficients for conductivity in cokebed 1.

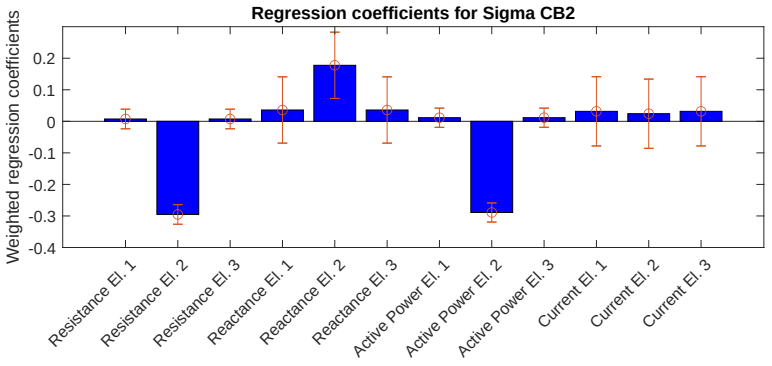

Figure D.5: Weighted regression coefficients for conductivity in cokebed 2.

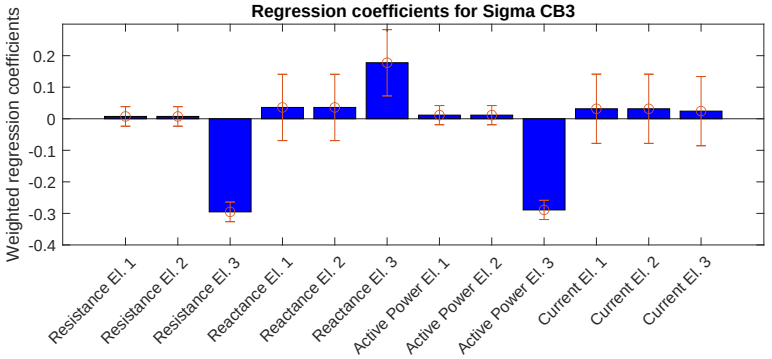

Figure D.6: Weighted regression coefficients for conductivity in cokebed 3.

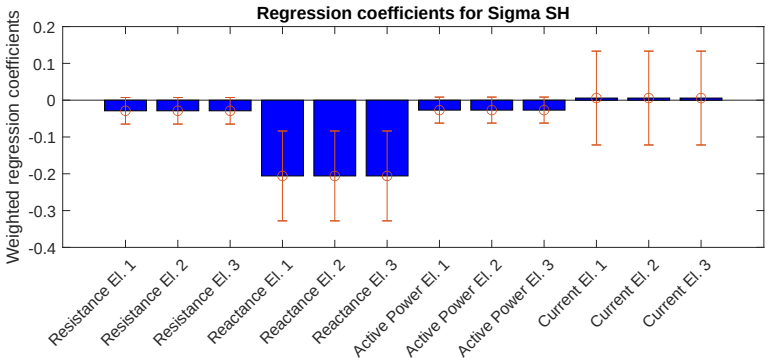

Figure D.7: Weighted regression coefficients for conductivity in charge material.

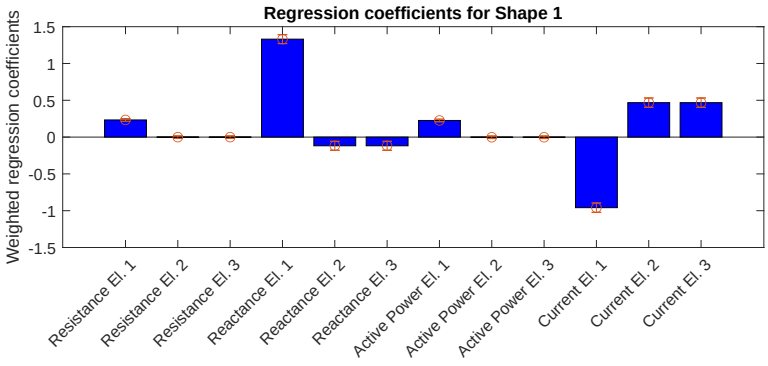

Figure D.8: Weighted regression coefficients for shape in cokebed 1.

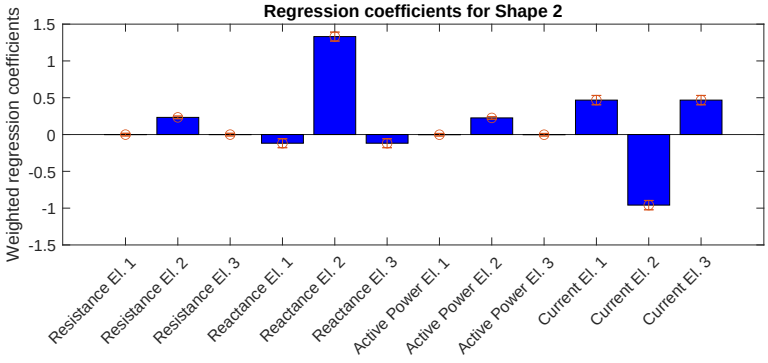

Figure D.9: Weighted regression coefficients for shape in cokebed 2.

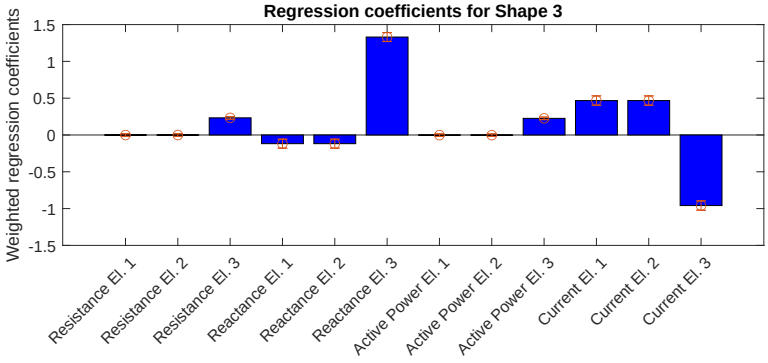

Figure D.10: Weighted regression coefficients for shape in cokebed 3.

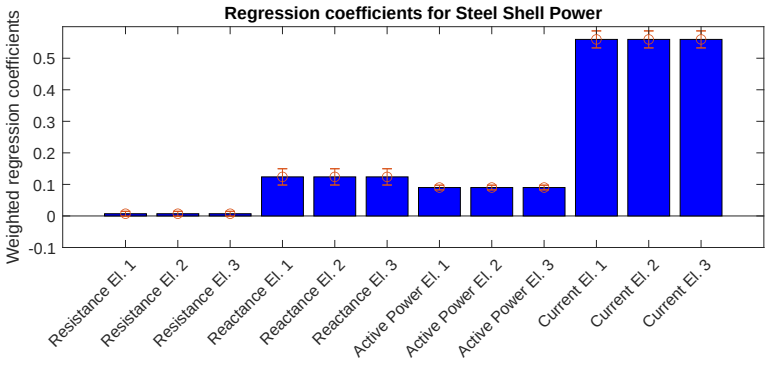

Figure D.11: Weighted regression coefficients for steel shell power.

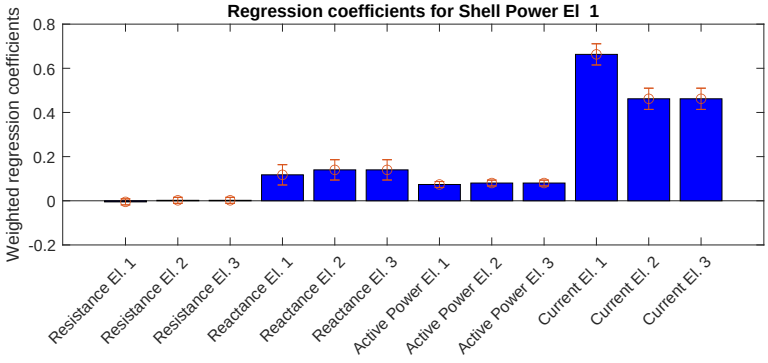

Figure D.12: Weighted regression coefficients for steel shell power El. 1.

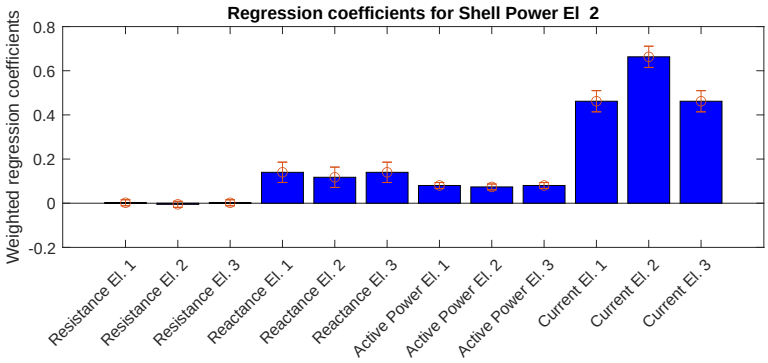

Figure D.13: Weighted regression coefficients for steel shell power El. 2.

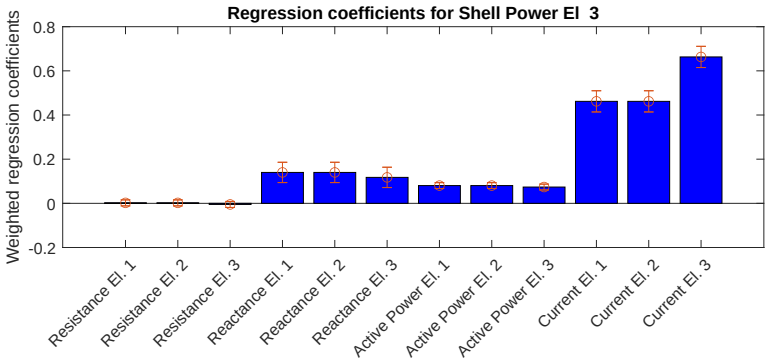

Figure D.14: Weighted regression coefficients for steel shell power El. 3.

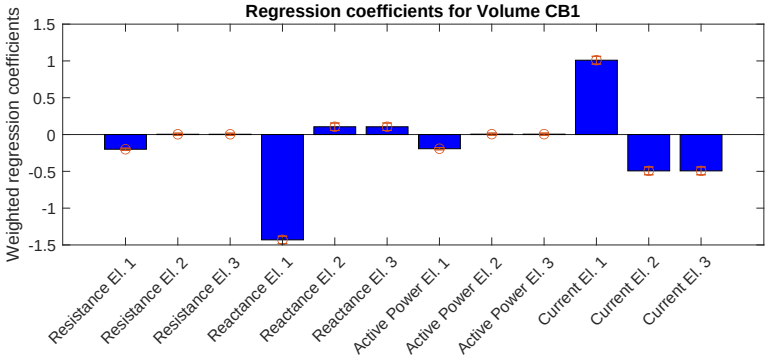

Figure D.15: Weighted regression coefficients for volume coke bed 1.

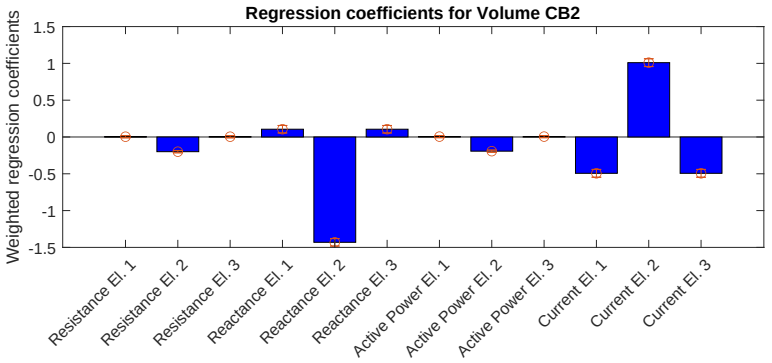

Figure D.16: Weighted regression coefficients for volume coke bed 2.

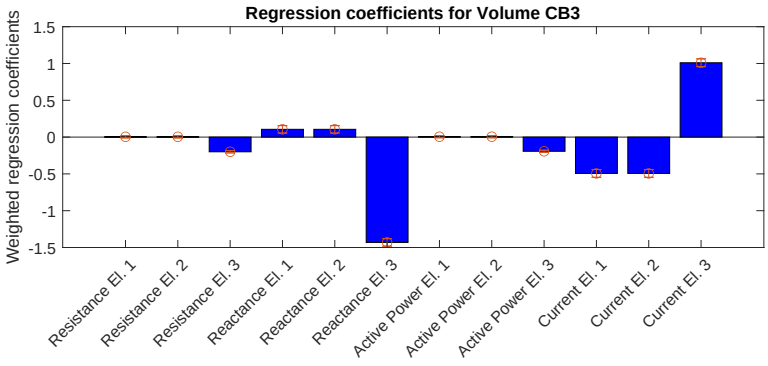

Figure D.17: Weighted regression coefficients for volume coke bed 3.

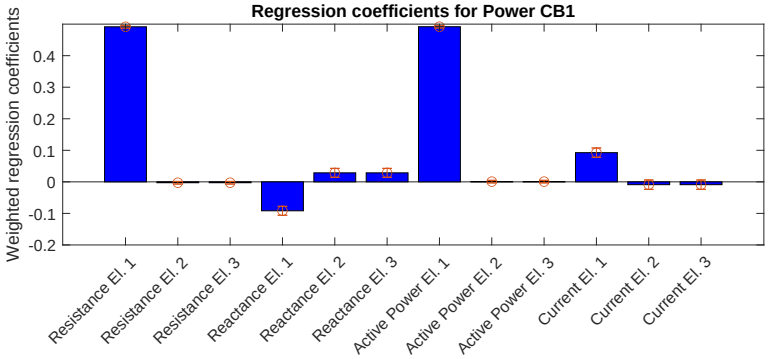

Figure D.18: Weighted regression coefficients for power coke bed 1.

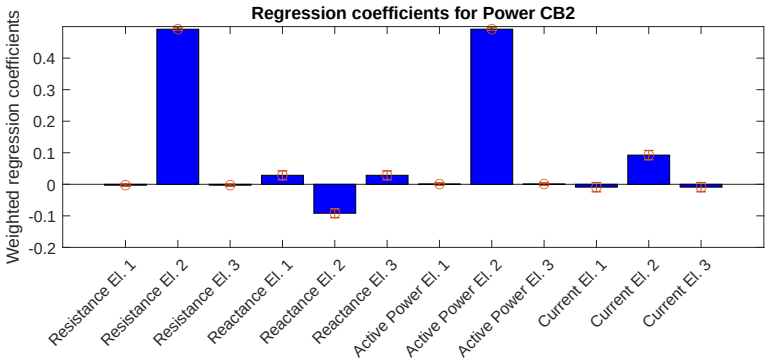

Figure D.19: Weighted regression coefficients for power coke bed 2.

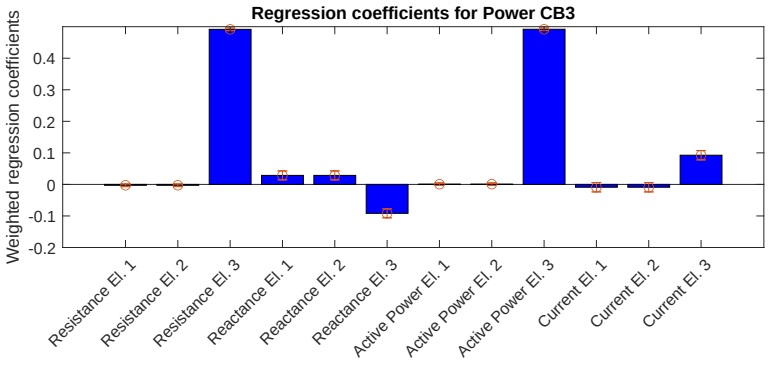

Figure D.20: Weighted regression coefficients for power coke bed 3.

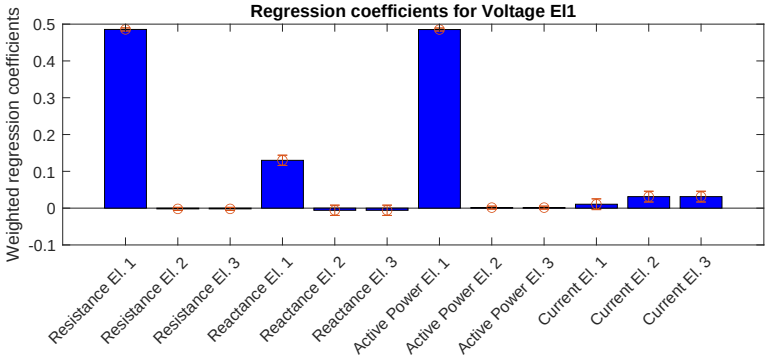

Figure D.21: Weighted regression coefficients for voltage in electrode 1.

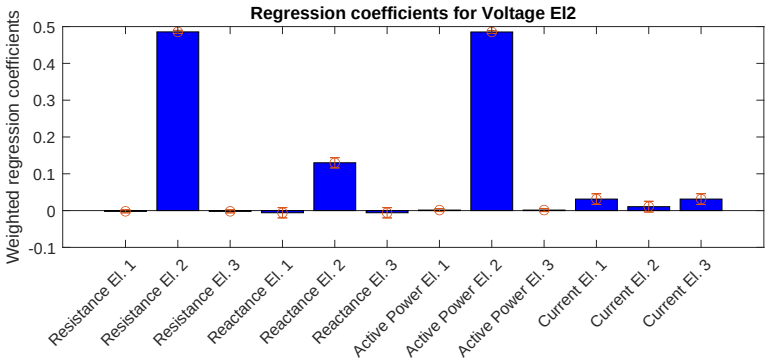

Figure D.22: Weighted regression coefficients for voltage in electrode 2.

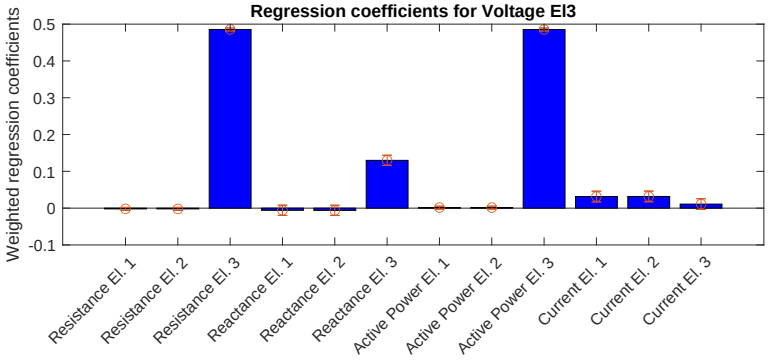

Figure D.23: Weighted regression coefficients for voltage in electrode 3.

Appendix E

Code

```
%% This document is for making metamodel

clc
clear
close all

% Giving information for opploading the X and Y for training
sSheetX = 'Input + eff';
sSheetY = 'Output';
ExcelFile = '../Data/Database_May.xlsx';
iNumberOfMainVariables = 13;

%% Model order selection'
% Using leave-one-out cross validation
% Plots the explained variance, both calibrated and validated
Save = 'True';

[afPctvar,                      ...
    afPctvarCV] =               ...
        LOOCV_EXPVA(            ...
            ExcelFile,          ...
            sSheetX,            ...
            sSheetY,            ...
            Save);

%% Making the PLSR model (direct metamodel)
disp('Making PLSR model...')
iNumberOfComponents = 17;
Plot = 'False';
```

```
Save = 'False';

[aafBeta,                                                    ...
    afB0,                                                    ...
    aafXWeightedLoadings,                                    ...
    aafXWeightedScores,                                      ...
    aafXWeights,                                             ...
    aafResiduals,                                            ...
    aafVarianceOfEstimates,                                  ...
    afYstdev,                                                ...
    afXstdev,                                                ...
    afXmean,                                                 ...
    afYmean,                                                 ...
    aafX,                                                    ...
    aafY,                                                    ...
    aafPerformanceIndexes,                                   ...
    afPctvar,                                                ...
    astrHeaderX,                                             ...
    astrHeaderY,                                             ...
    afVarianceOfEstimates] =                                 ...
        PLSR_function(                                       ...
            iNumberOfComponents,                             ...
            ExcelFile,                                       ...
            Plot,                                            ...
            sSheetX,                                         ...
            sSheetY,                                         ...
            Save);
disp('PLSR model made')

iNumberOfSamples = length(aafX);

%% Making the weights for the interaction effects

for col = 1:size(aafX,2)
    for row = 1:length(aafX)
        aafXcenteredsquared(row,col) =                       ...
            (aafX(row,col) - afXmean(col))^2;
    end
end
aafXSUMcenteredsquared = sum(aafXcenteredsquared)/           ...
    (iNumberOfSamples - 1);
for iNumberOfVariables = 1:size(aafX,2)
    afWeights(iNumberOfVariables) =                          ...
        1/sqrt(aafXSUMcenteredsquared(iNumberOfVariables));
end
```

```
75
76  % Making the weights for the original input
77  afWeightsOriginalInput = afWeights(1:iNumberOfMainVariables);
78  afXmeanMainVariables = afXmean(1:iNumberOfMainVariables);
79
80  %% LOOCV PLSR
81  [aafPerformanceIndexesCV,          ...
82      afExplainedVarianceCV]         ...
83      = LOOCV_PLSR(                  ...
84          ExcelFile,                 ...
85          sSheetX,                   ...
86          sSheetY,                   ...
87          iNumberOfComponents);
88
89  %% Uploading validation set
90
91  sSheetXValidation = 'Input_symmetry';
92  sSheetYValidation = 'Output_symmetry';
93  ExcelFile = '../Data/Database_May_Validation.xlsx';
94
95  [aafXValidation,astrHeaderXValidated,NotinUse]   =    ...
96      xlsread(ExcelFile, sSheetXValidation);
97  [aafYValidation,astrHeaderYValidated,NotinUse2]  =    ...
98      xlsread(ExcelFile, sSheetYValidation);
99
100 %% Prediction based on the validation set
101
102 % Normalizing the validation set
103 for i = 1:length(aafXValidation)
104     aafXValidationNormalized(i,:) =                    ...
105     (aafXValidation(i,:) - afXmeanMainVariables) .*    ...
106         afWeightsOriginalInput;
107 end
108
109 % Making the interaction effects
110 for number = 1:length(aafXValidation)
111     afXValidationNormalized = aafXValidationNormalized(number,:);
112     counter = 1;
113     for iMainInputvariable = 1:iNumberOfMainVariables
114         for j = iMainInputvariable + 1:iNumberOfMainVariables
115             afXinteractions(counter) = ...
116                 afXValidationNormalized(iMainInputvariable) * ...
117                 afXValidationNormalized(j);
118             counter = counter + 1;
119         end
```

```
    end
    aafXinteractions(number,:) = afXinteractions;
end

% Making the squared effects
for number = 1:length(aafXValidation)
    afXValidationNormalized = aafXValidationNormalized(number,:);
    counter = 1;
    for iMainInputvariable = 1:iNumberOfMainVariables
         afXsquares(iMainInputvariable) =  ...
             afXValidationNormalized(iMainInputvariable)^2;
         counter = counter + 1;
    end
    aafXsquares(number,:) = afXsquares;
end

% Merging x with interactions and squares
aafX0 = [aafXValidation, aafXinteractions, aafXsquares];

% Predicting validated y
aafY0 = aafX0 * aafBeta + afB0;

%% Assesing the model performance
fmeanYest = mean(aafY0);
fmeanYVal = mean(aafYValidation);

% Finding R2 and RMSE
iNumberOfOutputs = size(aafYValidation,2);
iNumberOfMeasurements = size(aafYValidation,1);
afR2 = zeros(1, iNumberOfOutputs);
afRMSE = zeros(1, iNumberOfOutputs);
for i = 1:iNumberOfOutputs
    afSquaredError = (aafYValidation(:,i) - aafY0(:,i)).^2;
    afMeanOfRealY = (aafYValidation(:,i) - fmeanYVal(i)).^2;
    fSumOfEst = sum(afSquaredError);
    fSumOfReal = sum(afMeanOfRealY);
    fR2 = 1 - (fSumOfEst/fSumOfReal);
    afR2(i) = fR2;
    fRMSE = sqrt(fSumOfEst/iNumberOfMeasurements);
    afRMSE(i) = fRMSE;
end

aafPerformanceIndexesVal = [afRMSE', afR2'];
aafPerformanceIndexesVal = table(aafPerformanceIndexesVal, ...
     'RowNames',astrHeaderY);
```

```
aafPerformanceIndexesVal = splitvars(aafPerformanceIndexesVal);
aafPerformanceIndexesVal.Properties.VariableNames = {'RMSE','R2'};

%% Plotting ref vs predicted

for iPlot = 1:size(aafYValidation,2)
    figure
    minste = min(aafYValidation(:,iPlot));
    storste = max(aafYValidation(:,iPlot));

    plot(aafYValidation(:,iPlot), aafY0(:,iPlot), 'o')
    hold on
    plot([minste, storste],[minste,storste] , 'k', 'MarkerSize', 2)
    xlim([minste, storste])
    xlabel('Reference Y');
    ylabel('Predicted Y');
    word = astrHeaderY(iPlot);
    title(word{1});
end
```

```
%% Function for PLSR
% 1. Gives the beta and b0 scaled back to
%    "raw" values
% 2. Provides scores and loadings
% 3. Give the calibrated perfomance in R^2 and RMSE
% 4. Gives plots of:
%   a) Beta coef with CI
%   b) Reference vs. prediction plots (calibrated)

function [aafBeta,                                  ...
          afB0,                                     ...
          aafXWeightedLoadings,                     ...
          aafXWeightedScores,                       ...
          aafXWeights,                              ...
          aafResiduals,                             ...
          aafVarianceOfEstimates,                   ...
          afYstdev,                                 ...
          afXstdev,                                 ...
          afXmean,                                  ...
          afYmean,                                  ...
          aafXUnscaled,                             ...
          aafYUnscaled,                             ...
          aafPerformanceIndexes,                    ...
          afPctvar,                                 ...
          astrHeaderX,                              ...
          astrHeaderY,                              ...
```

```
27          afVarianceOfEstimates] =                ...
28            PLSR_function(iNumberOfComponents,    ...
29                ExcelFile,                        ...
30                Plot,                             ...
31                sSheetX,                          ...
32                sSheetY,                          ...
33                Save)
34
35      C = strsplit(ExcelFile,'_');
36      ExcelID=C{end};
37      ExcelID = ExcelID(1:end-5);
38
39      % Upload data set
40      [aafXUnscaled,astrHeaderX,NotinUse]  = xlsread(ExcelFile, sSheetX);
41      [aafYUnscaled,astrHeaderY,NotinUse2] = xlsread(ExcelFile, sSheetY);
42
43      % Changing properties of headers
44      for i = 1:length(astrHeaderY)
45          astrHeaderY(i) = strrep(astrHeaderY(i),'.',' ');
46      end
47
48      % Making shorter names for astrHeaderX
49      for i = 1:length(astrHeaderX)
50          name = astrHeaderX{i};
51          name = name(1:7);
52          astrHeaderShortX{i} = name;
53      end
54
55      % Making shorter names for astrHeaderY
56      for i = 1:length(astrHeaderY)
57          name = astrHeaderY{i};
58          name = name(1:5);
59          astrHeaderShortY{i} = name;
60      end
61
62      % Set the percentile for the PI
63      fPercentile = 1.962;    % 95% confidence interval with 1000 df
64
65      % Standardizing
66      [aafX,afXmean,afXstdev] = zscore(aafXUnscaled);
67      [aafY,afYmean,afYstdev] = zscore(aafYUnscaled);
68
69      % Extracting info from data sets
70      iNumberOfMeasurements = size(aafX,1);
71      iNumberOfInputs = size(aafX,2);
```

```
72      iNumberOfOutputs = size(aafY,2);
73
74      %% Making weighted plsr model
75          % estimate the SCALED model
76      [   aafXWeightedLoadings,                   ...
77          aafYWeightedLoadings,                   ...
78          aafXWeightedScores,                     ...
79          aafYWeightedScores,                     ...
80          aafWeightedEstimatedBeta,               ...
81          aafPctvar,                              ...
82          fEstimatedWeightedMSE,                  ...
83          stats] =                                ...
84              plsregress(                         ...
85                  aafX,                           ...
86                  aafY,                           ...
87                  iNumberOfComponents);
88
89      aafXWeights = stats.W;
90      afEstimatedWeightedB0 = aafWeightedEstimatedBeta( 1, : );
91      aafEstimatedWeightedBeta = aafWeightedEstimatedBeta( 2:end, : );
92      afPctvar = cumsum(100*aafPctvar(2,:));
93
94      %% Computing Residuals of training set (weighted)
95      aafPredictedY = zeros( size(aafY) );
96      aafResiduals  = zeros( size(aafY) );
97
98      for iMeasurement = 1:iNumberOfMeasurements
99          %
100         aafPredictedY(iMeasurement, :) =    ...
101                 aafX(iMeasurement, :) *     ...
102                 aafEstimatedWeightedBeta    ...
103             +   afEstimatedWeightedB0;
104         %
105         aafResiduals(iMeasurement, :) =     ...
106                 aafY(iMeasurement, :)       ...
107             -   aafPredictedY(iMeasurement, :);
108         %
109     end %
110
111     %% Calculating the variance of estimates
112     aafVarianceOfEstimates = zeros(iNumberOfOutputs,iNumberOfOutputs);
113     %
114     for i = 1:iNumberOfMeasurements
115         %
116         aafVarianceOfEstimates = aafVarianceOfEstimates + ...
```

```
117             ( aafResiduals(i,:) )' * ( aafResiduals(i,:) );
118         %
119     end;%
120     %
121     % normalize to find the estimated variance
122     aafVarianceOfEstimates = ( 1 /                          ...
123         ( iNumberOfMeasurements - iNumberOfInputs - 1)) ...
124         * aafVarianceOfEstimates;
125
126
127     %% Making raw beta, gives aafBeta and afB0_raw
128     for i = 1:length(afXstdev)
129         aafBeta_new(i,:) = aafEstimatedWeightedBeta(i,:) / afXstdev(i);
130     end
131
132     % multiply in std_y into beta_new
133     for i = 1:length(afYstdev)
134         aafBeta(:,i) = aafBeta_new(:,i) * afYstdev(i);
135         aafB0_new(i) = afYstdev(i) * afEstimatedWeightedB0(i);
136     end
137
138     afB0 = - afXmean * aafBeta + aafB0_new + afYmean;
139
140     %% Calculating the CI for the betas
141     W = aafXWeights;
142     P = aafXWeightedLoadings;
143     T = aafXWeightedScores;
144
145     % Calculating the covariance matrix for Beta
146     aafZ = W * inv(P' * W) * inv(T' * T) * inv(W' * P) * W';
147     %
148     % Extracting the diagonal of Z (variance of each component in B)
149     afZ = diag(aafZ);
150     %
151     % Extracting the diagonal of the covariance matrix
152     afVarianceOfEstimates = diag(aafVarianceOfEstimates);
153     %
154     % Appending the aConfidenceIntervalBoundaries
155     aafConfidenceIntervalBoundaries = zeros(       ...
156         iNumberOfInputs, iNumberOfOutputs);
157     %
158     % Iterating such that the CI fo the betas for each y is calculated
159     for i = 1:iNumberOfOutputs
160         % Calculating the Beta CIs for one y in the Y set
161         %
```

```
        afConfidenceIntervalBoundaries = zeros(iNumberOfInputs, 1);
        for j = 1:iNumberOfInputs
            %
            afConfidenceIntervalBoundaries(j) =           ...
                        fPercentile                       ...
                    *   ( afVarianceOfEstimates(i) )^(1/2)...
                    *   afZ(j)^(1/2);
            %
        end
        aafConfidenceIntervalBoundaries(:,i) =     ...
            afConfidenceIntervalBoundaries;
    end;%

    %% Assesing the model performance (calibrated)
    aafYest = aafXUnscaled * aafBeta + afB0;
    fmeanYest = mean(aafYest);
    fmeanY = mean(aafYUnscaled);

    % Finding R2 and RMSE
    afR2 = zeros(1, iNumberOfOutputs);
    afRMSE = zeros(1, iNumberOfOutputs);
    for i = 1:size(aafYUnscaled,2)
        afSquaredError = (aafYUnscaled(:,i) - aafYest(:,i)).^2;
        afMeanOfRealY = (aafYUnscaled(:,i) - fmeanY(i)).^2;
        fSumOfEst = sum(afSquaredError);
        fSumOfReal = sum(afMeanOfRealY);
        fR2 = 1 - (fSumOfEst/fSumOfReal);
        afR2(i) = fR2;
        fRMSE = sqrt(fSumOfEst/iNumberOfMeasurements);
        afRMSE(i) = fRMSE;
    end

    aafPerformanceIndexes = [afRMSE', afR2'];
    aafPerformanceIndexes = table(aafPerformanceIndexes, ...
          'RowNames',astrHeaderY);
    aafPerformanceIndexes = splitvars(aafPerformanceIndexes);
    aafPerformanceIndexes.Properties.VariableNames = {'RMSE','R2'};

    %% Plotting the CI for betas
    if strcmpi('True',Plot)
        % Making a for loop for plotting Betas for all y's
        for iNumberPlot = 1:iNumberOfOutputs
            figure
            % Plotting betas for one y
            bar(1:length(astrHeaderX), ...
```

```
207                 aafEstimatedWeightedBeta(:,iNumberPlot), 'b')
208             hold on
209             % plot the limits
210             errorbar(aafEstimatedWeightedBeta(:,iNumberPlot) ...
211                 ,aafConfidenceIntervalBoundaries(:,iNumberPlot), 'o')
212             % labeling
213             set(gca,'XTickLabel',astrHeaderX);
214             xtickangle(45)
215             xTick=get(gca,'xtick');
216             set(gca,'xtick', 1:length(astrHeaderX));
217             %xlabel('X variables')
218             ylabel('Weighted regression coefficients')
219             word = strcat('Regression coefficients for ', ...
220                 {' '}, astrHeaderY(iNumberPlot));
221             title(word)
222             word = word{1};
223             word = word(find(~isspace(word)));
224             word(word=='.')=[];
225             %word = strcat(word{1},'.pdf');
226             if strcmpi('True',Save)
227                 set(gcf,'Units','centimeters');
228                 afFigurePosition = [1 1 20 8];
229                 set(gcf,'Position', afFigurePosition);
230                 set(gcf,...
231                 'PaperPosition',[0 0 afFigurePosition(3:4)],...
232                 'PaperSize',[afFigurePosition(3:4)]);
233                 saveas(gcf, word, 'pdf')
234             end
235         end
236
237         % Plotting the explained variance
238         figure
239         plot(1:iNumberOfComponents,cumsum(100*aafPctvar(2,:)),'-bo')
240         xlabel('Number of PLS components');
241         ylabel('Percent Variance Explained in y');
242         if strcmpi('True',Save)
243             set(gcf,'Units','centimeters');
244             afFigurePosition = [1 1 20 5.5];
245             set(gcf,'Position', afFigurePosition);
246             set(gcf,...
247             'PaperPosition',[0 0 afFigurePosition(3:4)],...
248             'PaperSize',[afFigurePosition(3:4)]);
249             ord = strcat('Explained variance', {' '}, ExcelID);
250             saveas(gcf, ord{1}, 'pdf')
251         end
```

```
252
253         % Plotting ref vs real
254         for i = 1:iNumberOfOutputs
255             figure
256             h1 = plot(aafYUnscaled(:,i), aafYest(:,i), 'bo');
257             set(h1, 'markerfacecolor', get(h1, 'color'));
258             word = strcat(astrHeaderY(i));
259             title(word)
260             word = word{1};
261             word = word(find(~isspace(word)));
262             xlabel('Reference Y')
263             ylabel('Predicted Y')
264                 if strcmpi('True',Save)
265                     set(gcf,'Units','centimeters');
266                     afFigurePosition = [1 1 20 5.5];
267                     set(gcf,'Position', afFigurePosition);
268                     set(gcf,...
269                     'PaperPosition',[0 0 afFigurePosition(3:4)],...
270                     'PaperSize',[afFigurePosition(3:4)]);
271                     ord = strcat('refVSpredplot', {' '}, word);
272                     saveas(gcf, ord{1}, 'pdf')
273                 end
274         end
275
276     end % for Plot = True
277
278
279 end %function
```